BILINGUAL PUBLISHING CO.
Pioneer of Global Academics Since 1984

Journal of Geological Research

Volume 3 · Issue 4 · October 2021 ISSN 2630-4961(Online)

BILINGUAL PUBLISHING CO.
Pioneer of Global Academics Since 1984

Editor-in-Chief

Editorial Board Members

Volume 3 Issue 4 • October 2021 • ISSN 2630-4961 (Online)

Journal of Geological Research

BILINGUAL PUBLISHING CO.
Pioneer of Global Academics Since 1984

BILINGUAL PUBLISHING CO.
Pioneer of Global Academics Since 1984

Volume 3 | Issue 4 | October 2021 | Page1-55
Journal of Geological Research

Contents

Articles

-

BILINGUAL PUBLISHING CO.
Pioneer of Global Academics Since 1984

Journal of Geological Research
https://ojs.bilpublishing.com/index.php/jgr-a

ARTICLE

Volcanogenic Deposits of Non-ferrous Metals in the Lesser Caucasus and Eastern Pontides

S. Kekelia* N.Gagnidze I. Mshvenieradze G. Kharazishvili

Department of mineral deposits and geochemistry, Al. Janelidze Institute of Geology of Ivane Javakhishvili Tbilisi State University, Georgia,the U.S.

ARTICLE INFO

Article history
Received: 16 August 2021
Revised: 6 September 2021
Accepted: 6 September 2021
Published Online: 28 September 2021

Keywords:
Kuroko-type deposits
Madneuli
Chayeli
Paleoisland
Undepleted mantle
Ore

ABSTRACT

The paper presents brief characteristics of geological environments of ore deposit occurrences in Turkey, Georgia and Armenia. They can be attributed to Kuroko-type deposits, being distinguished by the character of ore accumulation. To the west, in Turkey, there are epigenetic and hydrothermal-sedimentary copper-zinc deposits that were formed in deep restricted basinal settings. An example of the latter is the Chayeli deposit. To the east, in the Caucasus, we have predominantly only epigenetic deposits. Besides, in the Bolnisi mining district (Georgia) there is the Madneuli deposit which represents an example of polyformational deposit. Here, within the restricted territory, have been concentrated: barite, barite-polymetallic, gold-bearing secondary quartzite, large-scale stockworks of copper ores. Judged by the 87Sr/86Sr ratios, some volcanites which are spatially associated with ores, might have been products of the "differentiation" of undepleted mantle, or other magmas that were generated in the lower part of the earth crust.

In the Alaverdi ore district in Armenia, there are Jurassic volcano-depressions that host copper, copper-zinc and barite-sulfide ores. All the deposits of the Alaverdi district, porphyry copper including, contain economic reserves of ores.

On the basis of available literature material and our own data, there has been created a mental-logical geological-genetic model of volcanogenic deposits.

1. Introduction

Within the central part of the Alpine-Mediterranean-Himalayan mountain-fold belt there are fragments of ancient continental-margin structures – paleoisland arcs and backarc and interarc paleobasins. It is within these structures that economic volcanogenic deposits of non-ferrous metals have been concentrated. Among the most important geological events that have conditioned the tectonic setting of this segment of the mountain-fold belt are: (1) the partition of the South Armenian-Iranian microplate from the north margin of Gondwana in Permian-Triassic time and its accretion to the active Passific-type continental margin of the Eurasian continent [1-4]; (2) the opening of a rift in Late Triassic-Early Jurassic that was later trans-

*Corresponding Author:
S. Kekelia,
Department of mineral deposits and geochemistry, Al. Janelidze Institute of Geology of Ivane Javakhishvili Tbilisi State University, Georgia,the U.S.;
Email: sergokekelia@yahoo.com

DOI: https://doi.org/10.30564/jgr.v3i4.3572

formed into a branch of the Neotethys; (3) the obduction of oceanic complexes in the Senonian that heralded the "death" of the Tethys ocean [2]. The further development of the region during the late Alpine cycle was conditioned by the interaction of the Scythian and South Caucasian-Pontian microplates (active paleomargin of the Eurasian continent) with the northernmost lithosperic blocks of Gondwana (Kirşehir, East Taurus, Daralagez and some others). At present, the boundaries between these mobile blocks of the earth's crust (sometimes referred to as terrains) are represented by large fault zones commonly with evidence of significant dip-slip and strike-slip displacements and are marked by basitic and ultrabasitic ophiolitic complexes and tectonic melange (Figure 1).

It should be noted that the above-mentioned geologic events of the Alpine cycle were accompanied by the following processes: (1) the divergency of microplates (crustal blocks) in Triassic-Early Bajocian and the activation of the processes of mantle diapirism; (2) the convergence of the microplates in late Bajocian-earliest late Cretaceous accompanied by specific island-arc volcanism revealed in both uplifted blocks (subaerial environments) and restricted deep basins that existed within the South Caucasian-Pontian province. The maximum activity of this islandarc volcanism occurred in the South Caucasus in the Bajocian-late Jurassic and in the Pontides – in the Turonian-Santonian. A. Yilmaz and his co-authors [5] pointed out that in the geodynamic evolution of the western and eastern parts of the islandarc system there are obvious distinctions. It was also shown that the start of the collision between South Caucasian and Daralagez blocks happened in the Coniacian whereas that between Pontides and Anatolides – in the Campanian [2,6].

During the convergent stage, within the active continental margin of the Eurasian plate appeared thermoanomalies whose location was generally controlled by tectonic factors; these anomalies commonly coincide spatially with areas experienced maximum tectonic deformations and are characterized by increased fracturing and faulting. It is these areas that reveal enhanced magmatic and volcanic activity and wide development of hydrothermal processes. The submarine environments that dominated in the region during the early Alpine cycle (middle Jurassic – late Cretaceous) were conducive to the formation and preservation of volcanic-hosted mineral deposits.

At first, in the Jurassic time, epigenetic volcanogenic copper and barite-polymetallic deposits were formed (Alaverdi, Shamlug, Kafan, Akhtala) which were followed in the early Cretaceous by the Tekhut-type porphyry copper deposits. All the above deposits are located within the Armenian part of the Lesser Caucasus. In the activated deep restricted volcano-depressions epigenetic copper, gold-bearing and barite-polymetallic deposits of the Bolnisi-type (Georgia) were formed. To the west, in the Eastern Pontides, in the late Cretaceous intra-ark basins are developed volcanic- and sediment-hosted copper-zinc ores of the Chayeli-type as well as the large-scale epigenetic mineralization (Murgul and some others).

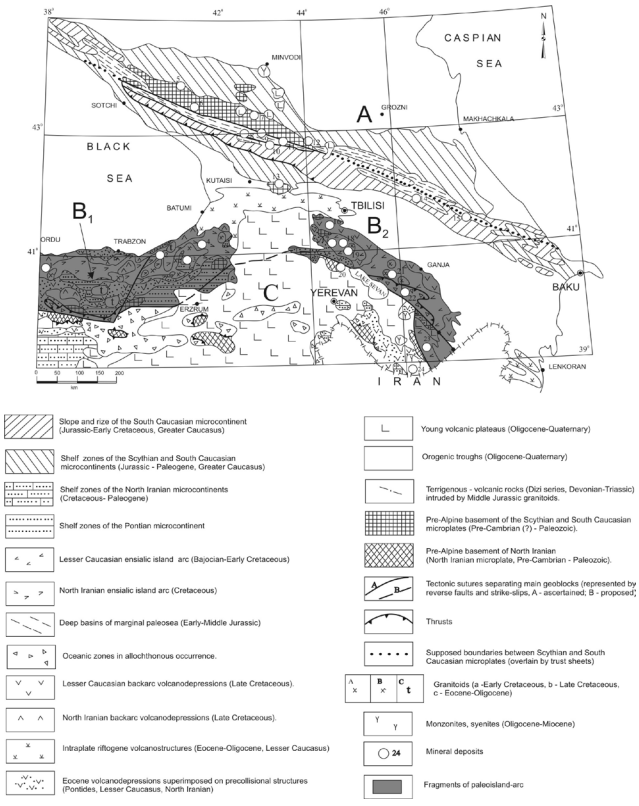

Figure 1. Distribution of main metal-bearing deposits within the geological structures of eastern Turkey and the Caucasus.

Main metal-bearing deposits of the Eurasian active paleomargin: 1. Aşikoy (Cu); 2. Lachanos (Cu, Zn, Pb); 3. Chayeli – Madenkoy (Cu, Zn); 4. Murgul (Cu, Zn); 5. Urup (Cu); 6. Kti-Teberda (W); 7. Tirni-Auz (W); 8. Lukhra (Au); 9. Tsana (As, Au); 10. Luchumi(As); 11. Zopkhito (Au,Sb); 12. Sadon (Pb, Zn); 13. Chiatura (Mn); 14. Filizcay (Zn,Pb,Cu); 15. Kizil-Dere (Cu); 16. Madneuli (Cu,Zn, Pb, $BaSO_4$); 17. Alaverdi (Cu); 18. Shamlug (Cu); 19. Tekhut (Cu); 20. Megradzor (Au); 21. Dashkesan (Fe, Co); 22. Zot (Au); 23. Kafan (Cu); 24. Kadjaran (Mo, Cu). Microplates: Eurasian paleocontinent: A – Scythian, B – Pontian – South Caucasian (B_1 – Eastern Pontides, B_2 – South Caucasus); Afro-Arabian paleocontinent: C- North Iranian

The deposits reveal distinct relationships with the specific lithogeodynamic complexes of paleoislandarc constructions. Some of them (for example, some deposits in Turkey) create integral spatial-temporal associations with

enclosing volcanites; the others were formed somewhat later than the enclosing rocks, but the time of their formation remained within the limits of the formation of volcanic-host complexes.

It is generally known that the majority of ore deposits are located within the uppermost 10 km-thick layer of the earth's crust, the highest position (0-1 km) being occupied by the deposits of non-ferrous and noble metals that are the subject of the present paper. As examples we consider some deposits in the eastern Pontides (Turkey), the Bolnisi (Georgia) and Alaverdi (Armenia) mining districts, and also a porphyry copper deposit of Tekhut (Armenia) located within an uplifted block adjacent to the Alaverdi group of volcanogenic deposits.

2. Ore Deposits of the Eastern Pontides (Turkey)

During the last decades it has been established that the volcano-plutonic activity in the Eastern Pontides (Turkey), which developed during the Alpine cycle as a typical island arc, resulted in the formation of significant volcanogenic and plutonic economic concentrations of non-ferrous metals. The volcanogenic deposits were formed within volcanodepressions which in Cenomanian-Campanian time represented parts of interarc marine basins, whereas the plutonic copper-molybdenporphyric deposits were related to the emplacement of granitoids into uplifted blocks. Important economic deposits here are Ashikoy, Lahanos, Chayeli, Kuttular, Murgul, Cerat Tepe and Guzeliayla (Cu, Mo) (Figure 2). It should be noted that the Eastern Pontides is the only region in the Pontian-South Caucasian paleoisland arc where hydrothermal-sedimentary deposits of non-ferrous ores, such as Chayeli and Ashikoy, have been discovered. The Chayeli deposit (Figure 3), known as a pearl of the Pontides, is distinguished by a very large accumulation of non-ferrous metals with estimated resources of 15.9 million tons of ore averaging 4.4% Cu, 6.1% Zn, 0.8 g/t Au and 4.4g/t Ag. Mining in the deposit commenced in 1994. Massive sulfide ore (VMS) form a body 920 m long along the strike; the body is traced at a depth of 650 m and is still open at depth and along strike. The maximum thickness of the ore-body attains 100m.

Just as in other deposits of the Kuroko type, the Chayeli orebody is overlain by a thin (0.5 to 2 m) layer of jasper-like quartzite which is, in turn, overlain by a sequence of tuffites and basaltic flows. Overlying the basalts are green tuffs interbedded with dolomites that contain fragments of foraminifera fossils.

The orebody is divided, as is proposed by Turkish geologists, by a syn-ore fault into two parts forming two overlapping "lenses". The orebody itself consists of massive sulfides, mainly brecciated, and of subordinate gangue minerals – barite, dolomite, quartz, sericite and kaolinite. Sulfides are represented by pyrite, chalcopyrite and sphalerite with lesser amounts of galena, bornite and tetrahedrite. As in other Kuroko-type deposits, massive sulfide ores are of two types – yellow ores enriched in pyrite and chalcopyrite and black ores enriched in sphalerite. Sphalerite content in the matrix of brecciated black ores exceeds 10%.

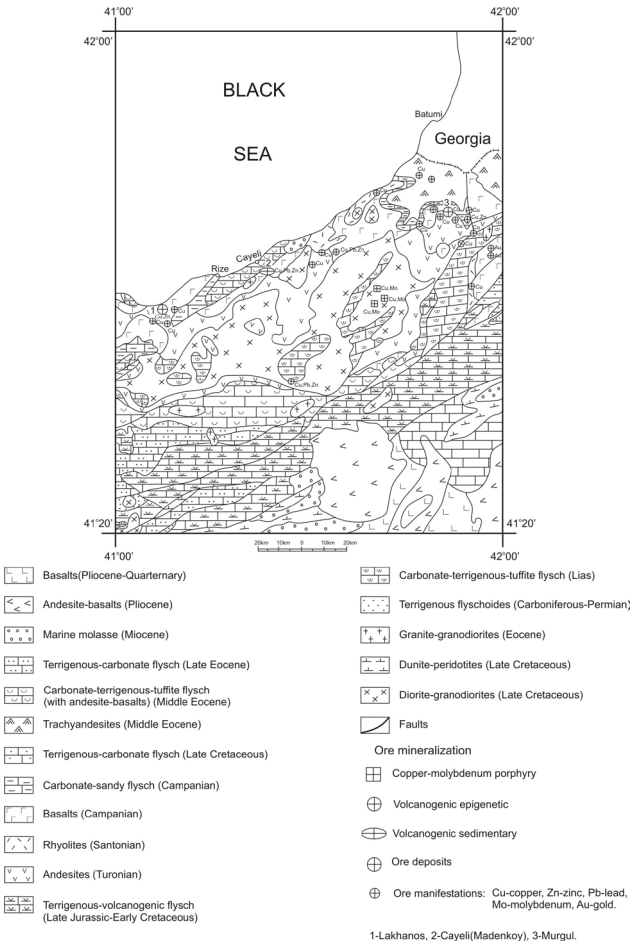

Figure 2. Schematic geological map of the uppermost eastern part of the Pontides (Turkey) showing mineralization. Materials used: 1) Geological map of Turkey on a 1:2 000000 scale (1989); 2) Geological map of Turkey on a 1:500 000 scale (2002).

Below the body of massive ores, veinlet-disseminated mineralization is developed. The hydrothermal-sedimentary system which preserved in Late Cretaceous volcanites in the form of orebody, underwent repeated process of brecciation under the influence of explosive (phreatic) activity associated with the functioning of hydrotherms. Clastic ores are dominant in the upper horizons of the deposit. Massive yellow ores and their powder varieties form the lower parts of the orebody and are most typical

of the thickest parts of the deposit. Massive ores overlie hyaloclastites that consist mainly of fragments of felsites and are intensely altered by the processes of pyritization and kaolinitization. Hyaloclastites are underlain by felsites with rare porphyric phenocrysts of quartz and feldspar. All the above rocks are superimposed by a quartz-pyrite-chalcopyrite stockwork.

Another type of hydrothermal-sedimentary mineralization was found in the allochthone that was removed into the paleoislandarc structure from the marginal sea basin of the Paleotethys. Rocks that form the allochthone are known in literature under the term of "Kure complex". The complex, aged as Triassic (?), is composed of ultrabasic tectonic slices, interbedded silicaclastic sediments and basaltic flows. According to reference [7] mineralization pattern and geological setting here are similar to those observed on the island of Cyprus – at the base of the section occur serpentinous peridotites that are successively overlain by gabbro, a diabase dyke complex, and green-stone-altered basaltic pillow-lavas. The section is terminated with a sequence of clays and shales. Copper-bearing massive sulfide mineralization is concentrated in pillow-lavas overlapped by the shale sequence. These data are in accordance with the reference [8] who attributes pyritic deposits ennobled with copper to the Cyprus-type volcanogenic massive sulfide (VMS) deposits. Other functioning ore deposits of the Pontides are characterized by epigenetic sphalerite-chalcopyrite specialization.

In the works of Turkish and West European geologists there is information about the composition and structure of volcanogenic formations that host non-ferrous metal deposits of the Eastern Pontides [9]. The basement for Cretaceous rocks that contain ore deposits is composed of andesitic volcanic rocks and terrigenous complexes of Early-Middle Jurassic age [10], and also of Late Jurassic – Cretaceous formations with insignificant copper and gold mineralization (Figure 2). In the 1960-ies among Cretaceous volcanites 4 series were distinguished: upper dacitic, upper basaltic, lower dacitic, and lower basaltic. Later ore-bearing Upper Cretaceous sediments were grouped into two series [9]: upper, represented by basalts intercalated with red limestones and purple tuffs, and lower made up of dacitic tuff-breccias and sandy tuffites. The deposits were formed after the eruption of dacitic series or at the beginning of functioning of volcanoes that produced basic lavas (upper series). Structurally, the region of copper mineralization is represented by a system of horsts and grabens that are bounded by faults of NE and NW directions. The age of the dacitic series defined by microfaunal data is Senonian, while the age of large granite-granodiorite-diorite intrusions by the data of radiometric measurements is about 30 mil. years (Late Oligocene-Miocene) [9]. Between the upper and lower series there is an unconformity registered by all investigators.

According to reference [9], basalts of the upper series are represented by plateau basalts sometimes showing pillow structure. Volcanic rocks of both series are deformed into folds whose axes trend into NE-SW and NW-SE directions, the first trend being older.

The rocks of dacitic series show widespread alterations of propylitization type; within the areas of development of quartz-sericite metasomatites the sulfide veinlet-dispersed mineralizetion type is also observed. Massive hydrothermal-sedimentary deposits are hosted in dacitic tuffs and tuffites and overlain by purple tuffs. In the lower levels of the basaltic series there are concordant lenses of massive ores of limited extension, and gypsum horizons. The marginal zones of the ore deposit of Chayeli are characterized by the presence of manganese minerals.

According to some researchers [11], bimodal volcanites which host VMS deposits are associated with large calderas and siliceous domes. VMS mineralization is developed at the ore deposits of Murgul, Cerattepe, Kutluler, Kotarakdere, Hrsit and Lahanos.

The study of published and unpublished (manuscript) materials shows that massive ores of non-ferrous metals in the Pontides were formed on the sea-floor of deep marine basins and, prior to diagenetic changes of sediments, ore deposits represented the so-called "ore hills". The marine basins were, most likely, of intra-arc origin in Cretaceous that is confirmed by the composition of volcanites and the presence of basaltic dykes that cut both the ore deposit and upper basalts and purple tuffs. The rocks that cover the ore deposit of Chayeli are practically unaltered, not counting diagenetic changes.

The clastic ores of Chayeli are characterized by well-expressed bedding. The ores are represented by angular or semi-rounded fragments of sulfides–sphalerite, pyrite and chalcopyrite. Most likely that the "clastic ores" formed as a result of the disintegration of "sedimentary" varieties and their re-deposition on the slope and the foot of the ore hill (like submarine colluvium).

At our disposal there are two analyses of sulfur isotopes (chalcopyrite +3.1 and sphalerite +4.8) defined in laboratory of the U.S. Geological Survey (Denver, Colorado). We can propose that sulfur from sulfides was derived from a biogenic source. At the deposit of Chayeli quartz-sulfidic veins (Figure 3) that served as ways for ascending hydrothermal fluids are devoid of any appreciable amount of gaseous-fluidal inclusions. The fact probably indicates the considerable depths of the sea during the period of the ore-formation.

The massive ores are, as a rule, gold-bearing; gold is found in sulfides as grains measuring 200 μ. The ores often show not clearly-expressed vertical zonality (from top to bottom): sphalerite-galena-barite-pyrite-chalcopyrite; pyrite-chalcopyrite; pyrite-chalcopyrite-clays; pyrite-chalcopyrite-quartz. The size of pyrite crystals increases with depth. The thickness of clastic ores in Chayeli increases to the south where probably was located the paleoslope of the ore hill. Here stockworks are absent beneath the sedimentary ores, whereas to the north, beneath the yellow ores, occurs veinlet-dispersed mineralization which is of economic significance.

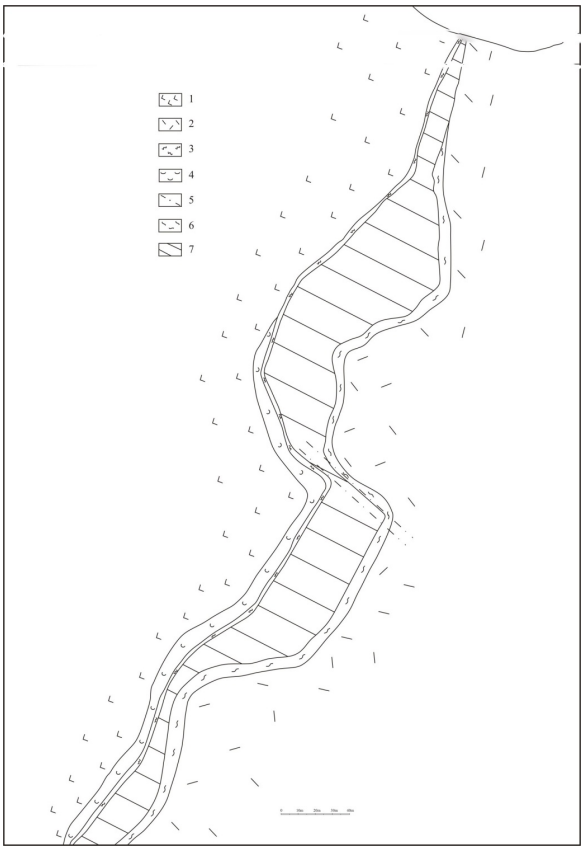

Figure 3. Section through the ore body of the Chaeli deposit (Madenkoy, Turkey).

Late Cretaceous: 1-basalt lavas; 2- rhyodacites; 3-jasper quartzite; 4-tuffite; 5- synvolcanic faults; 6- hyaloclastites; 7 - ore body of chalcopyrite-pyrite-sphalerite composition (copper > 5%, zinc - 9%). (Graphics courtesy of Turkish geologists working at the Madenkoy mine.

It has been revealed that in the Kure region (North Turkey), at the Ashikoy deposit [12] (Figure 4), basalts of the ophiolitic complex should be attributed, by their chemical parameters, to volcanites of sea-floor spreading zones. It is assumed that in Early Jurassic the spreading axis was located in a back-arc basin.

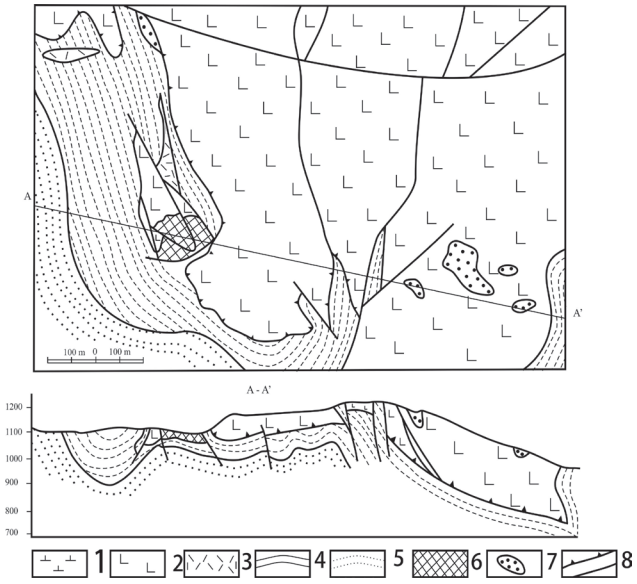

Figure 4. Diagram of the geological structure of the Ashikey deposit (Turkey Geological Survey, 1966)

1. Ultrabasic rocks (in allochthonous occurrence); 2. greenstone altered basalt; 3. dacite; 4. shale; 5. intercalation of sandstones and shales; 6. massive fine-grained pyrite-chalcopyrite ores; 7. iron "hats"; 8. faults: a-thrusts, b-near-vertical.

The examples of stockwork-vein deposits within the Eastern Pontides that have strong similarities with copper ore deposits in Madneuli (Georgia) are Lahanos and Murgul hosted by Late Cretaceous volcanites (Figure 5). At Lahanos, the stockwork of sphalerite-pyrite-chalcopyrite composition occupies a dacitic stock. Here, the veinlet-disseminated mineralization is concentrated within the area of quartz-sericite-chlorite metasomatites. Similar geological conditions are observed in the Murgul deposit. Here, the stockwork of pyrite-chalcopyritic ores is limited from the top by quartz-ferruginous (jasperous) rocks on the level of which gypsum lenses were located. Orehosting dacitic lavas are eroded and overlain uncomformably by Campanian-Maastrichtian volcanites. Not far from Murgul (Figure 5), at a site of Kizilkajia [13] occur hydrothermal-sedimentary deposits of "black" and "yellow" ores with characteristic banding and framboidal texture. Here also, ore-containing rocks are overlain uncomformably by unaltered andesite-dacitic lava flows.

Finally, it should be noted that in the Eastern Pontides there are known gold prospects proper, for example Behcecik [14] and Maradit [10] associated with Late Cretaceous volcanites and Eocene quartz diorites. The economic significance of these prospects is still to be studied and evaluated.

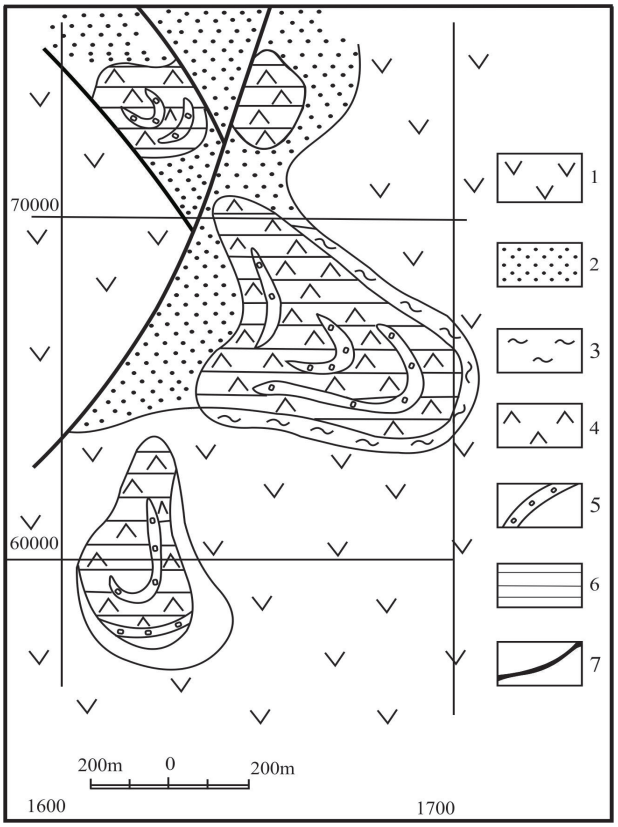

Figure 5. Schematic plan of the geological structure of the Murgul deposit (data of the Geological Survey of Turkey, Ankara, 1994).

Late Senonian (Campanian-Maastrichtian) rocks: 1. andesites and dacites; 2. mudstones, sandstones, tuffites, unconformably overlapping mineralized blocks; Early Senonian (Santonian) ore-bearing rocks: 3. siliceous-ferruginous sediments; 4. lavas of dacites and their pyroclastolites (within mineralized blocks brecciated and experienced quartz-sericite-chlorite alteration); 5. gypsum lenses; 6-stockwork-disseminated pyrite-chalcopyrite-sphalerite ores; 7. faults.

3. Ore Deposits of the Bolnisi Mining District (Georgia)

The Cretaceous volcano-tectonic depression of the Bolnisi ore district was formed in a back-arc residual sea basin environment at the end of the convergence phase, and took its final configuration at the beginning of the collision between the South Caucasus and Iranian lithospheric microplates. The depression is filled with Cretaceous volcanogenic-terrigenous rocks within which we distinguish three complexes (Figure 6). The lower, pre-collisional (Early Cretaceous -Turonian), one is composed of submarine terrigenous-volcanogenic rocks, with rare andesitic flows and marly limestones at the bottom. Within this complex there are necks of volcanoes (mainly of fissure-type) that host dioritic bodies. Majority of vents outpouring subaerial silicious volcanites were located at the intersections of earlier sublatitudinal faults with later NE – SW trending ones. The eruption of ignimbrites and felsic lavas was followed by the subsidence of the volcanic dome-shaped swellings formed as a result of squeezing of rhyodacitic extrusions on the slopes of large volcanic edifices. The areas of acidic and intermediate extrusive rocks are characterized by the development of volcanic cones (Figure 7 and 8), various collapse calderas (David Gareji), lava domes (Darbazi, Mushevani). Earlier works [15] suggest that ore-bearing volcanites on the FMA plot show two independent "differentiation" trends located within the calc-alkaline field. Some rocks are normal alkaline and aluminous andesites, others are rhyodacites. The latter are characterized by the increasing content of K_2O relatively to Na_2O, when passing from earlier differentiates to later ones.

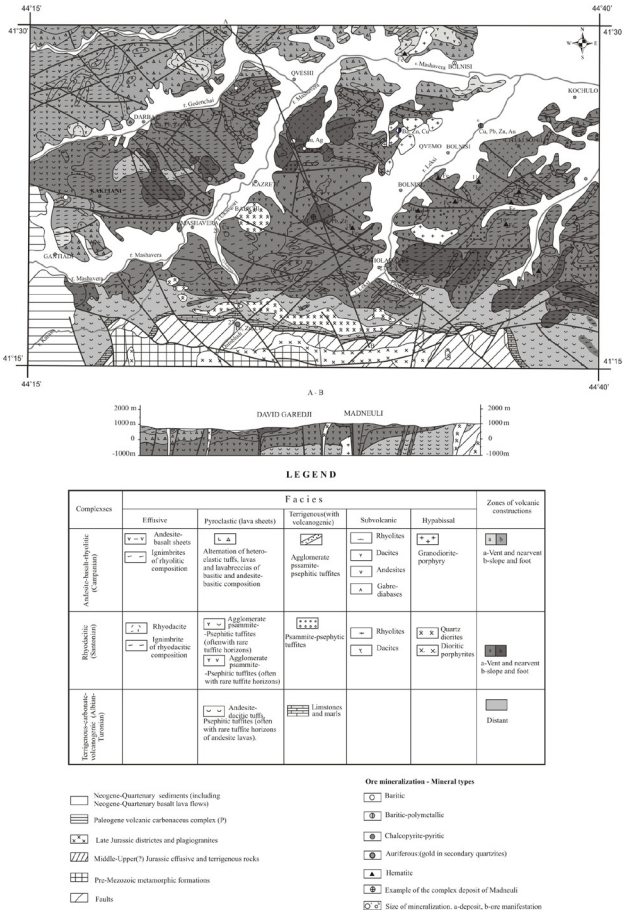

Figure 6. Paleovolcanological map of the Bolnisi district with ore deposits.

List of deposits and ore manifestations: 1. Bektakari - Zn, Pb, Au ore manifestation; 2. Ratevani - Fe ore manifestation; 3. Musafriani - Ba ore manifestation; 4. Darbazi - Zn, Pb, Au,

Cu ore manifestation; 5. Kvemo-Bolnisi – Cu, Ba, Zn, Pb deposit; 6. Tsiteli Sofeli - Cu, Au deposit; 7. David Gareji - Ba, Zn, Pb, Ag, Au deposit; 8. Mushevani - Ba, Zn, Pb, Cu ore manifestation; 9. Abulmulk (Sakdrisi) - Au, Cu deposit; 10. Guzalchai - Fe ore manifestation; 11. Shulaveri - Fe ore manifestatio; 12. Bolidari - Fe ore manifestation; 13. Kakliani - Ba, Zn, Pb, Cu ore manifestation; 14. Sarkineti - Fe ore manifestation; 15. Tashkesani - Fe ore manifestation; 16. Darklisi - Fe ore manifestation; 17. Madneuli - Cu, Au, Ba, Zn, Pb deposit; 18. Demursu - Fe ore manifestation; 19. Sangari - Fe ore manifestation; 20. Balichi - Cu, Zn ore manifestation; 21. Samtsverisi - Cu ore manifestation; 22. Kudroi - Fe ore manifestation; 23. Dambludi - Zn, Pb, Cu, Au deposit.

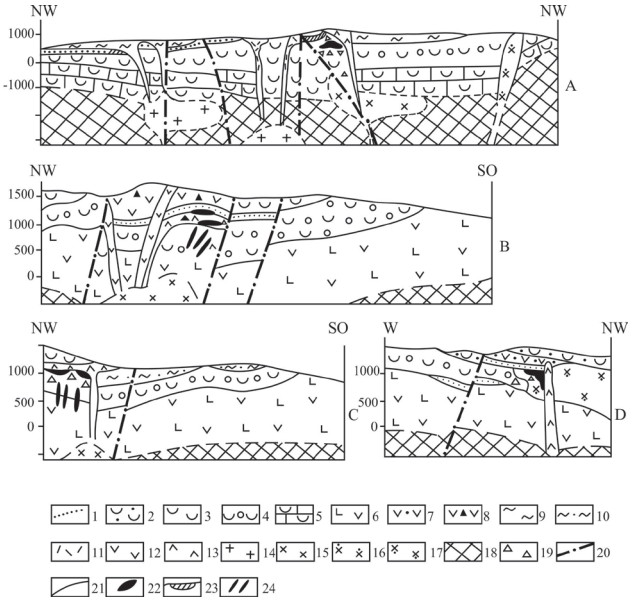

Figure 7. Fragments of the Lesser Caucasus ore-bearing volcano structures.

A - Late Cretaceous residual volcano-depression (Madneuli and David-Gareji deposits); B, C, D - Middle-Late Jurassic intra-arc volcanic depression (B - Alaverdi, C - Shamlug , D - Kafan deposits).

1. Carbonate-sandy thin horizons; 2. Late Jurassic volcanogenic-terrigenous flysch; 3. Late Cretaceous andesite-dacite lavas, psammo-psephitic tuffs and tuffites; 4. Late Cretaceous (a) and Middle Jurassic (b, c, d) agglomerate (to block) tuffs, tuffites and lavas of andesite-dacites; 5. Early Cretaceous tuffites, limestones, sandstones, lavas of andesite-dacites and andesite-basalts; 6.Early Bajocian lavas and lavobreccias of andesite-basalts and basalts, tuffites; 7-Middle Jurassic andesite lavas; 8-Bathonian lavas and lavas of andesite-basalts; 9.Late Cretaceous ignimbrites; 10. Middle Jurassic hyaloclastites; 11. Late Cretaceous rhyolites; 12. Middle Jurassic andesite-dacites; 13. Dacites and rhyodacites; 14. Late Cretaceous potassium-sodium granodiorites and granites; 15. Sodium granodiorites; 16. Late Cretaceous quartz diorites; 17. Middle Jurassic quartz diorite porphyrites; 18. pre-Mesozoic foundation; 19. explosive breccias; 20. faults; 21. assumed boundaries of geological bodies; 22. copper ore bodies (stockworks and brecciated stock-like bodies); 23. barite deposits; 24. copper ore vein-like bodies.

The middle (Coniacian-Santonian) complex is mainly of rhyo-dacitic composition and hosts mineralization; it was formed as a result of functioning, in subaerial conditions, of at least 5 volcanoes of central type. Lithologically it is composed of volcanogenous rocks characteristic of near-vent zones (breccia ignimbrites, coarse-grained tuffs, explosive breccias showing ore mineralization, extrusive and lava domes) and zones of volcanoes' slopes and basement (mainly dacite-rhyolite tuffs, lahars, ignimbrites, rhyolitic lavas). Characteristic features of this complex are parasitic lava domes squeezed on the slopes of some volcanoes, beneath which ore concentrations are often observed.

The uppermost volcanic complex was most likely formed at the end of the Cretaceous and is represented by contrast basalt-andesite-rhyolitic volcanites. Within this complex, relics of three central type volcanoes can be recognized. To this complex belong, as comagmates, granodiorites and granodiorite-porphyries occupying the central part of the base of the volcanodepression and being responsible, in our opinion, for copper-gold mineralization in the region. In the largest Madneuli deposit (where originally were mined only baritic ores, and now copper and gold-bearing ores are being extracted as well) coexists copper, barite-polymetallic and gold (in secondary quartzites) mineralization of differrent age. The following ore specialization is observed within smaller deposits: copper and gold – in Tsitelsopeli, gold and barite-polymetallic – in Sakdrisi, and barite, barite-polymetallic and silver-gold – in David-Gareji. The example of the Madneuli deposit shows that the process of ore accumulation was preceded by the formation of a metasomatic column the upper part of which is enriched in monoquartzite-solfataric material, lower part – in quartz-cericite metasomatites, and the flanks and deepest horizons – in propylites. In Madneuli, beneath the screen produced by the lava domes, two distinct levels of mineralizetion are distinguished: the upper one – barite and barite-polymetallic, and the lower – copper pyrite. The upper and, partly, the lower horizon host bodies of auriferous quarzites.

In the deposits of the Bolnisi ore district, the Georgian geologists have fulfilled extensive thermobarogeochemical and isotope-geochemical investigations. Earlier studies

[16,15] indicate that two-phased gaseous-fluidal inclusions in quartz from copper pyrite ores become homogenous at the temperature of 320-370°C, in quartz from copper-zinc ores – at 280-300 °C, and in the barite from barite-polymetallic ores – at 120°C.

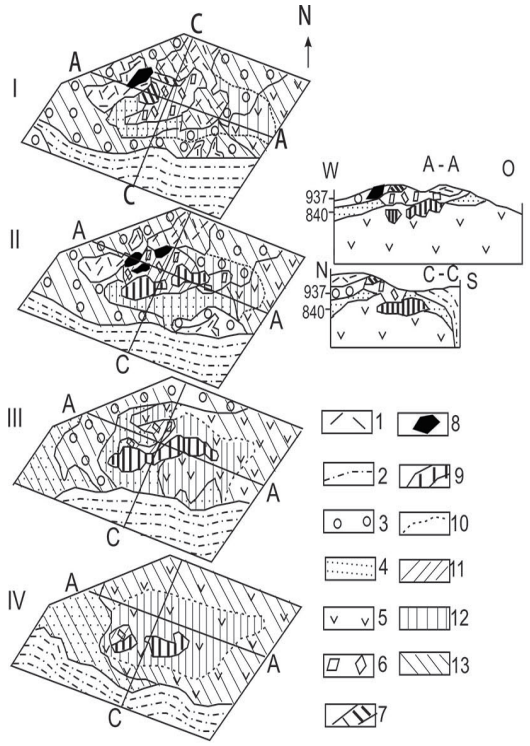

Figure 8. Distribution scheme of ores and metasomatites at different levels at the Madneuli deposit (Compiled by the authors, 1986).

1. Rhyodacites; 2. lava breccias and rhyolite lavas; 3. vitroclastic tuffs; 4. intercalation of mixed-clastic tuffites; 5. xenotuffs; 6. explosive breccia. Ore bodies: 7. barite; 8. barite-polymetallic; 9. copper; 10. boundaries of metasomatites; 11. secondary quartzite; 12. quartz-sericite-chlorite metasomatites; 13. propillites. I-Projection of the surface of the deposit before the opening of the quarry; II-projection of the open pit surface (as of 1.01.1985); III-cut 937m; IU-cut 840m.

The solutions were chloride-sulphate K-Na ones containing nitrogen and CO_2. They contain also insignificant amount of heavy hydrocarbons and methane (less than 4% mol.)

The following data have been obtained concerning the sulphur isotope composition: the average figures of $\delta^{34}S$ from sulphides only slightly deviate from standard meteoric values; in most cases values of $\delta^{34}S$ range from +10 to +20‰. The isotope composition data on carbon, oxygen and hydrogen are ambiguous and may be interpreted in favour of the participation in ore-forming process both meteoric and "magmatogenic" waters. The values of $\delta^{13}C$ from calcite and fluidal inclusions are around – 7.1±2.1‰ and +0.3±1.6‰, respectively; the hydrogen isotope composition (δD of water) from present-day waters of the region – from –50 to –70‰; $\delta^{18}O$ of quartz from copper ores ranges from +10.35 to +9.25‰, whereas $\delta^{18}O$ of barite from barite-polymetallic ores is within –1.07 and –1.53‰.

It should be also noted that economically significant volcanogenic deposits in the Bolnisi district are located in the upper parts of blocks made up of effusive-sedimentary rocks of the Turonian-Santonian age where the latter are cut by extrusive and lava domes. The blocks are bounded by NW- and NE- trending faults that serve as magma and ore-channelways. Extrusions and lava domes within the Madneuli deposit were squeezed out along fault systems which collectively form a ring structure. As a result of the hydrothermal "collapse", under the cover of rhyodacitic lavas there were formed explosive breccias which experienced transformation into "secondary" quartz-hydromica metasomatites and propylites. It is noteworthy that the process of propylitization also affected unaltered tuffites with distinctly expressed traces of their original bedding. Tectonic contacts between propylitically altered tuffites and explosive, intensively silicified and sulphide-impregnated, breccias are exposed in the eastern part of the quarry (horizon 957 m).

Our field works have confirmed that the Madneuli volcanic dome is located on the slope of the Dalidag paleovolcano composed of andesite-dacitic pyroclastolites, ignimbrites and rhyodacitic flows. In the vicinities of Madneuli some other ore-bearing volcanostructures are known: (1) David –Gareji caldera-type barite-polymetallic, within which mineralizationis related to lacustrine sediments is overlain by ignimbrites, and (2) Sakdrisi gold-bearing, represented by a steeply-dipping NE-trending fault along which rhyodacites and tuffites are turned into secondary quartzites. Economic significance of the Sakdrisi deposit has been revealed lately as a result of prospecting works (21 tons of gold, with average gold content 2-3 g/t). At present, within the Madneuli deposit relatively poor veinlet-disseminated ores are exploited.

At our disposal there are data on the isotopic composition of strontium and concentration of rubidium and strontium in rocks occurring in the vicinities of volcanogenic ore deposits [17]. According to these data, basalts of the Bolnisi mining district ($^{87}Sr/^{86}Sr$-0.704910) might have been products of the differentiation of the undepleted mantle whereas rhyolites of Murgul (Turkey) might be derived from the bottom of the earth's crust ($^{87}Sr/^{86}Sr$-0.707739) and rhyolites from the Madneuli deposit – from the upper part of the earth crust ($^{87}Sr/^{86}Sr$-0.7100269). The upper-crust source of magmas that produced rhyolites and

ignimbrites is also substantiated by the specific europium ratios Eu/Eu* characteristic of these rocks (0.65 – 0.68 for rhyolites and 0.52 – 0.58 for ignimbrites), and also by their enrichment in light REE and large-ionic lithophilic elements (K, Rb, Ba, Sr) (Table 1) [18].

It seems relevant here to adduce geochemical data on ore-hosting rocks at the Rapu-Rapu deposit in Philippines [19]. (Sherlock et al., 2003). Massive sulfide ores of the Rapu-Rapu deposit are spatially associated with dacites that underwent greenstone alterations. By its characteristics, this deposit can be attributed to Kuroko-type VMS deposit. The geological section of the Jurassic ore-hosting sequence contains, apart from ore-bearing dacites, mafic and quarts-feldspar sedimentary layers. The dacites by their geochemical parameters are similar to dacitic rocks developed in the back-arc Sumisu basin; the basic rocks are characterized by low concentrations of TiO_2 (≤0.9%) and Zr (40-50ppm), low ratio Zr/Y (2.5-3.0) and slight enrichment in REE. These rocks are typical representatives of island arc tholeiites and can be compared with Miocene andesite-basalts of the Kuroko deposit and Oligocene basalts of the Fiji arc. Some authors [19] propose that volcanogenic rocks of the Rapu-Rapu deposit enriched in REE were formed at the stage of the active riftogenesis of an oceanic island arc or a Jurassic back-arc basin. It is noteworthy that in the Philippine Islands there is another deposit (Canatuan) that was formed within the immature arc environment that is evidenced by the abrubt decrease of REE concentrations in both acid and basic rocks. Our data (Table 1) show that values of Zr/Y are somewhat higher (9.5-11.2 for dacites, 2.7-6.2 for rhyolites and 3.7-4.1 for basalts) that are characteristic of more matured paleoisland arc.

4. Ore Deposits of the Alaverdi Mining District (Armenia)

In the Alaverdi district (Figure 9), copper-bearing stockwork ore bodies are concentrated in Upper Bajocian aleurolite-sandstone horizons, and vertically-dipping vein-shaped bodies – in rhyodacitic hyaloclastites and andesite-basaltic effusions of Early Bajocian age. Vein bodies are marked by narrow zones of quartz-sericite-chlorite metasomatites. Besides the Alaverdi volcanogenic ore deposits (Figure 10 and 11), the authors also examined the nearby Tekhut copper-porphyry deposit. The Tekhut deposit is located within a Shnokh-Kokhb tonalite intrusion whose age is defined as Late Jyrassic-Early Cretaceous. Within the Somkhito-Karabakh zone, besides the Shnokh-Kokhb intrusion, there are a number of smaller intrusive bodies (Tsakhkashat, Dashkesan, Kedabek, Tsav) associated with magmatic porphyric bodies and insignificant porphyry copper bodies. K-Ar dating of the phaneritic intrusions gives a Neocomian age of 133±8 m.y. [20]. Phaneritic magmatic rocks as well as porphyric bodies show essentially sodic and high-aluminous character that attributes them to the group of tonalities [15]. V. Jaroshevich who studied gaseous-fluidal inclusions [21] suggests that fluids from which the precipitation of ore material took place were high-salinity chloride-sodic-potassic (50-20 wt % NaCl equivalent). According to this author, the formation of minerals occurred at temperatures of 400-220°C and pressure perhaps more than 100 bars. Sulfidic sulfur from the Tekhut deposit is characterized by the insignificant dispersion of $\delta^{34}S$ and approach the meteoric standard. The isotopic composition of oxygen from water ranges between +3.0 and -4.1‰ that may indicate some dilution

Table 1. Chemical analyses of magmatic rocks of Bolnisi ore district (TiO_2 - wt %, rare elements - ppm)

Sample №	1-99	2-99	12-99	32-99	7-99	8-99	14-99	15-99	18-99	22-99
Rock	Rhyolites				Basalts		Andesite-basalts		Dacites	
TiO_2	0.63	0.53	0.44	0.40	1.13	0.99	1.00	1.01	0.23	0.22
Y	44	49	52	58	36	34	141	145	35	33
Zr	224	190	226	222	90	82	388	383	56	57
La	17.97	14.12	19.11	26.71	18.50	19.04	43.42	46.54	8.72	8.59
Ce	38.45	31.20	39.79	57.25	40.06	39.34	88.68	92.61	15.47	15.29
Pr	4.54	4.03	5.19	7.01	5.30	5.04	10.01	11.02	1.80	1.89
Nd	17.86	11.75	18.61	28.31	18.63	14.87	37.19	40.65	5.91	6.79
S m	4. 19	3.46	4.97	5.58	4.34	4.05	8.20	7.00	1.42	1.55
Eu	1.01	0.87	1.32	1.35	1.43	1.39	1.62	1.74	0.42	0.41
Gd	3.64	3.99	5.39	4.66	4.14	3.96	5.72	6.32	1.01	1.06
Dy	3.57	4.12	6.24	3.96	3.63	3.52	4.81	5.02	0.92	0.98
Er	2.47	2.52	4.19	4.39	2.02	2.11	2.91	2.95	0.62	0.56
Yb	2.33	2.19	4.40	2.31	1.71	1.59	2.32	2.38	0.41	0.42
Lu	0.37	0.34	0.66	0.36	0.28	0.24	0.35	0.36	0.07	0.08
La_n/Yb_n	5.2	4.6	2.9	7.8	7.5	7.6	12.7	13.6	14	13.5
La_n/Sm_n	2.7	2.5	2.3	2.9	2.7	2.9	3.3	4.1	3.5	3.3
Zr/Y	5	4.3	3.8	2.7	4.1	3.7	10.7	10.9	11.2	9.5

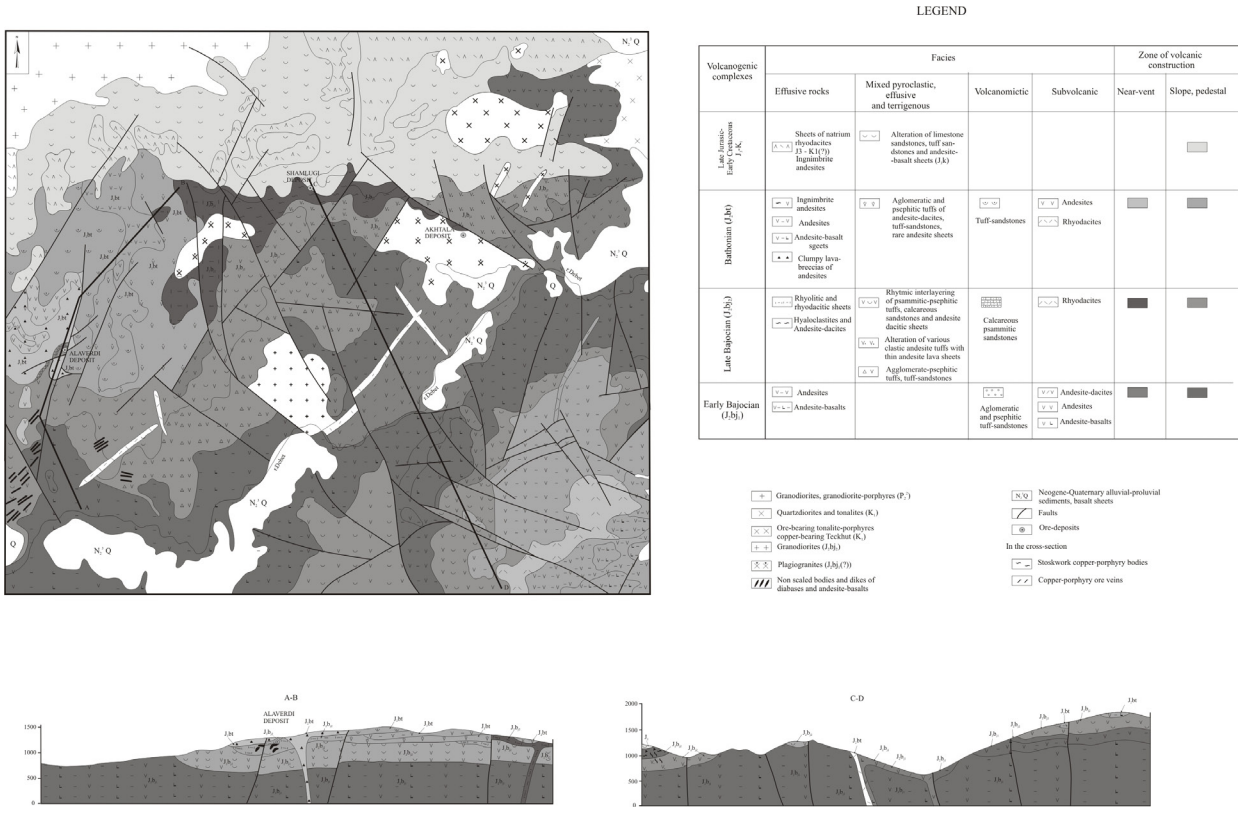

Figure 9. Paleovolcanological map with ore deposits of the Alaverdi district (Armenia).

of magmatic fluids by meteoric waters. The copper porphyry mineralization here is associated with stockworks and dykes of quartz-dioritic porphyries that are developed in the south-western apical part of the Shnokh-Kokhb massif. The contacts of porphyry bodies with the intrusive massif underwent intensive metasomatic reworking – the monoquartz "core" is replaced by quartz-feldspathic metasomatites and quartz-sericite-anhydrite metasomatites.

The Alaverdi ore-bearing region occupying the southwesternmost part of the Somkhito-Kafan tectonic unit – a fragment of a paleoislandarc structure – is composed, in its central part, mainly of Bajocian-Bathonian and Upper Jurassic-Lower Cretaceous volcanic complexes. The paleovolcanological map on a 1:25 000 scale, compiled by the authors shows that the Alaverdi volcanostructure was formed as a result of at least three strong phases of volcanic activity (Figure 7B). At first, in early Bajocian, volcanoes of fissure type were functioning, outpouring lavas of andesite-basaltic and, to somewhat lesser degree, basaltic composition. In our opinion, these lavas are pre-subduction formations generated during the divergent stage between the South Caucasian and North Iranian lithospheric microplates. In late Bajocian, within the areas of previous outpouring, two volcanodepressions formed which were subsequently filled with andesite-dacitic lavas, their pyroclasts and breccias and, at the later stage of functioning of volcanoes of central type, with rhyodacites and their pyroclasts and hyaloclastites. In the most eroded parts of the volcanic necks there are outcrops of the Akhpata plagiogranitic and Akhtala granodiorite-porphyritic intrusions. The latest phase of Middle Jurassic volcanism occurred, most likely, in the Bathonian. In the western part of the Alaverdi ore field are developed volcanites characteristic of the neck and proximal volcanic facies of a local volcano represented by very coarse breccias and agglomerates of andesite-basalts. As the volcano rose, these volcanites experienced intensive erosion, that resulted in the appearance of the stratified colluviums on its eastern slope. It is noteworthy that on the AFM diagram [15] the trend of "differentiation" of the Upper Bajocian volcanites occupies the transitional zone between the tholeitic field and calc-alkaline strip, while the trends of later Middle Jurassic volcanites are localized within the calc-alkaline strip. In the study region four groups of endogenic deposits are identified according to general geological considerations. It is thought that the earliest of them are barite-polymetallic ores located in the apical part of the Akhtala intrusion. The Alaverdi and Shamlug copper deposits (Figure 10 and 11) was formed, most likely, in Late Bajocian-Bathonian, while the Shamlug deposit– in Late Jurassic, because here massive porphyry copper stocks are overlapped by Upper Jurassic rhyodacites. The latest mineralization of the

subduction stage of the development of the paleoislandarc system is the above-mentioned Tekhut porphyry copper deposit which reveals the paragenetic relationship with the Lower Cretaceous tholeitic complex.

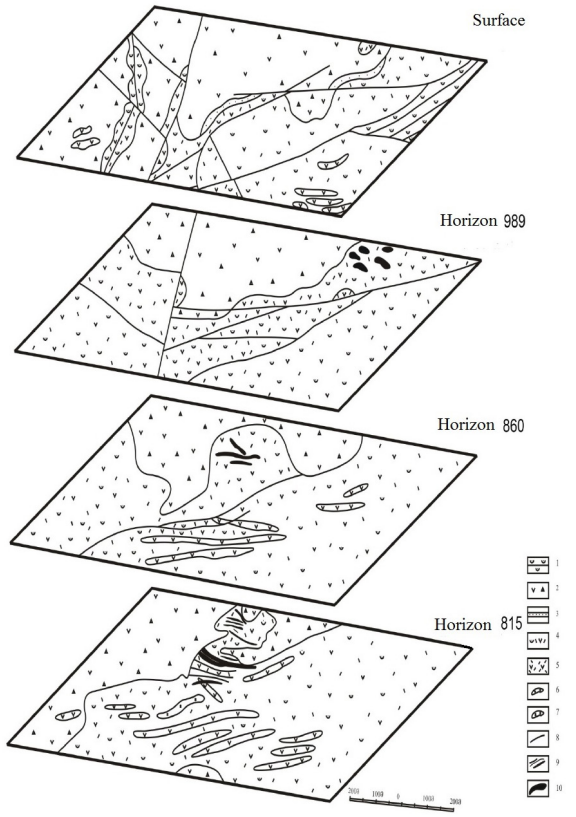

Figure 10. Horizontal sections of the Alaverdi deposit.

GPS Coordinates: 44 ° 65 'E, 41 ° 13' N. 1. Tuff sandstone (Bahtonian); 2. andesite tuffs and andesite-basalts (Bahtonian); 3. calcareous tuffaceous sandstones (Bajocian); 4. rough rhythmic interbedding of calcareous tuffaceous sandstones, tuffs and nappes of andesite-dacites and dacites (Bajocian); 5. dacite stocks; 6. andesites; 7. plagioclase porphyry; 8. faults; 9. ore-bearing veins (quartz-pyrite-chalcopyrite; 10 . ore-bearing stocks (massive and stockwork ores of pyrite-chalcopyrite composition).

The available data (the temperature of homogeneity of gaseous-fluidal inclusions in ore-containing quartz) [15,16] indicate that the Alaverdi deposit was formed at the temperatures 205-280°C, the Shamlug deposit – at 185-270 °C, and the Akhtala deposit – at 170±20°C. The gases that have been identified in inclusions are represented by N_2, CO_2 and minor amount of H_2O. The water extractions from gaseous-fluidal inclusions in ores of the Kafan deposit (which is an analog with the Alaverdi deposit) contain high concentrations of SO_4^{2-}, Ca and Na. Besides, the water extractions also contain, along with common cations (K, Na, Ca, Mg), considerable concentrations of heavy metals. In the deposits of the Alaverdi ore district, isotopic composition of oxygen in quartz from copper deposits proved to be equal to +10,3±0.5‰. Hydrogen of the water from fluidal inclusions (the Alaverdi deposit) is characterrized by values of δD equal to -75±0.5‰.

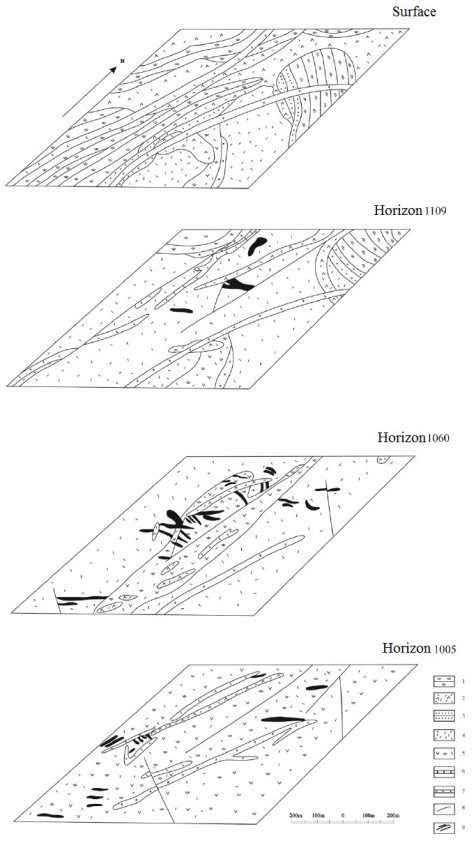

Figure 11. Horizontal sections of the Shamlug deposit.

1. Calcareous tuffaceous sandstones (Callovian); 2. rhyodacites and rhyolites (Callovian); 3. calcareous tuffaceous sandstones (upper Bajocian); 4. dacites and rhyodacites (Bajocian); 5. calcareous tuffaceous sandstone, andesite-dacite (Bajocian); 6. granodiorite-porphyry (Lower Jurassic); 7. diabase (Lower Jurassic (?); 8. tectonic faults; 9. Ore bodies (quartz-pyrite-chalcopyrite composition).

The authors possess new figures on the isotopic ratios of sulfur from sulfides and oxygen from quartz of the rocks of the Bolnisi and Alaverdi mining districts (see Table 2 and 3) (analyses were carried out by our co-author at the USGS laboratory in Denver).

In the laboratory of USGS were also determined the temperatures of homogenization of gaseous-fluidal inclusions in quartz from epigenetic deposits of the Lesser Caucasus. These temperature proved to be: for the Madneuli copper ores – 315-325°C, for the polysulfidic de-

posit of Akhtala (Armenia) – 245-250°C, and for the porphyry copper deposit of Tekhut (Armenia) - 325-330°C. The isotopic ratios of oxygen in quartz from copper ores of Madneuli, Tekhut and Shaumian (see Table 3) may evidence in favour of the participation of magmatic waters in the process of ore-formation [22]. At the epigenetic deposits of the Lesser Caucasian paleoislandarc, isotopic ratios of sulfur from sulfides are somewhat ambigupus but the authors assume that majority of sulfur had a magmatic source. It should be noted that these data are generally in compliance with the results of thermobarogeochemical investigations carried out earlier in the Caucasian institute of Mineral Resources (the results are given above).

Table 2. Isotopic ratios of sulfur from sulfides

№	Sample description	δ34S b‰
1	Madneuli 9, PY	3.3
2	Madneuli 9, PY	3.6
3	Madneuli 32, PY	-1.2
4	Madneuli 32, PY	-1.3
5	Madneuli 33, CPY	-1.4
6	Madneuli 35, CPY	2.5
7	Madneuli 40, PY	2.2
8	Madneuli 40, PY	3.3
9	Madneuli 41, PY	2.7
10	Alaverdi 1, CPY	2.6
11	Shamlug 2, CPY	0.9
12	Shamlug 3, CPY	0.3
13	Tekhut 9, CPY	1.4

Table 3. Isotopic ratios of oxygen from quartz

№	Sample description	δ18O ‰
1	Madneuli- 32, copper-pyrite-chalcopyritic ore	9.1
2	Madneuli- 33, copper-pyrite-chalcopyritic ore	8.1
3	Madneuli- 34, copper-pyrite-chalcopyritic ore	9.0
4	Madneuli- 35, copper-pyrite-chalcopyritic ore	9.2
5	Madneuli- 33, copper-pyrite-chalcopyritic ore	11.4
6	Tekhut – 9, copper-porphyry ore	10.05

5. Geological-genetic Model of Volcanogenic Deposits of Non-ferrous Metals of Paleoisland Arc Systems

Volcanogenic deposits are concentrated largely within complexes that were formed in the process of interaction of oceanic and continental lithospheric plates. Commonly, this interaction occurs along the active continental margins (subduction zones) where the oceanic crust plunges beneath the continental plate. Active continental margins at various stages of their geologic history underwent disintegration and now represent "pilings" of microplates and blocks. As far back as in the 1980s, some authors [23-26], distinguished blocks of the earth's crust that corresponded to fragments of both active and passive continental margins. Amongst these fragments there are complexes hosting various kinds of ore mineralization. In our case, we deal with Alpine fragments of the Pontian-Lesser Caucasian paleoisland arc which is distinguished by the presence of both vocanogenic-sedimentary and epithermal (epigenetic) ore deposits known in literature as the Kuroko-type deposits [27].

The ore-forming process is identified with the evolution of a high-energy geological system practically open for its moveable components [28]. As makroelements of the dissipative fluidal systems may be present: (1) areas of the formation of fluids (this point is however disputable [29]); (2) ways of fluid migration; (3) areas of discharge with structural (physical) and geochemical barriers where ore accumulation takes place. In the present work, we propose a mental-logical model of the evolution of ore-generating systems and, in the first place, that part of the latter that is responsible for the precipitation and preservation of ore material. In the model we distinguish those signs and factors that are necessary and sufficient for the functioning of ore-generating processes. For substantiating proposed inferences, besides general geological data, we have presented results of thermobarogeochemical studies and data on isotopic correlations of main ore-forming elements. It is noteworthy that the genetic model should be regarded as a certain abstraction in which the main significance is attached not to the outer resemblance between individuals (ore deposits, ore bodies) but to the standardization of processes proceeding within a system.

It should be noted once more that data on isotopic ratios of strontium and consentrations of rubidium indicate that basalts and dacites developed near the volcanogenic deposits represent products of the "differentiation" of undepleted mantle whereas magmas giving birth to rhyolites of the Madneuli and Murgul deposits had most likely their source in the base of the earth's crust.

According to geophysical data [30], the roots of magmatic bodies beneath island arcs with mature sialic crust are usually located at depths of 60 km. Since these depths correspond to the very bottom of the crust, many authors [30-32] assume the relationship between the magmas of orogenic series and the partial melting of amphibolites.

Usually, beneath (Madneuli) or above (Chayeli) volcanic domes there are evidences of intensive activity of heated fluids – hydrothermally-altered rocks and various kinds of ore accumulations. The idea about the magmatic source of fluids of volcanogenic deposits has lost,

during the last two decades, its attractiveness because of the difficulties related to the necessity of explanation of participation of very large volumes of water in the hydrothermal process. The mechanism of separation of fluids is considered a relatively short-term process. Its "traces" in magmatic bodies are expressed by autometasomatic alterations, and uniform distribution of submicroscopic particles of oxides and sulfides in the crystals of silicates or in the groundmass of rock-forming minerals. Results of isotopic-geochemical studies of volcanogenic deposits give evidence of a significant role of meteoric waters in hydrosystems [33]. Experimental works also indicate the insignificant amount of magmatic waters in the hydrosystems, not exceeding 0.0005% of the total mass of water [34].

It is widely known that there is a correlation between ore components and their concentration in ore-containing rocks [35,36]. Moreover, the hydrothermally-altered rocks are characterized by the deficiency of metals in the direct closeness to ore accumulations. Experimental works on the extraction of elements from rocks [34,37] under the P-T-conditions corresponding to the functionning of fluids also confirm the supposition that ore-containing magmatic and sedimentary sequences may be regarded as a possible source of metals. Hydrothermal solutions with ore elements are similar by their salinity to sea water, but at the same time, they are enriched, at several orders, with Fe, Ag, Pb, Cu and Zn in comparison with the sea water [38]. The initial redistribution and exsolution of ore components are realated to the conditions of crystallization of magmatic rocks characterized by a certain component composition. Some authors [39] identified, in the basalts of mid-oceanic ridges and, earlier, in the siliceous rocks, spherical aggregates of oxidic-ore material of liquational nature. In ore-bearing subalkaline effusive rocks of rift valleys of midoceanic ridges were also found sulfides impregnated in form of small "drops" in clinopyroxene and feldspar [40]. In these ore liquates were identified nickel pyrrhotite, sphalerite, chalcopyrite, silver, albite and potassium feldspar.

The further way of migration of ore elements in volcanic environments is conditioned by the involvement of sea and ground (meteoric) waters in the convective flow, in connection with the decreasing of their density due to the heat produced by cooling intrusions [41]. The resulting aggressive heated waters acquire properties and composition characteristic of ore-bearing fluids interacting with surrounding intrusive rocks and volcanites.

According to vast material collected on the base of studying the world ocean [42-44], the large-scale ore-genesis is successively realized in the process of: (1) crystallization of magmas; (2) interaction between "aggressive" meteoric waters and surrounding volcanites; (3) stable functioning of physical-chemical barriers in areas of discharge of hydrotherms (whether it be the sea floor or the ground surface).

Volcanogenic deposits of non-ferrous metals are characterized by the following features: (1) Both sedimentary-hydrothermal and veinlet-impregnated deposits are related to volcanodepressions. The former are usually located in the axial zones of the depressions whereas the latter occur in their peripheral parts being controlled by extrusive domes.

(2) The component composition of ores reveals dependence on petrochemical pecurialites of ore-bearing volcanites and their comagmatites. Potassium-sodic rhyodacites are usually associated with barite-polymetallic mineralization, whereas andesite-basalts and sodic rhyolites are largely accompanied by the copper-zinc mineralization [45].

(3) The scope of economic mineralization depends on the capacity of ore-bearing depresssions (and the volume of volcanites filling them) and on the content of metals in the volcanites [15].

(4) Within the ore knots, ways of migration of fluids are marked by the traces of hydrothermal alterations. Zones of down-going flows are distinguished by argillization of rocks (the presence of hydromica-montmorillonitic and chlorite-montmorillonitic neomineralization minerals); above-intrusion and flank parts of the depressions are intensly propylitized. At barite-sulfidic near-surface and shallow deposits the up-going branches of therms (the discharge zones) are marked by explosive breccias in which hydrothermal alterations are represented by secondary quartzites and quartz-adular-sericite (hydromica) metasomatites. The host rocks of veinlet-impregnated copper and copper-zinc ores, as well as the volcanites underlying hydrothermal-sedimentary mineralization are transformed, by the up-going branches, into quartz-chlorite (with sericite) metasomatites often containing anhydrite and gypsum.

Recently experimental works (5-29 days of duration) reconstructed conditions under which the formation of hydrothermally-altered rocks occurred as a result of interaction of sea waters with felsic magmatites [46]. The latter lost their K and Na and instead became enriched in Mg and Ca. The process leads to the formation of smectites, and from the hydrotherms enriched in rock components emanate barite, anhydrite and gypsum.

(5) Barite-sulfidic ores usually hosted in secondary quartzites (Madneuli) are characterized by a not-very-distinct zonality of minerals: barite-sulfidic and baritic (in vein zones) associations are replaced downwards by sphalerite-galena-chalcopyritic ones. It is noteworthy that the veinlet- impregnated bodies are confined from the top

by a screen (effusives, subvolcanic gently-dipping bodies), and from the bottom – by gypsum zones and jaspery quartzites, and small bodies of fine-grained pyrite and, less frequently, chalcopyrite [15]. Stockworks of copper-pyritic and zinc ores contain, in their upper parts, schlieren infilled with druses of quartz, pyrite, chalcopyrite, and also, probably hypergene bornite and covellite. Above the copper mineralization, besides gypsum-anhydritic lenses, there are also, not unfrequently, quartz-hematite concentrations. The described pattern of copper-zinc veinlet-impregnated mineralizetion is also valid for hydrothermal-sedimentary mineralization of the Kuroko-type (e. g., Chayeli in Turkey). This circumstance was underlined by T. Matsukama and E. Khorikosi [47] as far back as 1973.

(6) Fluids responsible for volcanogenic deposits were subacid chloro-sodic low-salinity solutions [27,33,48]. Our data indicate solution salinity equal to 1.5-3.5 wt% NaCl equiv., taking into account the melting of frozen gaseous-fluidal inclusions [49]. Low-salinity fluids are also characteristic of the recent accumulation of sulfides in the world ocean [50,51]. However, in some sites of sulfide formation, brines with salinity up to 30 wt.% NaCl eq. (at temperatures 200-400°C) have been discovered [51]. Data obtained from the Lesser Caucasian deposits do not contradict these figures [15,52].

B.W.D. Yardley [53] summarized information on crustal fluids pointing out that temperature was one of the main factors influencing on the concentration of metals in solution. Such metals as Fe, Mn, Zn and Pb are in solutions, most likely, in form of chloridic complexes. For example, in case of Zn, this metal is represented chiefly by $ZnCl_3^-$ and $ZnCl_4^{2-}$ [54]. The concentration of above metals also increases with increased content of chlorides. Metals, most probably, are concentrated in brines of evaporitic sequences where Pb-Zn deposits of the Missisipi-type have been formed.

Maximum temperatures of ore-accumulation seem to be comparable with temperature of boiling up the solutions [27]. Within the areas of recent volcanic activity, the lower boundary of boiling the solution with generation of water steam, under the temperature more than 270°C, lies at depths of 300-400 m [33]. The material from the Lesser Caucasus shows that maximum temperatures of homogenization of fluidal inclusions at copper deposits are 410-390°C, and at barite-sulfidic deposits ~280°C [21]. According to our data (Table 4) maximum pressure of fluids in epigenetic deposits reached 150-200 bars, and the formation of minerals took place at depths of 400-600 m from the surface. In case of trapping gaseous-fluidal inclusions under temperature of 320°C minimum pressure may be perhaps about 80 bars; however, under greater temperature about 350°C pressures could reach 500 bars (but no higher). (Figures obtained from the water-NaCl system liquid-vapor curve on the P-T plot) [49].

(7) Available data on isotopic composition of hydrogen and oxygen of fluidal inclusions in quartz, barite and calcite from barite-polymetallic ores were earlier interpreted in favour of the significant participation of meteoric waters in the ore-generating process. As for copper ores [27,21,45], here meteoric waters might have played an inferior role as compared with magmatic waters. Our new results on oxygen isotopy, obtained, as was mentioned above in the laboratory of USGS in Denver, also do not condradict to these data.

(8) Data on the isotopic composition of sulfur in sulfides and sulfates are, as was mentionned above, somewhat ambigious: S in sulfides is close to meteoritic standards whereas sulfur in sulfates is increased in density at 14±3‰ [21]. As an example of hydrothermal-sedimentary barite-sulfide deposit where sulfur in sulfides is characterized by lesser density ($\delta^{34}D$= -2÷-11‰, unpublished data by V. Buadze) it may be adduced the deposit of Wed Al Kebir in Algeria.

(9) At the majority of hydrothermal-sedimentary deposits, the boiling up of fluids did not take place at all, or might happen possibly before thermae's outflow on the sea floor thus favouring the formation of ore-conveying systems. The most conducive conditions for the stable accumulation of hydrothermal-sedimentary ores were on the sea bottom, at depths of 2-3 km [55,56]. Lesser depths are not completely forbidding, taking into consideration physical-chemical peculiarities of ore-forming minerals, but they are not altogether conducive to stable proceeding of ore-forming processes because of the upwelling and high-energy conditions characteristic of shelf and transitional zones.

We assume that the onset of functioning of hydrosystems within the volcanic complexes was preceded by the following succession of events: deposition of terrigenous-volcanogenic sediments in the local depressions of sea basins (backarc or/and intraarc); intensification of volcanic activity giving rise to the formation of andesite-dacitic and rhyolitic complexes; final stage of volcanism with outflow of andesite-basalts and subordinate sodic rhyolites. After some attenuation of volcanic activity (that was reflected by partial washout of previously formed volcanites and deposition of tuffites) there was an emplacement of intrusions that cooled and crystallized at depths of about 2 km from day-surface, perhaps even deeper. It should be noted that hydrothermal-sedimentary ores were formed after the accumulation of andesite-dacite-rhyolitic complexes (ore-concentrations at the Kuroko-

type deposits are usually localized on rhyodacitic domes). Mineral zonality observed in hydrothermal-sedimentary deposits may be explained by the re-distribution of ore-forming components as a result of the destruction of "hills" and their diffusion from lower levels to upper ones in the process of leaching of ores by fluids [57,58]. An example of this may serve a recent ore-bearing structure in the Pacific ocean, on the Explorer ridge, where high-temperature sulfides underlie beds of relatively low-temperature sulfides of Fe and Mn, barites and silica. According to [59] who proposed a thermodynamic model, the anhydrite-pyritic mineralization is in due course replaced by a later silica-sulfidic substance. The emergence of anhydrite in "ore hills" is explained by the involvement of sea waters in the discharge zones. The sea waters are heated and as a result anhydrite is precipitated from them [60].

Unfortunately, as was mentioned above, we did not succeed in studying of gaseous-fluidal inclusions at the Chayeli deposit. For that reason, we use published data on deposits that are typical representatives of the Kuroko-type one of which is a hydrothermal-sedimentary deposit in the Kermadek island arc [61]. Thermobarogeochemical investigations of gaseous-fluidal inclusions showed that the salinity of hydrothermal solutions ranged between 1.75-3.9 wt % NaCl-equiv., and temperatures of homogenization – between 175-322°C. Two-phased inclusions are predominant, although rare monophased aqueous inclusions are also found. The average salinity is approaching the standard salinity of sea water (3.2wt % NaCl equiv.). Here, there are no any signs of boiling, such as the co-existence of inclusions enriched in gas and in liquid under the equal values of T_h. It should be also noted that the method of gaseous chromatography allowed identifying in massive sulfides the following volatiles: H_2O (99.8-99.98 mol %), CO_2 (0.03-0.17 mol %), N_2 (0.004-0.023 mol %) and CH_4 (0.002-0.026 mol %). It is assumed [61] that part of methane might be of abiogenic origin. Thus, numerous examples of deposits, both hydrothermal and epigenetic types, confirm an earlier idea [48] about the standardpattern of PT – conditions of ore accumulation at volcanogenic deposits.

For the deposits of the Madneuli type which were formed after the squeezing of rhyodacitic domes (baritic and barite-polymetallic bodies) and later, as a result of the emplacement of porphyry granodiorites (stockwork dissemination copper mineralization), the way of their generation was somewhat different. Before the beginning of intensive volcanic activity that gave rise to processes of ore-formation, there existed vast territories with subaerial conditions, and within the volcanodepressions artesian basins with buried sea waters were developed. The paleodepressions were bounded by blocks of hydrogeological massifs.

As a result of the emplacement of rhyodacites and eruption of felsic lavas and ignimbrites, the meteoric ground waters became overheated and saturated with volatile magma components that finally led to catastrophic blasts and explosions and formation of explosive breccias beneath the impermeable screen. Two hydrochemical zones were formed within the depressions: the upper one - sulfate-ammonium and the lower one – chloride-sodic [15]. The boundary between these zones is marked by gypsum-anhydrite concentrations, jasper-like quartzites and iron sulfides. In our opinion, the presence of hydrochemical zonality was promoted: (1) at first, by the boiling up of the solution at a temperature more than 350°C [62] and at shallow depths, with the differentiation into fluidal and gaseous phases (with separation of sulfides, quartz, carbonate and, locally, adular); (2) later, by the efflux of volatiles (H_2S, SO_2, HCl, CO_2, NH_4, etc.) into the near-surface zone and their oxidation; (3) by the boiling up of the solution retaining part of soluble acidic components, hydrogen sulfide in the first place.

It should be noted that the destabilization of the solution in the sea-bottom conditions related to the drop of temperature and its oxidation may be a cause for the mass precipitation of ore matter. Since "black smokers" are commonly made up of pyrite, pyrrhotite and sphalerite suspensions, it is very likely that copper- and zinc-containing solutions might have transported metals in form of hydrosulfidic complexes. The enrichment of hydrotherms within the volcanodepressions was probably realized in the process of degasation of a shallow-occuring magmatic body (intrusions that are often observed beneath ore bodies). According to experimental works [48], among gases at temperatures below 600°C a dominant one is hydrogen sulfide, and at higher temperatures – sulfurous gas. The latter in mixture with a fluid at temperature 500-600°C is capable of producing hydrogen sulfide and sulfuric acid.

Levels of mineral generation in epigenetic deposits are generally compared with zones of "black smokers" whose bordering anomalous physical-chemical parameters cause a synchronous crystallization of anhydrite and iron sulfides. These conditions correspond to zones of hydrotherms with minimum activity of PO_2 coinciding with the lower boundary of the field of barite stability under equal activities of H_2S-SO_4^{2-} [27].

At the barite-sulfidic deposits, the zonal distribution of metals is conditioned by the following factors: (1) different stability of complex compounds [27,48]; (2) greater dependence of the solubility of copper minerals on temperature as compared with that of sphalerite and galena

[27]; (3) dependence of precipitation of metals on the concentration of S^{2-}. Under the equal concentrations of metals in solution, precipitation of copper and zinc demands higher concentrations of H_2S than it needs for lead [63]; (4) functioning of a H_2S – barrier efficiency of which is determined by low concentrations of S^{2-} [64].

It can be supposed that in the zones of discharge of fluids, ΣS proves to be sufficient for the precipitation of copper, whereas lead, zinc and silver reveal a trend of passing through the hydrogen sulfide barrier. The excessive ion-settler plays a role of a solvent-complexgenerator.

It seems possible that in polyformational deposits of the Madneuli-type, the origin of quartz veinlets coincides in time with that of the explosive breccias and the arising of the above-mentioned hydrochemical zonality within volcanostructures. Precipitation of gold, quartz and sulfides can be regarded as an one-act process related to the destabilization of magmatic fluids. This process proceeded within the medium characterized by high oxidizing potential, corresponding to the level of formation of secondary quartzites.

Basing on physical-chemical studies [65] points out that low-salinity magmatic waters are capable of transporting gold under high temperature regime. One of the main requirements is the presence of a sufficient quantity of H_2S that plays the role of a bisulfide complex. Under high pressure, vaporized magmatic fluids pass into liquid form, without heterogenous phase transition. These fluids are responsible for significant potassium and propylitic alterations of rocks hosting epithermal mineralization. In his paper, Ch. Heinrich considers Au-Cu porphyry deposits; however, in our opinion, the results of this work may be used for gold-bearing deposits of the Madneuli-type as well. In spite of the fact that fluids producing low-sulfide Au-bearing epithermal deposits contain considerable portion of meteoric water, their gold "reserves" have been formed, mainly, at the expense of metal dissolved in an insignificant part of vapor-condensed fluids of magmatic origin.

In conclusion, it should be once more underlined that hydrothermal-sedimentary deposits of "ore-hill" type obtain their zonality in the process of recrystallization, solution and redeposition of ore material. Usually, the stifling of the sulfide-forming process takes place where the therms reach zones with high partial oxygen pressure – outside depressions and above ore-concentrations where precipitation of oxides of Fe and Mn and formation of jasper in supra-ore horizons occurs.

Some authors [45] explain the formation of large mass of sulfide deposits by better, providing of hydrotherms with water in submarine environments as compared with epigenetic deposits. We think that the mechanism of ore-formation on the sea floor – frequently-repeated supply of ore matter – was decisive under the generation of volcanogenic massive sulfide deposits (VMS).

6. Conclusions

The above material allows to draw a conclusion that most ore deposits in paleoisland arc environments, and in the Pontian-Lesser Caucasian arc in particular, can be expected within and around volcanic vents or on the slopes of large volcanoes located in volcanodepressions and, also, in silicious parts of volcanogenic-sedimentary sequences or directly above the latter (as in case of hydrothermal-sedimentary deposits). As a rule, ore accumulations are overlain by basic volcanites, but there may be exceptions, e.g. the Madneuli deposit. In the flank zones of ore bodies and, often, in their hanging walls, concentrations of gypsum are commonly found. Mineral composition of ores is practically identical in all copper deposits, also with the exception of Madneuli, where one volcanostructure hosts an association of gold, barite-sulfidic and copper ores belonging to various stages of the ore-formation.

Of a particular interest is the composition of ore-containing sequences in the region: a) in the Alaverdi district ore-containing Middle Jurassic unit is represented by thin chemogenic-sedimentary rocks, hyaloclastites, accumulations of submarine colluviums, tephroidal turbidites, andesitic and dacitic lavas; the ore-containing sequence is overlain by the Upper Jurassic complex represented by andesite-basaltic flows alterating with carbonate clastic tuffites; b) in the Bolnisi district, the ore-containing stratified sequences (tuffites with rare dacitic flows, and crater-lacustrine deposits) are overlain by subaerial ignimbrites and rhyodacitic lavas; c) the Chayeli volcanostructure containing hydrothermal-sedimentary ores is composed of supra-ore basalts (pillow lavas) alternating with limestones and "purple" tuffs, and also with propylitized dacites. The latter are overlain by massive sulfidic ores (VMS) in the lower part of which quartz-chlorite-hydromicaceous metasomatites host veinlet-impregnated copper ores. According to Turkish geologist, the volcanostructure represents a large caldera located on the floor of a deep-marine basin.

The Lesser Caucasian deposits by their genesis are undoubtedly epigenetic: in the Alaverdi district, veinlet-impregneited and vein mineralization is superimposed on hyaloclastites and tuffites; in Bolnisi, mainly veinlet-impregnated copper mineralization is developed in silicified tuffites; besides, gold and barite-sulfide mineralization in veins and shallow-dipping sills is present in second-

ary quartzites. In Chayeli, ores show similarity with "ore hills" in the present-day middle-oceanic ridges and rift zones of marginal seas.

It should be noted that ore bodies in the Alaverdi district are located in narrow zones of quartz-sericite-chlorite metasomatites; in the Bolnisi district, the vertical metasomatic "column" contains in its upper part secondary quartzites (near-surface solfataric alterations), while the lower part shows more high-temperature silicification (quartz-chlorite-sulfidic metasomatites with little sericite). Here ore metasomatites are surrounded by propylites. At the Chayeli-type deposits (Madenkoy), the dacite unit that underlies the hydrothermal-sedimentary mineralization contains, at the background of regional propylitization, veinlet-impregnated "yellow" ores. The latter mark ways of migration of hydrothermal solutions to the paleo-sea floor.

In the Alaverdi district small stocks and thin veins containing copper ores, are predominant; in the Bolnisi district main ore bodies are large copper stockworks; in the Eastern Pontides both stockworks and thick lens-shaped bodies of massive sulfidic ores (VMS) consisting mainly of pyrite, chalcopyrite and sphalerite are present.

Most likely, that these differenences are caused chiefly by different geodynamic regimes dominating in various blocks of the earth crust of the study region. Thermobarogeochemical studies indicate that the principal copper deposits, in spite of the existing differences in the mechanism of ore accumulation, were formed in similar PTX-conditions and, therefore, can be attributed to the same genetical class of volcanogenic ore deposits.

It has been established that depending on the stage of geological investigation, it is necessary to know main parameters characterizing both an ore-magmatic system on the whole and its individual components. The search for hydrothermal-sedimentary ores of non-ferrous metals within the Georgian and Armenian part of the Lesser Caucasian paleoislandarc is condemned to failure due to the absence of "geodynamic basis" for their accumulation. Previously proposed prospecting model had been created for the certain area – the Bolnisi ore district in Georgia. In the proposed model, the main consideration was given to the relationship between the basic parameters of mineralization and dimensions of a volcanodepression [15]. When planning large scale (1:50,000) mapping at the stage of the prognostication works, it is necessary to take into account the results of geophysical and geochemical investigations. Thus, in the Bolnisi district, it has been delimited areas corresponding to source zones (overlying magmatic bodies and defining mineralized blocks). In the gravity field, these areas are expressed as low intensity minimums. As for the geochemical data, they show the aureoles of titanium, zircon, arsenic, zinc, molybdenum, bismuth, copper, manganese, iodine around the copper bodies, Gold-bearing quartzites are marked by aureoles of silver, gold, arsenic, bismuth and iodine.

It is noteworthy, that the prognosis of ore concentrations should be made with due regard for the standard object: morphostructural peculiarities of the upper parts of ore-magmatic paleosystems; degree of differentiation of rhyodaitic magmas; relation between size and structure of ore bodies and dimensions of local volcanostructures; character of pre-ore and syn-ore re-working of rocks; component composition of aureoles.

References

[1] Biju-Duval B., Dercourt J., Le Richon X. 1977. From the Tethys ocean to Mediterranean seas; a plate tectonic model of the evolution of the western Alpine system. Histoire Structural de Bassins Mediterraneens, p.143-164.

[2] Monin A.S., Zonenshain L.P. (eds.). 1987. History of the Ocean Tethys. Institute of Oceanology, 155 p., (in Russian).

[3] Yilmaz Y., Tuysuz O., Genc S., Sengor A.M.C. 1997. Geology and tectonic evolution of the Pontides. In: Robinson A.C. (ed) Regional and petroleum geology of the Black Sea and surrounding region. American Association Petroleum Geologists Memoir, 68, p.183-226.

[4] Okay A.I., Sahinturk, O. 1997. Geology of the Eastern Pontides. In: Robinson A.G. (ed) Regional and petroleum geology of the Black Sea and surrounding region. American Association Petroleum Geologists Memoir, 68, p.291-311.

[5] Yilmaz A., Adamia Sh., Chabukiani A., Chkhotua T., Erdogan K., Tuzcu S., Karabiyikoglu M. 2000. Structural correlation of the Southern Transcaucasus (Georgia) - Eastern Pontides (Turkey). In: Bozkurt E., Winchester L.A , Piper J.D.A (ed). Tectonics and Magmatism in Turkey and the Surrounding Area. Geological Society Special Publication, 173, 17, London, p.185-198.

[6] Dixon, C.J., Pereira, J. 1974. Plate Tectonics and Mineralization in the Tethyan Region. Mineralium Deposita, 9, p.185-198.

[7] Ustaomer T., Robertson A.H.F. 1993. Late Paleozoic-Early Mesozoic marginal basins along the active southern continental margin of Eurasia: evidence from the Central Pontides (Turkey) and adjacent regions. Geological Journal, 120, p.1-20.

[8] Guner M. 1980. Sulphide ores and geology of the

Küre area Pontid in N Turkey. Mineral Research and Exploration Bulletin, p.65-109.

[9] Altun Y. 1977. Geology of the Chayeli-Madenkoy copper-zinc deposit and the problems related to mineralization. Ankara, Mineral Res. Expl. Bull., 89, p.10-24.

[10] Popovic R. 2004. Auriferous mineralization in the Murgul-Artvin-Maradit area (Northeastern Turkey). Mineral Res. Expl . Bull., 129, p.17-29.

[11] Akcay M., Arar M. 1999. Geology, mineralogy and geochemistry of the Chayeli massive sulfide ore deposit, Rize, NE Turkey. In: A. Stanley (ed), Mineral Deposits: Processes to processing, Balkema, Rotterdam, p.459-462.

[12] Chakir Ü. 1995. Geological characteristics of the Ashikoy-Toykondu (Küre-Kastamonu) massive sulfide deposits. Mineral. Res. Expl. Bull., 117, Ankara, p.29-40.

[13] Lethch Graig H.B. 1981. Mineralogy and textures of the Lakhanos and Kizilkaya massive sulphide deposits, Northeastern Turkey, and their similarity to Kuroko ores. Mineral deposita, 16, p. 241-257.

[14] Yigit O., Nelson E.P., Hitzman M.W. 2000. Early Tertiary epithermal gold mineralization, Bahcecik prospect, northeastern Turkey. Mineralium Deposita, 35, p.689-696.

[15] Kekelia S.A., Ambokadze A.H., Ratman I.P. 1993. Volcanogenic deposits of non-ferrous metals of paleoislandarc systems and methods of their prognosis. Metsniereba Publications, 96 p., (in Russian).

[16] Arevadze D.V., 1989. Physical-chemical conditions of endogenic deposits of Transcaucasus. Abstract of doctoral thesis,Tbilisi, Metsniereba, p.54, (in Russian).

[17] Kekelia S., Kekelia M., Otkhmezuri Z., Moon Ch., Ozgür N. 2004. Ore-forming systems in volcanogenic-sedimentary sequences by the example of non-ferrous metal deposits of the Caucasus and Eastern Pontides. Ankara (Turkey), Mineral. Res. Expl. Bull, 129, p.1-16.

[18] Gugushvili V.I., Kekelia M.A., Moon Ch., Natsvlishvili, M. P. 2002. Crustal and Mantle Sources of Cretaceous Volcanism and Sulphide Mineralization in the Bolnisi Mining District. In: Topchishvili M.V. (ed.) Georgian Academy of Sciences, Geological Institute Proceedings, New Series, 117, p.412-419, (in Russian).

[19] Sherlock R.L., Barret T.I., Lewis P.D. 2003. Geological setting of the Rapu Rapu gold-rich volcanogenic massive sulfide deposits, Albay Province, Philippines. Mineralium deposita, 38, p.813-830.

[20] Aslanian A.T., Gulian E.Kh., Pidjian G S., Amirian Sh.S., Faramzian A.S., Ovsesian E.Sh., Arutiunian S.G. 1980. Tekhut copper-molybdenite deposit. Proceedings of the Academy of Sciences of Armenian SSR, Earth Sciences, #5, p.3-24, (in Russian).

[21] Yaroshevich, V.Z. 1985. Genetic features of the deposits of the Caucasus base ore formations according to data of isotopic studies. Abstract of dissertation. Tbilisi, 52 p.

[22] Taylor H.P., jr. 1982. Oxygen and hydrogen isotopes in hydrothermal ore deposits. In: H.L. Barnes(ed.). Geochemistry of hydrothermal ore deposits. Moscow, Mir, p.200-237.

[23] Zonenshain L. P., Kovalev A. A. (ed). 1974. New global tectonics. Moscow, Mir, 471 p., (in Russian).

[24] Mitchel A., Garson M. 1984. Global tectonic position of mineral deposits. Moscow, Mir, 496 p., (in Russian).

[25] Rona P. 1986. Hydrothermal mineralization of spreading areas in the ocean. Moscow, Mir,160 p. (in Russian).

[26] Abramovich I.I., Klushin I.G. 1987. Geodynamics and metallogeny of folded zones. Leningrad, Nauka, 247 p., (in Russian).

[27] Franklin, J.M., Lydon, J.W., Sangster, D.F. 1984. Base metal massive sulfide deposits of volcanogenic affinities. In: Skinner B.S. (ed) Genesis of Ore Deposits 2. Mir Publishers, p.39-252, (in Russian).

[28] Korzhinski D.C. 1982. Theory of metasomatic zonality. Moscow, Nauka, 104 p., (in Russian).

[29] Chukhrov F.V. 1978. Ore material sources of the endogenic deposits. Moscow, Nauka, p.340, (in Russian).

[30] Ringwood A.E. 1981. Composition and petrology of the earth mantle. Moscow, Nedra, 584 p., (in Russian).

[31] Belousov A.F., Krivenko A.P. 1983. Magmatogenesis of volcanic formations. Novosibirsk, Nauka, 167p, (in Russian).

[32] Wyllie P.J. 1983. Petrogenesis and physics of the earth. In the article of Yoder H.S. Evolution of igneus rocks. Moscow, Mir, p.468-503.

[33] Sinyakov V. I. 1986. General ore genesis models for endogenous deposits. Nauka Publications, Novosibirsk, 243 p., (in Russian).

[34] Grinchuk G.D., Borisov M.B., Melnikova G.L. 1984. Thermodynamic model of hydrothermal systems in the oceanic crust: evaluation of solution evolution. Geology of ore deposits, #4, p.3-23, (in Russian).

[35] Baranov A.H., Arkhangelski A.N. 1990. Scientific foundations of geochemical method of prognosis of

concealed sulfur deposits by the dispersion aureoles. In: Ovchinikov A N. (ed) Theory and practice of geochemical exploration in modern conditions. Moscow, "Nauka", p.108-124, (in Russian).

[36] Farfel L.C. 1988. Prognostication of ore deposits. Moscow, Mir. 150 p.

[37] Hodgson C.L., Lyndon S.M. 1977. The geological setting of the volcanogenic massive sulfide deposits and active hydrothermal systems: some implications for explorations. Canadian Mining Metallurgical Bull., v.70, p.95-106.

[38] Mottl M.J., Holland H.D., Corr R.F. 1979. Chemical exchange during hydrothermal alteration of basalts seawater. Experimental results for Fe, Mn and sulfur apecies. Geochim et acta. v43, p.869-884.

[39] Prokoptsev G.N., Prokoptsev N.G. 1990. Formation of metalliferrous hydrotherms at oceanic floor. USSR Academy of Sciences Transactions, Geological Series 4, p.34-44, (in Russian).

[40] Akimtsev V.A., Sharapov V.N. 1993. Ore effusions of the rift valley of the middle-Atlantic ridge. Proceedings of the Academy of Sciences of Russia, 331, #3, p.329-331, (in Russian).

[41] Norton D., Cathhes M. 1982. Thermal aspects of ore-deposition. In: "Geochemistry of hydrothermal ore deposits", Moscow, "Mir", 1982, p.481-496.

[42] Grinberg I.C., Krasnov C.G., Ainimer A.U., Porshina I.M., Stepanova T.V. 1990. Hydrothermal sulfur mineralization in the ocean. Soviet Geology, #12, p.81-91, (in Russian).

[43] Elianova, E.A. 1999. Formation of recent and ancient submarine pyrite ores: composition and structure. In: Popov V.E. (ed) Models of volcanogenic-sedimentary ore formation system. Abstracts of International Conference), St. Petersburg, p.26-27, (in Russian).

[44] Elianova E.A. ,Mirlin E.G. 1990. The oceanic ore-genesis, Soviet Geology, #6, p.47-55, (in Russian).

[45] Krivtsov A.I. 1989. Applied metallogeny. Nedra Publications, p. 288, (in Russian).

[46] Ogawa Y., Shikazono N., Ishiyama D., Sato H., Mizuta T. 2005. An experimental study on felsic rock - artificial seawater interaction: implications for hydrothermal alteration and sulfate formation in the Kuroko mining area of Japan. Mineralium Deposita, 39, p.813-821.

[47] Matsukama T., Khorikosi Ei. 1973. A review of Kuroko deposits in Japan. In: Tatsumi.T. (ed) Volcanism and ore formation. Mir Publishers, p.129-151, (in Russian).

[48] Ovchinnikov L.N. 1988. Formation of ore deposits. Nedra Publications, 255 p., (in Russian).

[49] Shepherd T.J., Rankin A.H., Alderton D.H.M. 1985. A practical guide to fluid inclusion studies. Blaskie, Glasgow and London, 239 p.

[50] Bortnikov N.C., Simonov B.A., Bogdanov I.A. 2004. Fluid inclusions in minerals of modern sulfur constructions: physical-chemical conditions of mineral formations and evolution of fluids. Geology of ore deposits, v. 46, #1, p.74-87, (in Russian).

[51] Bortnikov N.C., Vikentiev I.V. 2005. Modern sulfur polymetallic mineral formation in the world ocean. Geology of ore deposits, v. 47, #1, p.16-50, (in Russian).

[52] Kekelia S.A., Yaroshevich V.Z., Ratman I.P. 1991. Geological and genetic models for Alpine volcanogenic non-ferrous deposits in the Mediterranean Metallogenic Belt. Geology and Geophysics 8, p.71-79, (in Russian).

[53] Yardley Bruce W.D. 2005. Metal Concentrations in Crustal Fluids and their Relationship to Ore Formation. Economic Geology, Vol.100, #4,613 p, (in Russian).

[54] Seward T.M. 1984. The formation of lead (II) chloride complexes to 300^0C: A spectrophotometric study: Geochimica et Cosmoshimica Acta, v.48, p. 121-134, (in Russian).

[55] Stackelberg I., 1985, Van and the shipboard scientific party. Hydrothermal sulfide deposits in back-arc spreading centers in the Southwest Pacific. BGC Circulair, 27, p. 3-14.

[56] Gablina, I.F., Mozgova, N.N., Borodaev, Ju.C., Stepanova, I.V., Cherkashev G.A., Ilijin M.L. 2000. Associations of Cu sulphides in recent oceanic ores of the hydrothermal field Logachev (Mid-Atlantic ridge, 14°45N). Geology of Ore Deposits 42, #4, p.329-349, (in Russian).

[57] Hannigton M.D., Peter J.M., Scott S.D. 1986. Gold in sea-floor polymetallic sulfide deposits. Econ. Geol.,vol. 81, p.1867-1883.

[58] Elianova E.A. 1989. Formation of composition and structure of ores during the modern and old sulfide generation. Soviet Geology. #12, p. 17-26, (in Russian).

[59] Grinchuk G.D. 1999. Model of pyrite ore body formation in submarine hydrothermal system. In: Popov V.E. (ed) Models of volcanogenic-sedimentary ore formation systems. Abstracts of International Conference, St. Petersburg. p.19-21, (in Russian).

[60] Cherkashev, G.A., Zhirnov, E.A., Stepanova T.V., Mozgova N. N. 1999. Zonality and oceanic sulphide structure model (by the data on deep sea drilling). In:

Popov V.E. (ed) Models of volcanogenic-sedimentary ore formation systems. Abstracts of International Conference, St. Petersburg, p.141-142, (in Russian).

[61] de Ronde C.E.J., Faure K., Bray C.J., Chappell D.A., Ian C. Wright I.C. 2003. Hydrothermal fluids associated with seafloor mineralization at two southern Kermadec arc volcanoes, offshore New Zeland. Mineralium Deposita, 38, p.217-233.

[62] Barns H.L. 1982. Solubility of ore minerals. H.L.Barnes (ed.) Geochemistry of Hydrothermal Deposits. Moscow, Nauka, p.176-193, (in Russian).

[63] Ganeev I.G. 1989. Material transportation by hydrothermal solutions. Proceedings of All-union mineralogical society, vol.1, p.3-16, (in Russian).

[64] Kraynov S.P., Matveev L.I., Solomin G.A. 1988. Geochemical conditions of lead and zinc sedimentation from brines in sedimentary basins on a sulfide barries. Geochemistry, 2, p.1708-1719, (in Russian).

[65] Heinrich Ch.A. 2005. The physical evolution of low-salinity magmatic fluids at the porphyry to epithermal transition: a thermodynamic study. Mineralium Deposita, 39, p.864-889.

BILINGUAL PUBLISHING CO.
Pioneer of Global Academics Since 1984

Journal of Geological Research
https://ojs.bilpublishing.com/index.php/jgr-a

ARTICLE

Investigations on River Sediments in Chak Sedimentary Basin, Wardak Province, Afghanistan

Hafizullah Rasouli[1*] Roya Quraishi[2] Kaltoum Belhassan[3]

1. Department of Geology, Geoscience Faculty, Kabul University, Kabul, Jamal Mina 1006, Kabul, Afghanistan
2. Department of Hydrometeorology, Geoscience Faculty, Kabul University, Kabul, Jamal Mina 1006, Kabul, Afghanistan
3. Geology Department, Faculty of Sciences Dhar Mehraz, Fez, Morocco

ARTICLE INFO

Article history
Received: 16 August 2021
Revised: 10 September 2021
Accepted: 14 September 2021
Published Online: 30 September 2021

Keywords:
Minerals
Gravel analysis
Sieving analysis
Sediments
Terraces

ABSTRACT

This sedimentary is from a largest basin of Afghanistan, which covers an area of 9772 km2. It is located about 80 km, at west side of Kabul. In this research, we studied different types of heavy and light minerals, gravel analysis in river sediments. Logar River is core stream flowing over basin, it carries diverse masses of sediments from dissimilar parts of surroding montians. Further, in the months of summer while snowmelting is started, transfer diverse materials and cause different traces to be made. Area of basin is enclosed by mountain range and separated into two sections, majore part is Khawat Olya and second one is Khawat Sufla. The main aim of study is to characterize different sizes and types of minerals in river load for the previous geological periods. This research is therefore essential to explain different sizes and type of minerals in river sediments, which is no any study has been conducted in the study area. This study found out that the category of sediments is related to the parental materials that are placed in the close mountains such as; gneiss, limestone, and granite, dissimilar varities of conglomerate, slate, schist, reefs, conglomerate and sandston.

1. Introduction

As it is clear, we have been suffering from clashes for more than forty years. So, geological researches have not been conducted in this equivalent basin (Chack Basin). Thus, as research in this basin is very important due to its importance and before some researches might be conducted, but were not be like this one. Therefore, we decided to work hard and conduct this geological research. Chak Basin is one of the biggest basins in Afghanistan that has 9772 km^2 area and is surrounded by high mountains ranges. Further, nature of sediments which are in this basin directly related to the parent rocks those are located in the nearby mountains such as gneiss, limestone, granite, conglomerates, slate, schist, reefs and sandstone [1-26].

The Chak Sedimentary Basin is surrounded by Wardak Mountain series, the maximum height reaching 3500 ① m a.s.l, in Daimirdad, Wardak Mountain range, and least height is 2092 m a.s.positioned in Ambokhak village, the

① m a. s. l = meter average sea level

*Corresponding Author:
Hafizullah Rasouli,
Department of Geology, Geoscience Faculty, Kabul University, Kabul, Jamal Mina 1006, Kabul, Afghanistan;
Email: hafizullah.rasouli133@gmail.com; Hafizullahrasouli778@gmail.com

DOI: https://doi.org/10.30564/jgr.v3i4.3574

Paghman Mountains in the direction of the east side of study area. Heights of the central plains range from about 2200 m in the Central Chak Basin and subbasins to 2900 m in the Asiab, Bigsamend, Alisha then Gardan Masjeed subbasins [1]. In Chak Basin the Loger River is the main streams transitory over this basin and via streams from mountain regions transported dissimilar particles and kinds of sediments throughout snow-melting period (from April to June), occasionally during flush floods seasons (May to August) transference altered bulks of sediments and falling by one another creation dissimilar beds and terraces [2]. The forms of sediments is connected to the rocks that are placed and fragmented by unlike types of exogenetic powers in the near mountains and transported by watercourses at the priorer geological stages [3]. Study area strike is similar longitudinal valley and it is parallel with the mountain states [4]. Younger deposits from different parts of this basin based on their depth and arrangement are changed according to the settings, for example, the upper and steep areas of this basin are not very thick and they belong to the Quaternary Period [5], and commonly involves conglomerate but nonetheless the lower basin consisting of young tertiar sediments and normally containing of different clay, silt,sand and gravels.The landforms inside the basin are characteristics of a dry to semiarid, technically dynamic regions [7,6]. In the central plains of the Chak Basin are local depositional centers for sediments resulting from the adjoining surficial deposits and bedrocks outcrops [8]. The central parts gradually elevation towards the neighboring mountains and hills to piedmonts [8]. Alluvial fans have established on the margins of the mountains close the ChakWardak basin and on interbrain ridges.The alluvial fans generally grade beginning coarse materials nearby source to finer materials on the distal edge.Physical weathering brought via risky temperature variations takes created breakdown in elevation at the edge of the basin [9,10]. This permanent weathering route maintains the steep, rocky mountain slope.This basin is portion of the dynamically tectonic of Kabul Mass in the transpresional plate borderline region of Afghanistan [11]. The north eastern parts of Chak Depositional Basin is distinct by Paghman fault system [12]. The Paghman fault movement north toward northeast and is evident in the continues fault scarp and piedmont alluvium the north eastern border of this basin.The Chak basin can be defined a valley fill basin and range setting where the valleys are filled with Quaternary and tertiary sediments, and the ranges are composed of uplifted crystalline and sedimentary rocks [13]. Quaternary sediments are classically fewer 80 m thick in the valleys [14,16]. The underlying tertiary depositions have been estimated to be as much as 800 m thick in the city of Kabul [15,27]. Also possibly additional 1000 m thick in certain areas of the valley [17,28]. The Quaternary and Tertiary remains and rocks have been categorized by divides the sediments into younger and older basin deposits [19,20]. The younger deposits, reworked loess series, are described as reworked loess, gravel, sand and talus. The gavel and were deposited mostly in the river channels [29,30].

The main objective of this research is to find out heavy and light minerals, gravel analysis for determining the quality of rocks as well as the types of mineral in river terraces. This research is important for industrial, geology, construction material, arts in the equivalent ministries and other organizations in Afghanistan. The reason that I prefer this research to be conducted is that such researches have not been conducted before in Afghanistan, if conducted couldn't response the needs of time.

The challenges that I faced during this research are; lack of research in this area and lack of geological equipment for research.

2. Study Locations

This inquiry carried out in the particular geological features and three altered terraces (upper, middle and lower) of Chak District (Figure 1) [22,23]. This is located at the south west side of Kabul happening Hindu Kush Mountain range in Afghanistan. The Chak Wardak Basin hiding place an area of 9772 km^2 with a maximum altitude of 3500 m in Wardak Daimirdak Mountain range and least elevation is 2092 m positioned in Ambokhak [24,26]. Loger River is one of the very significant streams of this district and it's started from (3500 m a.s. l) Daimirdad Mountain (Wardak range related Hindu Kush mountain range in Afghanistan) belong to Wardak Province [25]. At the first steps this river flows from west to east, and pass from Chack and Saidabad Districts in Wardak Province and then enters into Loger Province and it joins with Charkh River in Barakibarak District of Logar Province. After that, it enters to Kabul Province and juncture with Kabul River at the Sheena village related to the Bagramy District [26].

3. Method and Materials

In this exploration we studies different river terraces. From every terrace we got 1 kg sample and analysed in the test room of geology, Kabul University.The bigger size is boulders (50×80 cm), and smaller size is silt. For extrication smaller size we done sedimentological analysis and we used different size of sieving as shown in Figures 7 and 8. For separating heavy and light minerals, we mixed sediment fractions that are passing from 6.2

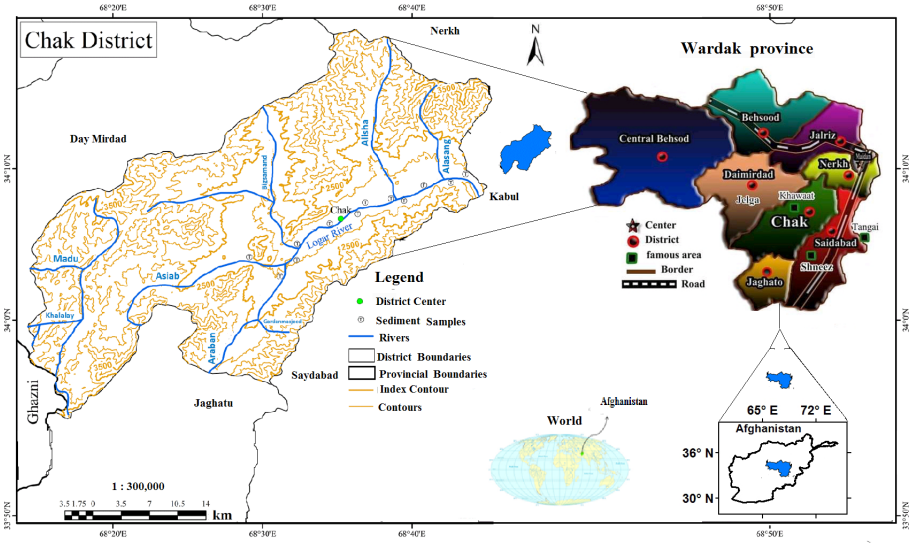

Figure 1. Geological setting of study locations, Wardak, Afghanistan.

mμ and150 mμ sieving sizes and mixed with one another, from these we got 300 mgr (milli gram) sample and put in the chemical solution of Bromoform (2.8 gr/cm^3), and for 24 hours staying in this chemical solution after 24 hours light minerals was at the suspension condition, and heavy minerals was precipitated at this solution, after we dried at the 30^{0}C of temperature, and we made thin section for determination type of heavy and light minerals we used polyresasion microscoph, at the result achieved different type of heavy and light minerals as shown in Tables 1 and 2. From bigger sizes (Pebbl, Granul) we did gravel analysis method to find different kinds of rocks.

4. Results and Discussion

Small and bigger tributaries at the different locations of Khawat Olya and Sufla junction with Loger River streams, normally these flows after west to east. The diverse kinds of sediments inter mountain backing basin accumulation and one by others making different kinds of terraces. The sediments inter mountain basin belonging near the tertiary (Iocene and Oligocene). It is about 20-45 million years old and its name is tertiary formation. At the higher parts of these sediments found not the same terraces it's related to the lower tertiary (Pleistocene) and it's younger than lower sediments. The slopes of Chak Basin are in north west to south east that belong to the relief of this basin from Daimirdad 3500 m to Ambokhak 2092 m [19]. The thickness of younger sediments between inter mountains backing basin belonging to the form of basin and distance from mountains ranges. The depth of sediments close to the source consolidated angular gravels and at the plains areas generally soft clay, silt, sand and some rounded gravels. The thickness of sediments at the plain areas at the Chak Dam is more than 1500 m and generally its clay, silt and sand. The quality and quantity of deposits in Chak Basin belonging near the adjacent mountains and that weathered by exogenetic force and transported by different phenomenon of gravity, waters, winds and made different types of sediment layers at the different location of basin. From sediments samples we found epidote, kyanite, muscovite, biotite and grarnet minerals belong to all metamorphic rocks that are located in surrounding mountains, others minerals rutile, biotite, and zircon because these belong to igneouse rocks.

4.1 Gravel Analysis

In this part of research, we got from five terraces different bigger sizes of gravels (Cobbles, Pebbles, granuls, grites). The sizes of terrace gravels belong to the slope and distance from mountains ranges, the formations of that terraces located near to the mountains and slope areas. Generally, there are bigger sizes in terraces, but apositlly those are far from mountain ranges and plains areas composetes from smaller sizes of gravels. From gravel analysis of lower terrace of Najuya we find different kinds of gravels according to the location of terrace. In this terrace 80% Limestone, 16% Quarsite and 4% Gnaize (Figure 2). Size bigger is 11×15 cm and smaller is 5×6 mm.

In lower terrace of Baghcha being limestone 70%, quarzite 20% and gneiss 10% (Figure 3), the bigger size is 10×10 cm and the smaller is 6 × 6 mm. If we compare two terraces, we can find more limestone because of surrounding mountains of bomb, and that are transported by water and deposited in these terraces. In this existing more than bigger particles on the river bed slope.

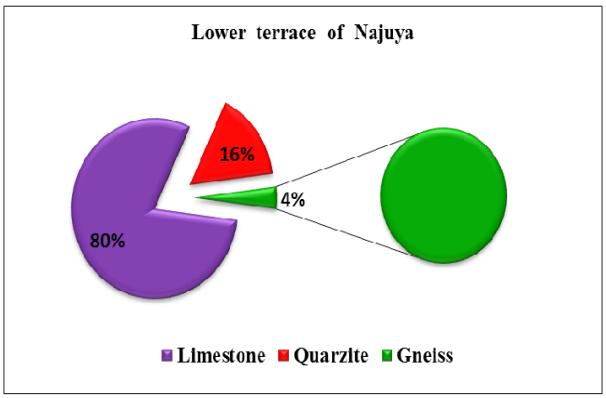

Figure 2. the percentage of rock type gravels in the formation lower terrace of Najuya.

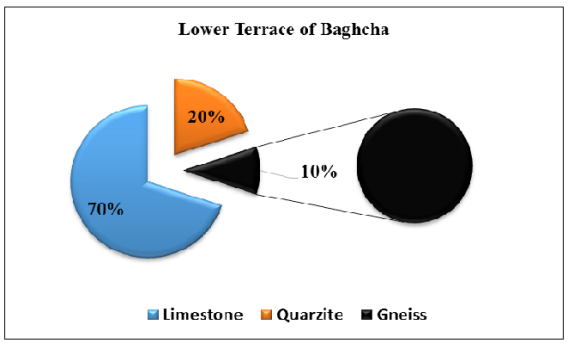

Figure 3. Different percentage rock type at gravels in lower terrace of Baghcha.

In the middle terrace of Baghcha, being gneiss 80%, guarzite 10% and granite 10% (Figure 4), bigger is 9×8 cm and smaller is 6 ×7 mm, in this terrace the percentage of gneiss is more than others rocks, because of surrounding mountains that are transported by water from south west and north west mountains of wardak.

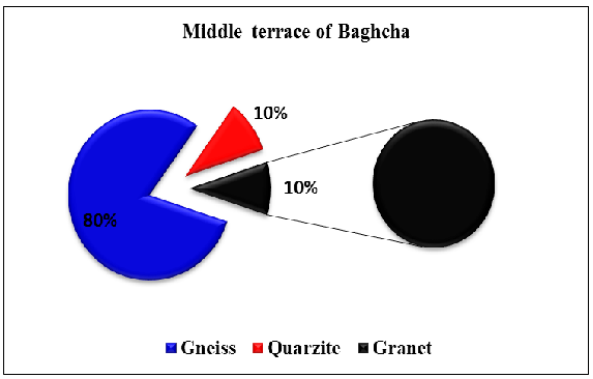

Figure 4. Different percentage rock type at gravels in middle terrace of Baghcha.

In middle terrace (molase) of west side of dam, being pegmatite 10%, conglomerate 30%, qarzite 50% and gneiss 10% (Figure 5), from these sizes the bigger one is 10× 11 cm and smaller one is 5× 6 mm.

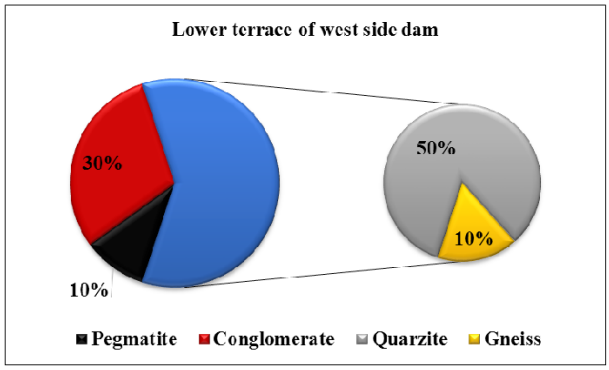

Figure 5. Different percentage rock type at gravels in lower terrace of west side of Chak dam.

In this limestone being 50% green schist 10%, and quarzite 40% (Figure 6), gneiss bigger one is 10 ×9 cm and smaller one is 6 × 5 mm. If look here, in these two terraces, we can find more metamorphic rocks there because these also transport from surrounding metamorphic (crystalline) of Kabul by water on that time.

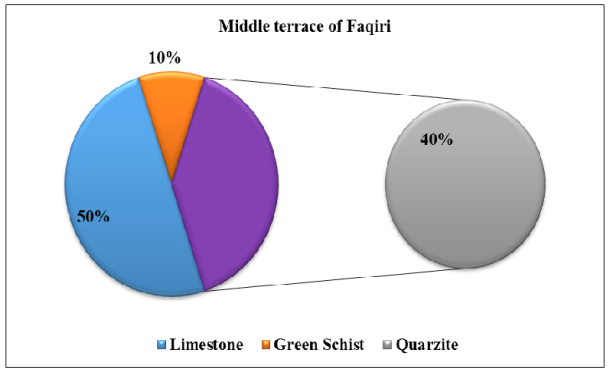

Figure 6. Different percentage rock type at gravels in middle terrace of Faqiri.

4.2 Sieving Analysis

After gravel analysis method we did sieving analysis method in this method we prepared different sizes and we got at the weight of 300 gr (gram) from every terraces and analyzed different sizes by sieving analysis method. In this method we achieved the following percentage of different sizes (Figure 7 and 8).

4.3 Heavy and Light Minerals

For heavy and light minerals studies in laboratory we mixed the sieving sizes of 125 µm (milli micron) with 6.3 µm and we futing these materials at the wight 30 mgr in the chemical solution of Bromoform (2.8 gr.cm^{-3}) and we found different heavy and light minerals. As shown in Tables 1 and 2 and Figure 9, 10, 11, 12, 13, 14, we can find a number of heavy and light minerals. In this research we

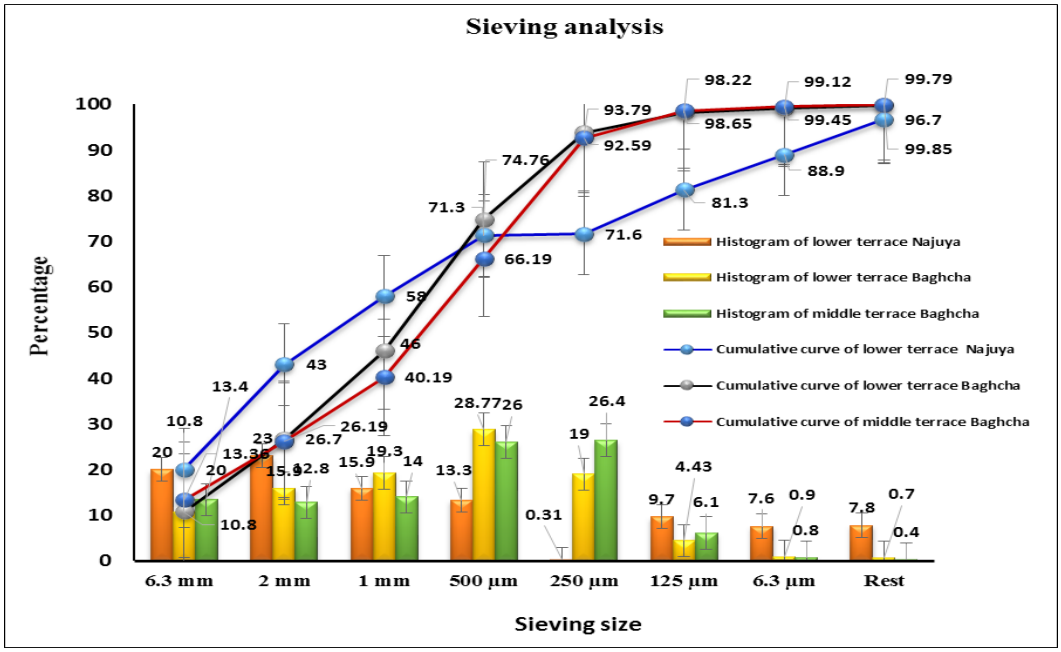

Figure 7. Cumulative Curve and histogram of middle, lower terraces of Najuya and Baghcha at the Chak, Wardak.

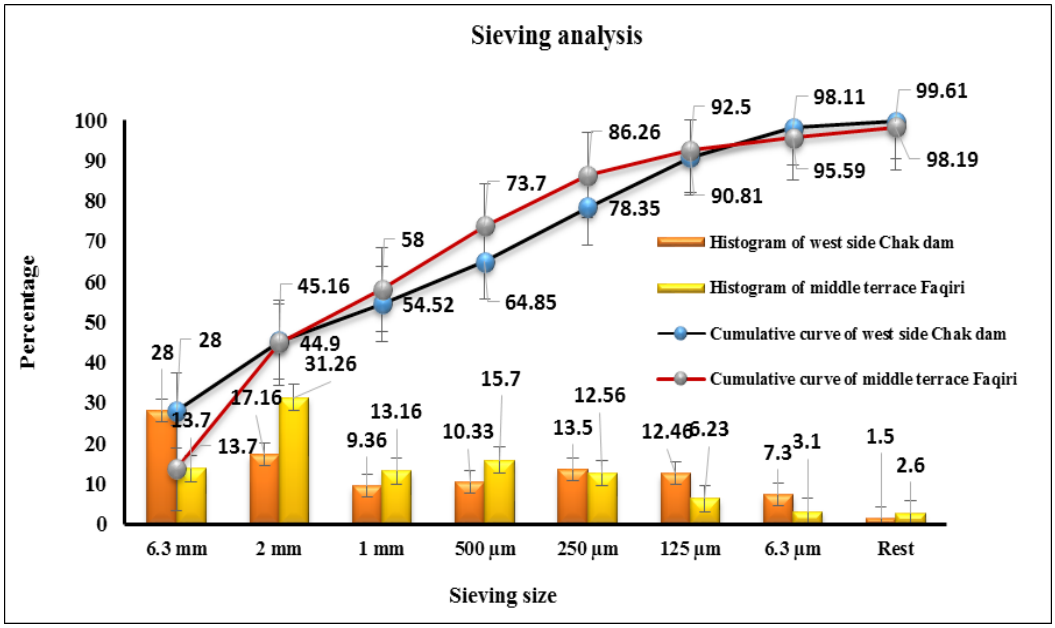

Figure 8. Cumulative Curve and histogram of lower and middle terraces of west side Chak dam and Faqiri at the Chak, Wardak.

found minerals of epidote, garnet and staurolite more than in Madukhel mountains range that is transported by water to Baghcha and Chak Dam terraces rutile, hornblende, zircon and tourmaline minerals, because of igneouse rocks at the Gardan Masjid surrounding mountains it's transported by water at the different times. Some light minerals for example muscovite, biotite in all terraces of middle and lower because these two kinds' minerals we can find in both metamorphic and igneous rocks that are located in mountains. As well as if we compare biotite mineral between Faqiri and Najuya terraces achieving that there is erosion of igneous rocks at mountains and it's deposited in these terraces. Also amphibole mineral in terraces, because of Gardam Masjid mountain igneous rocks. As well as tourmaline and zircon minerals because Gardam Musjeed mountain (Figure 15, 16, 17, 18). For good understanding also we can see some percentage in graphs. The percentage of heavy and light minerals in the Tables 1 and 2 are detail explained.

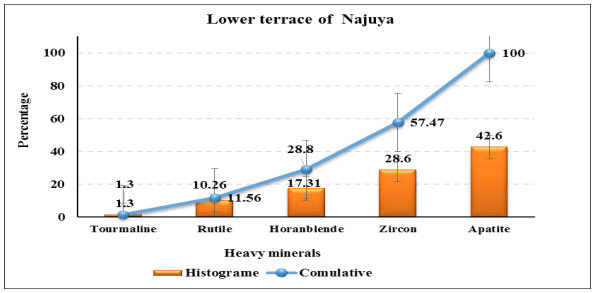

Figure 9. Cumulative curve and histogram of heavy minerals of lower terrace of Najuya.

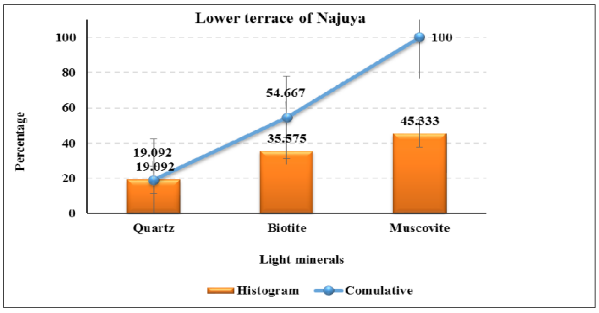

Figure 10. Cumulative curve and histogram of light minerals of lower terrace of Najuya.

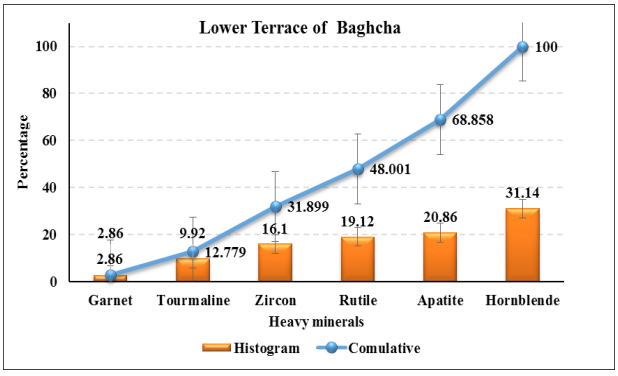

Figure 11. Cumulative curve and histogram of heavy minerals lower terrace of Baghcha.

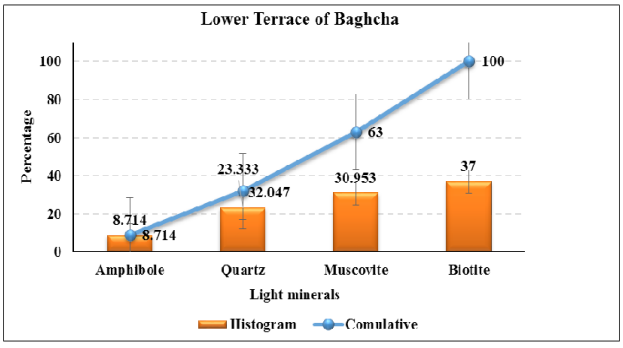

Figure 12. Cumulative curve and histogram of light at the lower terrace of Baghcha.

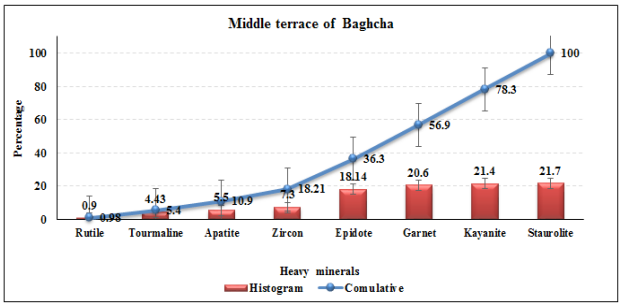

Figure 13. Cumulative curve and histogram of heavy minerals middle terrace of Baghcha.

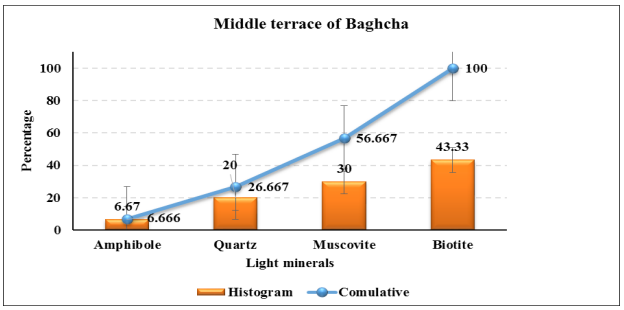

Figure 14. Cumulative curve and histogram of light minerals middle terrace of Baghcha.

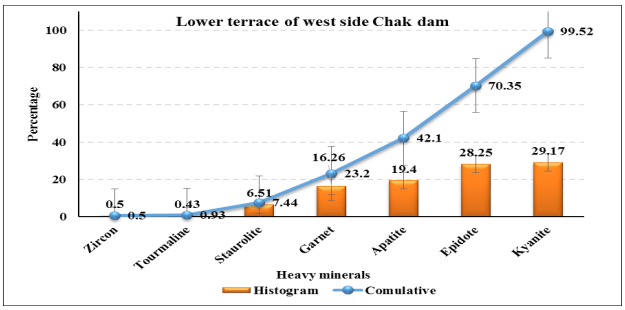

Figure 15. Cumulative cueve and histogram of heavy minerals of lower terrace west side Chak dam.

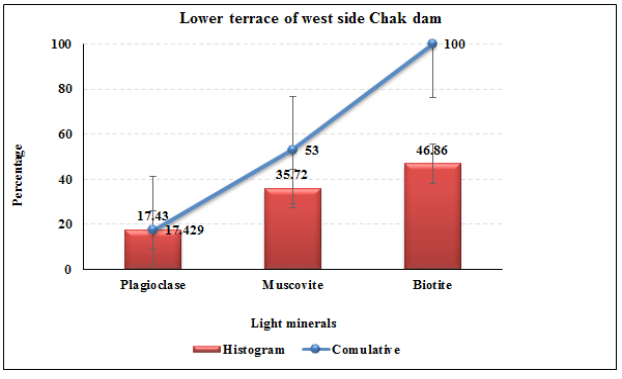

Figure 16. Cumulative curve and histogram of light mineralsLower terrace of west side Chak dam.

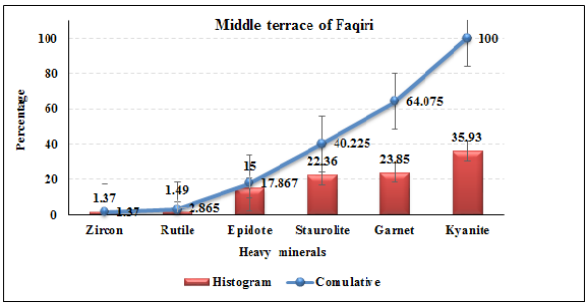

Figure 17. Cumultive curve and histogram of heavy minerals Middle terrace of Faqiri.

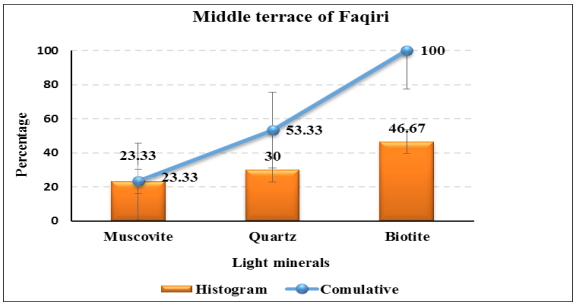

Figure 18. Cumulative curve and histogram of light minerals middle terrace of Faqiri.

Table 1. Summary of heavy minerals of this research

River sediments	Locations	Minerals	Percentage
Loger River	lower terrace of Najuya	Tourmaline	1.3
≈	≈	Rutile	10.26
≈	≈	Hornblende	17.30
≈	≈	Zircon	28.6
≈	≈	Apatite	42.56
≈	lower terrace of Baghcha	Garnet	2.86
≈	≈	Tourmaline	9.92
≈	≈	Zircon	16.1
≈	≈	Rutile	19.12
≈	≈	Apatite	20.87
≈	≈	Hurnblende	31.14
≈	middle terrace of Baghcha	Rutile	0.9
≈	≈	Tourmaline	4.42
≈	≈	Apatite	5.5
≈	≈	Zircon	7.3
≈	≈	Epidote	18.14
≈	≈	Garnet	20.6
≈	≈	Kayanite	21.4
≈	≈	Staurolite	21.7
≈	lower terrace west side Chak dam	Zircon	0.5
≈	≈	Tourmaline	0.43
≈	≈	Staurolite	6.51
≈	≈	Garnet	16.26
≈	≈	Apatite	19.4
≈	≈	Epidote	28.25
≈	≈	Kyanite	29.17
≈	Middle terrace of Faqiri	Zircon	1.37
≈	≈	Rutile	1.49
≈	≈	Epidote	15
≈	≈	Staurolite	22.36
≈	≈	Garnet	23.85
≈	≈	Kyanite	35.93

Table 2. Summary of Light minerals of this research

River sediments	Locations	minerals	Percentage
Loger River	lower terrace of Najuya	Quartz	19.09
≈	≈	Biotite	35.5
≈	≈	Muscovite	45.3
≈	lower terrace of Baghcha	Amphibole	8.71
≈	≈	Quartz	23.33
≈	≈	Muscovite	30.95
≈	≈	Biotite	37
≈	middle terrace of Baghcha	Amphibole	6.7
≈	≈	Quartz	20.1
≈	≈	Muscovite	30
≈	≈	Biotite	43.3
≈	lower terrace west side Chak dam	Plagioclase	17.42
≈	≈	Muscovite	35.7
≈	≈	Biotite	46.86
≈	Middle terrace of Faqiri	Muscovite	23.3
≈	≈	Quartz	30
≈	≈	Biotite	46.6

5. Conclusions

This geological research used to distinguish different sediments sizes, rock and minerals types in river sediments that are transported at snowmelting season by Loger River discharges from different parts of surrounding mountains in Chak District. At formation of lower terrace in Najuya 80% limestone, 16% quarzite and 4% gneiss, bigger size is 11×15 cm and smaller is 5×6 mm. In lower terrace of Baghcha limestone 70 %, quarzite 20% and gneiss 10%, bigger size is 10×10 cm and smaller is 6 × 6 mm. In middle terrace of Baghcha, gneiss 80%, quarzite 10% and granite 10%, bigger is 9×8 cm and smaller is 6 ×7 mm. In middle terrace of west side dam, pegmatite 10%, conglomerate 30%, qarzite 50% and gneiss 10%, bigger size is 10× 11 cm and smaller is 5× 6 mm. In middle terrace of Faqiri limestone 50% green schist 10%, and quarzite 40%, bigger is 10×9 cm and smaller is 6 × 5 mm. From chemical analysis (Bromoform solution). In the research we found different kind of heavy and light minerals of epidote, garnet, staurolite, rutile, hornblende, zircon and tourmaline, muscovite, biotite, tourmaline, zircon. In this research some heavy minerals such as; epidote, garnet and staurolite related to metamorphic rocks, rutile, hornblende, zircon, amphibole and tourmaline minerals are related to igneouse rocks. Some light minerals such as; muscovite, biotite exist in all terraces, because these two minerals exist in both metamorphic and igneous rocks. All these minerals belong to the surrounding mountains rocks. Those transferred by Loger River in the snowmelting seasons.

The results attained propose that the sedimentological analysis can be used professionally for petrographical, aquifere, geological mapping, stratigraphy, geochronology and engineering geological studies for other mountain basins in Afghanistan.

References

[1] Anthony E. J. & Héquette A., 2007. The grain-size characterization of coastal sand from the Somme estuary to Belgium: sediment sorting processes and mixing in a tide-and storm-Dominated setting. Sedimentary Geology.

[2] Avouac, J.P., and E. Burov,1996. Erosion as a driving mechanism of intracontinental Mountain growth, J. Geophys. Res., 101, 17,747-17, 769.

[3] Böckh, E.G., 1971.Report on the groundwater resources of the city of Kabul, report for Bundesanstalt für Geowissenschaften und Rohstoffe BGR file number 0021016, 43 p.

[4] Ball, M. M., 2003. Carbonate sand bodies of Florida and Bahamas. Journal of Sedimentary petrology, P. 91.

[5] Banks, David, and Soldal, Oddmund, 2002. Towards a policy for sustainable use of Groundwater by non-governmental organizations in Afghanistan: Hydrogeology Journal, v. 10, no. 3, p. 377.

[6] Belhassan, K. 2020. Hydrogeology of the Ribaa – Bittit springs in the Mikkes Basin (Morocco).International Journal of Water Resources and Environmental Science 9 (1): 07 -15, 2020 ISSN 231-2492, © IDOSI Publications, 2020.
DOI: 10.5829/idosi.ijwres. 2020.9.1.14537.

[7] Belhassan, K., 2020. Relationship between River and Groundwater: Water table Piezometery of the Mikkes Basin (Morocco. International Journal of Water Resources and Environmental Science 9 (1): 01-06, 2020 ISSN 2311-2492, © IDOSI Publications, 2020.

DOI: 10.5829/idosi.ijwres. 2020.9.1.14536.

[8] Bentley S. J., Sheremet A. & Jaeger J. M.,2006. Event sedimentation, bioturbation, and Preserved sedimentary fabric: Field and model comparisons in three contrasting marine Settings. Continental Shelf Research 26, P. 2108-2124.

[9] Bohannon, R.G., 2005. Geologic map of quadrangle 3468, Chak-e-Wardak (509) and Kabul (510) quadrangles: Afghan Open-File Report (509/510) 2005-1001.

[10] Bohannon, R.G., and Turner, K.J., 2007. Geologic map of quadrangle 3468, Chak Wardak-Syahgerd (509) and Kabul (510) quadrangles, Afghanistan: U.S. Geological Survey.Open-File Report 2005-1107-A. 1 sheet.

[11] Broshears, R.E., Akbari, M.A., Chornack, M.P., Mueller, D.K., and Ruddy, B.C.,2005. Inventory of ground-water resources in the Kabul Basin, Afghanistan: U.S. Geological Survey Scientific Investigations Report 2005-5090, 34 p.

[12] Colella, A and di Geronimo, I.,1998. Surface sediments and macro fanas of the Grati submarine fan (Ionian sea, Italy a) sedimentary geology.

[13] Elliontt, T., 2001. Siliciclasstic shorlines Sedimentary Environments and facies, 2nd ed., Black wall scientific pub., Oxford.

[14] Folk, R. L.,2004. spectral divission of Limestone types. In: Classification of carbonate Rocks(ed w. E. Ham), 62-84, memoirs of the American Association of petroleum geology, Tulsa, Oklahoma.

[15] gela L. Coe ,2003. The sedimentary Records of sea Level change, british Library, ISBN 052, 831113 hard back.

[16] González-Álvarez R. *et al.*,2005. Paleoclimatic evolution of the Galician continental shelf (NW of Spain) during the last 3000 years: from a storm regime to present conditions. Journal of Marine Systems.

[17] Goff J., McFadgen B. & Chagué-Goff C.,2004. Sedimentary differences between the 2002 Easter storm and the 15th-century Okoropunga tsunami, southeastern North Island, New Zealand. Marine geology.

[18] Herman E. K., Toran L. & White W. B.,2009. Quantifying the place of karst aquifers in the Groundwater to surface water continuum: A time series analysis study of storm behavior in Pennsylvania water resources. Journal of Hydrology.

[19] Horikawa K. & Ito M. 2009. Non-uniform across-shelf variations in thickness, grain size, and frequency of turbidites in a transgressive outer-shelf, the Middle Pleistocene Kakinokidai Formation, Boso Peninsula, Japan. Sedimentary Geology.

[20] Mike Leeder, 2006. Sedimentology and sedimentary basins, by Grphicraft, Ltd, Hong Kong, Raplika press pvt Ltd, Kundli.

[21] Rasouli, H. and Safi, A. G., 2021. Geological, Soil and Sediment Studies in Chelston Sedimentary Basin, Kabul, Afghanistan. International Journal of Geosciences, 12, 170-193. https://doi.org/10.4236/ijg.2021.122011.

[22] Rasouli H. Sarwari, M. H., Khairuddin R.، Said A. H.,2020 Geological Study of Tangi Mahipar Mountain Range along Kabul Jalalabad road, Afghanistan https://dx.doi.org/10.4236/ojg.2020.1010044.

[23] Rasouli H.,2020. Application of soil physical and chemical parameters and its Comparing in Kabul sedimentary basins, Kabul, Afghanistan http://dx.doi.org/10.24327/ijrsr.2020.1102.5095.

[24] Rasouli H., 2020. WELL DESIGN AND STRATIGRAPHY OF SHEERKHANA DEEP WELL IN CHAK DISTRICT, WARDAK, AFGHANISTAN. International Journal of Geology, Earth & Environmental Sciences، ISSN: 2277-2081, and Open Access, Online International Journal Available at 10 (2) May-August, pp.54-68/Rasouli http://www.cibtech.org/jgee.htm2020Vol.

[25] Rasouli H., Shamal S. and Sarwari, M.H. 2021. Geological Study of Dasht-e-Top Sedimentary Basin, Wadak Province, Afghanistan. International Journal of Geosciences, 12, 531-540. https://doi.org/10.4236/ijg.2021.126029.

[26] Rasouli H., 2019. A STUDY ON SOME RIVER SEDIMENTS, HYDROLOGY AND GEOLOGICALCHARACTERISTICS IN CHAK SEDIMENTARY BASIN, WARDAK, AFGHANISTAN. International Journal of Geology, Earth & Environmental Sciences,ISSN: 2277-2081, and Open Access, Online International Journal Available at Vol.9 2 May-August, pp.49-61/Rasouli. http://www.cibtech.org/jgee.htm2019.

[27] Sun Y., Gao S. & Li J.,2003. Preliminary analysis of grain-size populations with Environmentally sensitive terrigenous components in marginal sea setting. Chinese Science Bulletin P. 184-186.

[28] Tang X., Chen M., Liu J., Zhang L. & Chen Z.,2004. The anisotropy of magnetic Susceptibility of Core NS97-13 sediments from the Nansha Islands sea area in the Southern South China Sea. Acta Oceanologica Sinica P. 69-70 (in Chiness with English Abstract).

[29] Wright, L. D.,2000. River deltas, in Dasvis, R. A., J.R(ed.), Caostal Sedimentary environments : Springer – Verlag, New Yark.

[30] Xiao S., Liu W., Li A., Yang S. & Lai Z.,2009. Pervasive autocorrelation of the chemical Index of alteration in sedimentary profiles and its palaeoenvironmental implications. Sedimentology.

BILINGUAL PUBLISHING CO.
Pioneer of Global Academics Since 1984

Journal of Geological Research
https://ojs.bilpublishing.com/index.php/jgr-a

ARTICLE

Interpretation of Aeromagnetic Data of Part of Gwagwalada Abuja Nigeria for Potential Mineral Targets

Priscillia Egbelehulu* **Abu Mallam** **Abel. U. Osagie**

Department of Physics, University of Abuja, Abuja, Nigeria

ARTICLE INFO

Article history
Received: 16 August 2021
Revised: 12 September 2021
Accepted: 14 September 2021
Published Online: 30 September 2021

Keywords:
Aeromagnetic
Lineament
Faults
Total magnetic intensity

ABSTRACT

This study analyzes aeromagnetic data over a section of Gwagwalada in Abuja. The data were obtained from the Nigerian Geological Survey Agency acquired at 100 m terrain clearance. The study area spans longitudes 7.0875 E to 7.1458 E and latitude 8.9625 N to 9.0 N (about 27 km2). The dataset was reduced to the equator (RTE) and downward continued by 50 m. Analytic signal filter was applied on TMI-RTE grid to detect the edges of the magnetic bodies present. The structure was observed to trend NE-SW. The CET lineament map reveals intersections such as junctions and corners on the map. This revealed structure liable for potential mineralization zone. Euler deconvolution technique applied over the transformed dataset ascertain the location and depth of the structure, having a maximum depth of about 421 m and a minimum of about 59 m. Variation in magnetic depth and susceptibility contrast is specified by the gridded SPI depth map.

1. Introduction

Minerals are usually deposited underneath the earth surface. Detecting them to a great extent depends on the characteristics or properties they possess which distinguish them from their surrounding media.

Geophysical method assumed for their survey depends on their properties [4].

Magnetic method plays a vital role in mineral exploration. Its importance is seen in its ability to delineate structures like faults, folds, contacts, shear zones, intrusions and detection of favorable areas of ore deposits [1]. It responds to ferromagnetic materials and detects metallic objects [11]. It is concerned with the measurement of the intensity of the earth's magnetic field.

Earth's magnetic field anomalies are usually a result of either induced or remanent magnetism, due to secondary magnetization which is induced in a ferrous body by the earth's magnetic field. The shape, dimension, and amplitude of an induced magnetic anomaly are functions of the kind of orientation, geometry, size, depth, intensity, inclination of the earth's magnetic field in the area of interest and magnetic susceptibility of the body [3].

Most magnetic rocks are known to contain several combinations of induced and remanent magnetization which affects the earth's primary field [10]. The magnitudes

*Corresponding Author:
Priscillia Egbelehulu,
Department of Physics, University of Abuja, Abuja, Nigeria;
Email: priscilliaegbelehulu@gmail.com

DOI: https://doi.org/10.30564/jgr.v3i4.3581

of these fields depend largely on the quantity, size of magnetic-mineral grains and their composition. Magnetic anomalies could be linked to primary igneous or sedimentary processes that build the magnetic mineralogy. They could also be as a result of secondary alteration that introduces or removes magnetic minerals.

The results of any geophysical survey are used to identify a target of interest, or to correlate the spatial variation of values of the rock property with variations in the geology. Thus, survey helps to get valuable information on the geology and possibly to find targets of economic interest and importance in the study area [13]. Understanding the nature of the mineralization and how it originates is an important factor in mining exploration, since minerals are structurally controlled and are associated with faults, fractures and shear zones. Delineating these structures aids future exploration, giving an idea of the mining potential of the region. This research aims at interpreting aeromagnetic data for potential mineral target.

Objectives of the study are

•To identify lineaments.

•To delineate geological structures that might host possible minerals.

•To ascertain the depth of the vein.

2. Location

The area of study is located in Abuja, Gwagwalada area council (Figure 2). It is about 55 km from the capital city (Abuja). It is bounded by 7.0875 E to 7.1458 E and latitude 8.9625 N to 9.0 N, which covers 27 km^2 north-eastern part of Gwagwalada. The contour obtained from the topographic map of the study area is used to produce a digital terrain model of the area (Figure 1) using The Generic Mapping Tools (GMT) software. This gives an idea about the geomorphology of the area. The area is located within the broken-line rectangular box is a low land terrain with hills located at the northeastern and central part with a height of about 400 m above sea level with valleys observed along the hills.

2.1 Geology of the Study Area

The geology of the Federal Capital Territory (FCT), Abuja is underlain by two major rock formations - the Basement Complex and sedimentary rock formations [8]. The dominant rock within the study area is banded gneisses. The outcrops are well foliated showing prominent gneissosity with the alternation of bands of mafic and felsic minerals. They are medium-to coarse-grained with large quartz intrusions exploiting joints and weak zones within the rock.

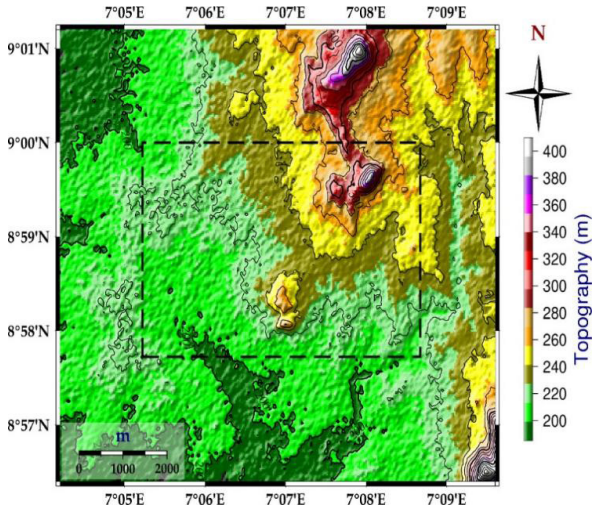

Figure 1. Topographic Map of Study Area

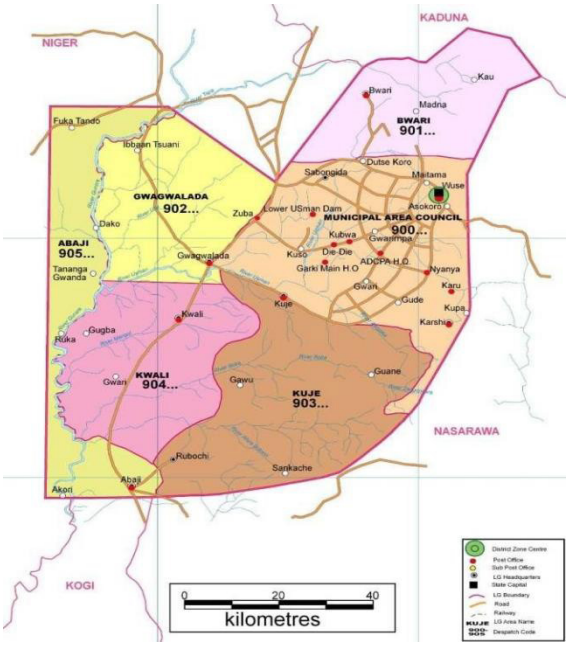

Figure 2. Location Map of Study Area

3. Materials and Method

The major component of the study involves image enhancement of the aeromagnetic dataset acquired from the Nigerian Geological Survey Agency (NGSA). The magnetic anomalies associated with local magnetic variations of the study area was obtained by the removal of the normal geomagnetic field that is, by subtracting 33000nT from the dataset. The International Geomagnetic Reference Field (IGRF) formula [2] which was computed by GEOMAG program is used for the reduction. The dataset is interpolated by employing the minimum curvature gridding algorithm obtainable in the Geosoft Oasis Montaj 8.4 software. The angle of inclination and declination was

taken at -6.4° and -1.7° respectively. These values were acquired from the eleventh generation international geomagnetic Reference Field (IGRF) formula [2] at latitude 8o59'N and longitude 7o07'E around the mid-point of the region. The map is also characterized by magnetic highs trending NE-SW. This configuration could be ascribed to a relatively deep-seated low relief basement structures with the igneous rocks composition. On the reduced to equator (RTE) map, analytic signal, centre for exploration targeting (CET), Euler deconvolution and Source parameter imaging (SPI) was applied over the dataset.

3.1 Analytic Signal

Analytic Signal method is used for detecting the edges of magnetic bodies. The conceptualization of analytic signal for magnetic data interpretation was initially introduced [6]. It reveals that amplitude yields a bell-shaped function over every corner of a 2D body with polygonal cross-section. For a remote corner, the maximum of the bell-shaped curve is detected precisely over the corner. At half its maximum amplitude, the width of the curve is equal to twice the depth to the corner. However, resolving for these parameters is not affected by the presence of the remanent magnetization. Horizontal locations are usually well verified by this method nonetheless depth determinations are only valid for polyhedral bodies [7]. The 3D analytic signal was employed to approximately estimate positions of magnetic contacts and acquire depth estimates from gridded data [12].

3.2 Center of Exploration Targeting (CET)

The CET grid analysis examines the texture of a laterally continuous line-like region of discontinuity such as lineament along ridges and edges as well as areas of deviation to locate deposit occurrence favorability.

3.3 Euler Deconvolution

This technique uses the first-order x, y and z derivatives to determine the location and the depth for different idealized targets (sphere, cylinder, thin dike, and contact). Every single one of them can be characterized by a specific structural index. Eigen values generated in Euler solution could be further analyzed to decide whether an individual anomaly was 2D or 3D.

$$X\frac{\partial T}{\partial x} + Y\frac{\partial T}{\partial y} + Z\frac{\partial T}{\partial z} + NT = x_0\frac{\partial T}{\partial x} + y_0\frac{\partial T}{\partial y} + z_0\frac{\partial T}{\partial z} + NB \quad (1)$$

Where;

x_0, y_0, z_0 *are coordinate of magnetic force.*

$\frac{\partial T}{\partial x}, \frac{\partial T}{\partial y}, \frac{\partial T}{\partial z}$ *are derviatives of total field with respect to* x, y, z

N-Structural Index (SI) helps relates rate of change of a potential field with distance.

B-It's a local background representing the "regional" field within a sliding window with an adjustable size [5]. The SI to a great extent depends on the type and physical parameters of the potential field this provides an excellent overview of the Euler's homogeneity equation properties in general and the SI in particular [15].

Estimating depth by applying Euler deconvolution technique helps in delineating geologic contacts where faults usually occur. This technique provides an automated estimation of the source location and depth. Thus, it is used as a boundary finder as well as a depth estimator. It is often deployed in magnetic interpretation due to its uniqueness-since it requires only a little precedent knowledge about the magnetic source geometry, and it requires no information about the magnetization vector [9] and [16].

3.4 Source Parameter Imaging

This technique was developed due to complex analytic signal. SPI is occasionally referred to as the local wave number method [17-19]. It has its maxima located over isolated contacts, and its depths is estimated without the presumption of the thickness of the source bodies [14]. Solution grids obtained from the SPI™ technique shows edge locations, depths, dips and susceptibility contrasts. The local wave number maps more closely similar geology compared to magnetic map or its derivatives.

4. Results and Discussion

The total magnetic intensity (TMI) grid Figure 3a is reduced to the equator Figure 3b. This ensures that the magnetic anomaly is directly positioned on the body causing them since the direction of magnetization varies. The magnetic signature is enhanced and trends in NE-SW direction of the study area.

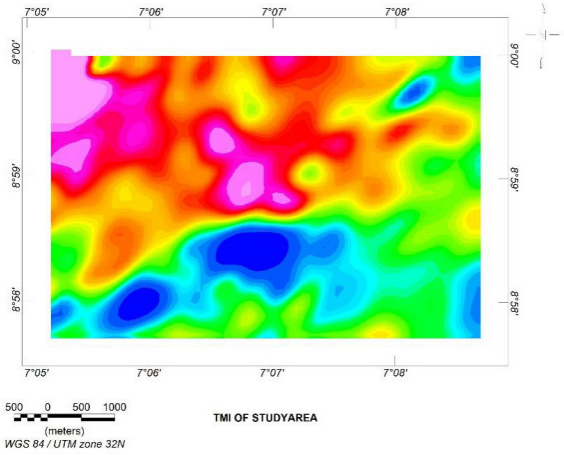

Figure 3a. TMI map of Study area

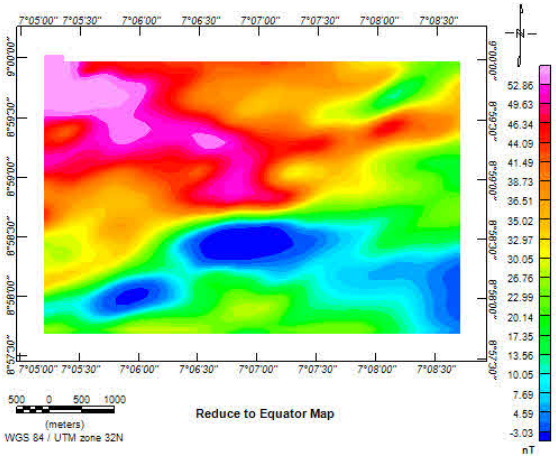

Figure 3b. TMI map reduce to Equator

4.2 Structural Analysis from Analytic Signal Plug

It is characterized with high and low amplitude thereby separating regions of outcrop and sedimentation. Since the result is amplitude domain, regions possessing outcrops have a significantly high amplitude shown in Figure 4 with red and pink color and areas having low amplitude identified with blue coloration. Analytic signal is more discontinuous than the simple horizontal gradient because a maximum generated directly over the discrete bodies along their edges.

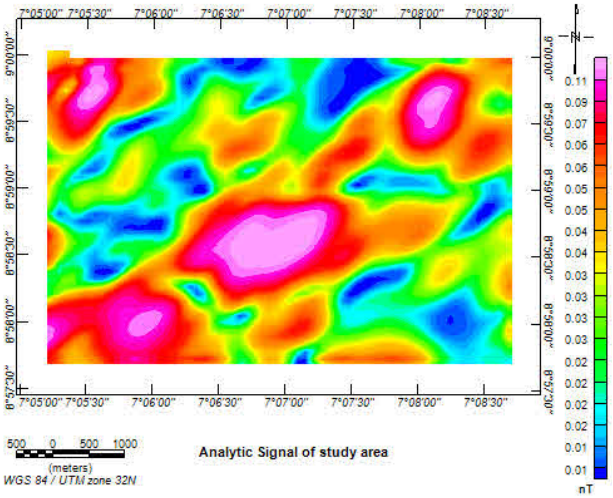

Figure 4. Analytical Map of Study Area

4.3 Application of Center of Exploration Targeting (CET) Grid Analysis and Results

CET grid analysis is applied to RTE grid so that anomalies are shifted over their causative structures. Standard deviation and phase symmetry plug-in was applied to produce the map in Figure 5a, while application of the amplitude threshing and the skeleton to vector plug-in yielded map Figure 5b. Form Figure 5a it can be deduced that the area shown in blue coloration represent areas with very low amplitudes are due to a deeper magnetic sources. The region is observed to follow NE-SW trends, which coincides with the trending of the area. The areas depicted by the pink colour are the outcrop of migmatitic-gneiss, which is the most abundant of the basement rock in the area. Rocks of lithological group of the basement complex also identified in the area are banded- gneiss (Biotite-gneiss), granite-gneiss and quartz veins which were observed at the northeastern part of the map, northwest, central part and the southwestern part of the map all trending NE-SW as shown in Figure 1. Figure 5b, which is the CET lineament reveals positions of selected intersections such as junctions and corners of the detected segmented lines. Areas where the line structure intercept or change direction are regarded as high mineralization areas.

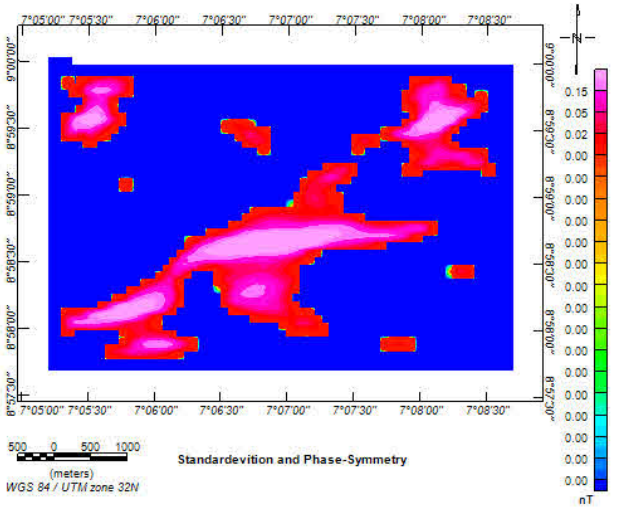

Figure 5a. Standard Deviation and Phase Symmetry Map of the Study Area

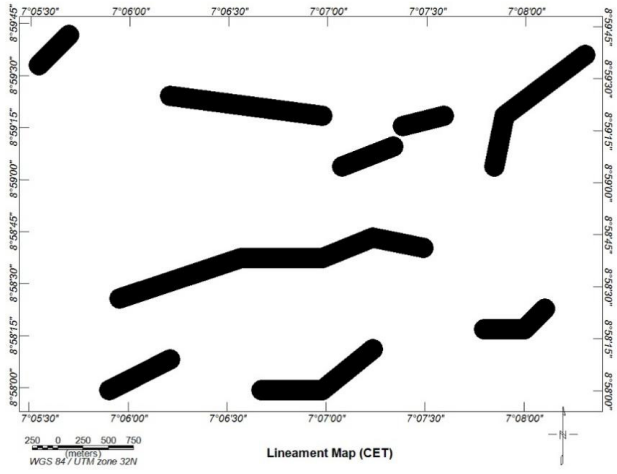

Figure 5b. Lineament Map (CET) of the Study Area

4.4 Application of Euler Deconvolution for Structural Analysis and Result

Euler deconvolution was carried out on the RTE. Its method for depth estimation is an automated technique used in detecting the source of potential field base on the amplitude and gradients. Structural index (SI) and window sizes are selected appropriately as (dyke =1) Figure 6. Euler deconvolution explore the area to locate structures and estimate the depth to which the structures exists. To achieve the best SI, structural indices were taken as 1.

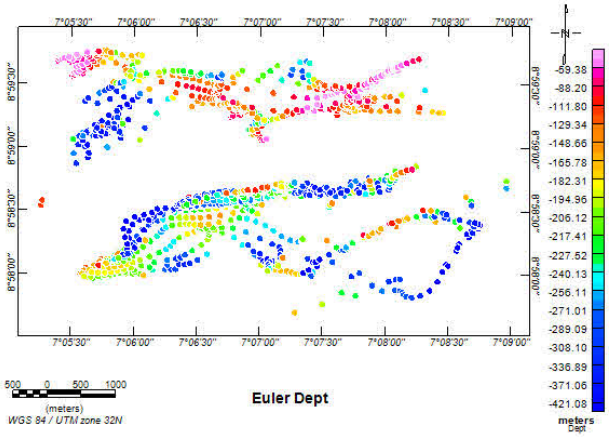

Figure 6. Euler Deconvolution of the study Area

Depth estimated in the west (W) to the East (E), Northeast (NE) and Northwest (NW) direction over the major anomaly decreases gradually. The pink circles represent the depths of the main anomaly having a depth about 59.38 m depth of the extrusive body (blue circles) which is about 421.08 m is different from the main anomaly. The degree of accuracy of Euler depth depends on the structures or on the anomaly falling on the center of the window.

4.5 Application of Source Parameter Imaging and Results

SPI method makes easier interpretation of magnetic data significantly Figure 7. Variation in magnetic depth and susceptibility dissimilarity within the study area is usually indicated by the gridded SPI map and colour legend. The negative values in the legend indicate depth of magnetic bodies, which could be deep-seated crystalline rocks or a shallow intrusion. The Pink coloration indicates area associated with near surface magnetic bodies with depth approximately 99.13 m, while the blue colour indicates area of deep seated magnetic bodies having a depth ranging from 246.71 m to 408.76 m. SPI depth ranges generally from 99.13 m (near surface depth) to 408.76 m (deep seated magnetic bodies).

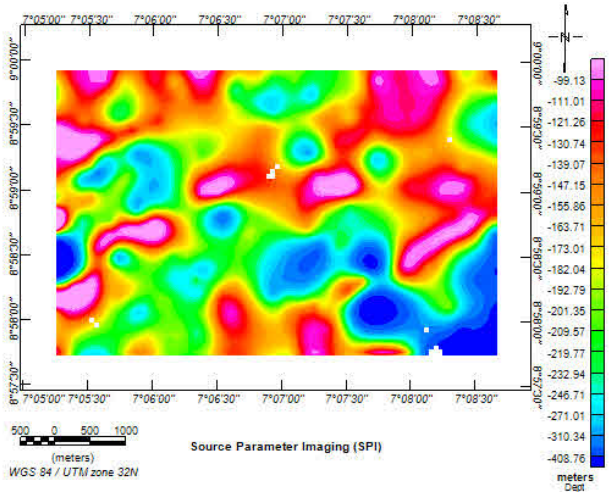

Figure 7. SPI Map of the Study Area

5. Conclusions

Analytical signal filter map Figure 4 is discontinuous and shows a prominent NE-SW trend. However, a maximum is generated directly over separate bodies alongside their edges. The maximum indicates contact depth with the condition that the signal originating from a single contact was obtained. Euler deconvolution plug-in was applied and obtained depth of the source potential field based on the amplitude and gradient. The depth of the main anomaly was 59.38 m. The center for exploration targeting (CET) plug-in applied on the RTE grid clearly revealed that the CET analysis was extremely effectual and useful in identifying the occurrence, location of favorable mineralization area and tracing the structural lineament. Which were traced to longitude 7005’30’’, 70 07’00’’, 70 08’00” and latitude 8059’32’’, 8058’45’’, 8059’15’’ also coincide with feature in Euler deconvolution (depth). Finally, source parameter imaging (SPI) Figure 7 applied using a pre-processing grid of horizontal and vertical derivative, indicated variation in magnetic depth and susceptibility contrast within the study area.

References

[1] Elkhateeb, O.S. Delineation Potential Gold Mineralization Zone in A Part of Central Eastern Desert, Egypt Using Airborn Magnetic and Radiometric data [J]. *NRIAG Journal of Astronomy and Geophysics* (2018). 55-70.

[2] Finlay C.C, Maus S, Beggan C.D, Bondar T.N, Chambodut A, Chernova T.A, Chulliat A, Golovkov V.P, Hamilton B, Hamoudi M, Holme R. International geomagnetic reference field: the eleventh generation [J]. Geophysical Journal International (2010).

183(3):1216-30.

[3] Hinze W.J. The role of gravity and magnetic methods in engineering and environmental studies. InGeotechnical an Environmental Geophysics: Volume I: Review and Tutorial [J]. Society of Exploration Geophysicists (1990). 75-126.

[4] Kearey, P, Brooks, M., & Ian, H. An Introduction to Geophyscial Exploration. Third Edition Blackwell Publishing (2002).

[5] Mushayandebvu M.F, Lesur V, Reid A.B, Fairhead J.D. Grid Euler deconvolution with constraints for 2D structures [J]. Geophysics (2004). 69(2):489-96.

[6] Nabighian, M. N. The analytic signal of two-dimensional magnetic bodies with polygonal cross-section - Its properties and use for automated anomaly interpretation [J]. Geophysics (1972), 37, 507-517.

[7] Nabighian, M. N. Additional comments on the analytic signal of two-dimensional magnetic bodies with polygonal cross-section [J] Geophysics (1974), 39, 85-92.

[8] Offodile, M. E. The development and management of groundwater in Nigeria. *Contributions of Geosciences and Mining to National Development, (NMGS)* (2003), 1-7.

[9] Reid, A.B., Allsop, J.M., Granser, H., Millett, A.J., Somerton, I.W. Magnetic Interpretation in Three Dimension Using Euler Deconvolution [J]. *Geophysics* (1990), 55, 80-90.

[10] Reynolds, R.L., Rosenbaum, J.G., Hudson, M.R and Fishman, N.S Rock Magnetism, the Distribution of Magnetic Minerals in Earth Crust and Aeromagnetic Anomalies. U.S Geological Survey Bulletin (1990). 24-45.

[11] Robert, J.H. Application of Magnetic and Electromagnetic Methods to Locate Buried Metal. U.S Department of Interior, U.S Geological Survey, Open-File Report (2003). 03-317.

[12] Roest, W.R., Verhoef, J., and Pilkington, M. Magnetic interpretation using the 3-D analytic signal. *Geophysics* (1992), 57, 116-125.

[13] Scott, W.J Geophysics for Mineral Exploration-A Manual for Prospectors (2014). 1-2, 11-14.

[14] Smith, R.S., Thurston, J.B., Dai, Ting-Fan, and MacLeod, I.N. SPI™ - the improved source parameter imaging method: Geophysical Prospecting (1998), 46, 141-151.

[15] Stavrev, P. and Reid, A. Degrees of Homogeneity of Potential Fields and Structural Indices of Euler Deconvolution [J]. *Geophysics* (2007), 72, 1-12.

[16] Thompson, D.T. A New Technique of Making Computer Assisted Depth Estimates from Magnetic Data [J]. Geophysics (1982), 47: 31-37.

[17] Thurston, J. B., Smith, R. S. and Guillon, J-C. A multimodel method for depth estimation from magnetic data [J]. Geophysics (2002), 67, 555-561.

[18] Thurston, J., Guillon, J. -C. and Smith, R. Model-independent depth estimation with the SPI™ method: SEG Expanded Abstracts (1999), 18,403-406.

[19] Thurston, J.B., and Smith, R.S. Automatic conversion of magnetic data to depth, dip, and susceptibility contrast using the SPI™ method: Geophysics (1997), 62, 807-813.

BILINGUAL PUBLISHING CO.
Pioneer of Global Academics Since 1984

Journal of Geological Research
https://ojs.bilpublishing.com/index.php/jgr-a

ARTICLE

Petrographic Characteristics and Geochemistry of Volcanic Rocks in the Kyaukmyet Prospect, Monywa District, Central Myanmar

Toe Naing Oo[1,2*] Agung Harijoko[1] Lucas Donny Setijadji[1]

1. Department of Geological Engineering, Faculty of Engineering, Gadjah Mada University, Yogyakarta, Indonesia
2. Department of Geology, Kyaing Tong University, Eastern Shan State, Myanmar

ARTICLE INFO

Article history
Received: 20 August 2021
Revised: 15 September 2021
Accepted: 16 September 2021
Published Online: 30 September 2021

Keywords:
Geochemistry
Petrography
Volcanic rocks
Calc-alkaline
Kyaukmyet prospect
Monywa district

ABSTRACT

The Kyaukmyet prospect lies approximately 5 km ENE of the high-sulfidation Kyisintaung copper-gold deposit, Monywa district, central Myanmar. Geologically, the research area is remarked by magmatic extrusion that occurred during the Late Oligocene to Middle Miocene of Magyigon Formation which led to the outcrops of volcanic rocks. Study detailed on petrographical and geochemical of the Kyaukmyet volcanic rocks has not been performed before the present work. The principal aim of this paper is to document the petrographical and geochemical characteristics of volcanic suite rocks exposed in the Kyaukmyet prospect. The results of this data have provided insight into the origin of the rocks and petrogenetic processes during evolution. Petrographically, all the studied volcanic rocks in the research area show that trachytic and porphyritic textures with phenocrysts of quartz, plagioclase, and K-feldspar which are embedded in a fine to medium grained groundmass. The accessory minerals of this rock consist of biotite, chlorite and opaque mineral. Geochemically, these volcanic rocks having calc-alkaline nature and classified as volcanic field (rhyolite) as well as volcanic arc setting. Based on the chondrite normalized spider diagram, LREE has enriched to HREE in this area which indicated negative Eu anomaly and subduction tectonic setting.

1. Introduction

Myanmar is a tectonically complex region which lies in the eastern margin of the India-Asia collision zone. It is characterized by the continuation of the 1500 km long still active dextral Sagaing Fault that extends from the eastern tip of Himalayan Syntaxis to the north and the Andaman Sea to the south [1-3]. Tectonogeographically, Myanmar is divided into two distinct geological provinces including the eastern part (Shan Thai Block) and the western part (West Burma Block) [4]. The eastern part is made up of the Shan Plateau, the Mogok Mandalay Mergui Belt and the Shan Scarps, whereas the western part is composed of the Indo-Myanmar Ranges, the Wuntho-Popa magmatic arc and overlying Cretaceous-Pliocene sedimentary formations [3,5] (Figure 1).

The Monywa district is tectonically situated in the active N-S trending the Wuntho-Popa magmatic arc which formed as a result of east dipping subduction in

*Corresponding Author:
Toe Naing Oo,
Department of Geological Engineering, Faculty of Engineering, Gadjah Mada University, Yogyakarta, Indonesia; Department of Geology, Kyaing Tong University, Eastern Shan State, Myanmar;
Email: toenaingoo.geol84@gmail.com

DOI: https://doi.org/10.30564/jgr.v3i4.3605

the Andaman-Sunda subduction zone that prolongs from the Gangdese through to the west of Myanmar, and to western Sumatra in the south [6] (Figure 1). In general, the Wuntho-Popa magmatic arc is one of the most important geological conditions as well as mineral belts in Myanmar. It is recognized by the occurrence of Late Cretaceous to Tertiary granodioritic batholiths, and minor Late Cretaceous to Quaternary volcanic rocks [7,8]. It is assumed that northern continuation of the Sunda-Andaman arc, is a N-S trending geanticlinal uplift which exposes Mesozoic intrusions and their host rocks.

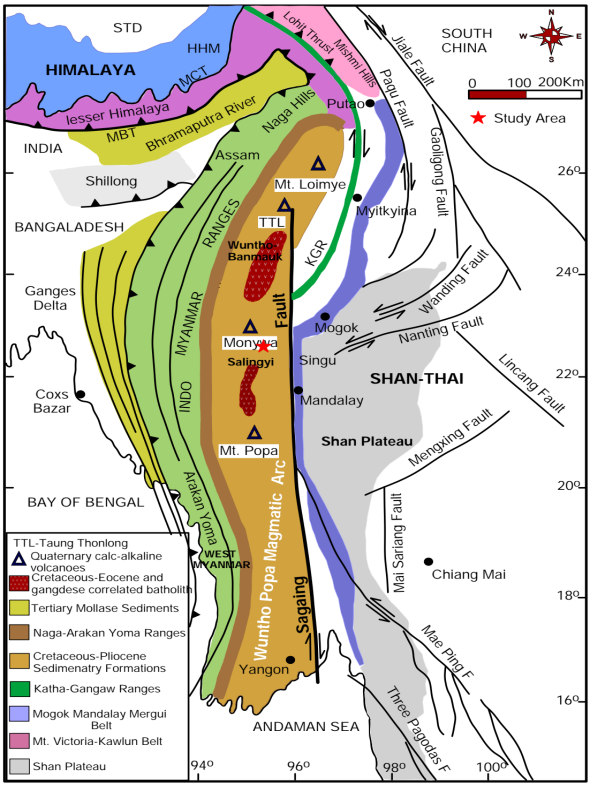

Figure 1. Simplified geologic map (modified from [1,3]) illustrating distribution of the main volcanoes and major geological units in Myanmar.

Accordingly, the Mesozoic rocks are further intruded by Cretaceous diorites and biotite granodiorites in the Monywa district. These units are subsequently overlain by Upper Oligocene to Middle Miocene volcanic and volcaniclastic rocks known as the Magyigon Formation including andesite, quartz andesite porphyry, dacite, rhyolite, tuff and lapilli tuff rock units (Figure 2). In addition, the sedimentary succession consists of a basal conglomerate with local limestone overlain by the Powintaung sandstone developing a west-facing scarp. Above are shales, cross-bedded sandstone, and local basalt breccia, with minor consist of interbedded andesitic tuff in the upper part, comprising the Magyigon Formation, which includes debris flow deposits with rhyolites (Figure 2). The basement rocks are overlain locally by volcanic rocks and both are overlain unconformably by eastward-dipping quartz-ofeldspathic sandstone of probable Eocene age, with a prominent west-facing scarp slope at Powintaung. Zircon geochronology data reveal that the rocks that area present within the Monywa district consist of Cretaceous-age basement, Oligocene rhyolitic volcanic formed 27-24 Ma, and Miocene andesite porphyry with an emplacement age of 19 Ma [9] respectively. Studies detailed on petrographical and geochemical of the volcanic rocks are still absent till date to constrain the petrogenesis and evolution of the volcanic rocks. In this paper contribution, we present our work on the petrography and geochemical data for the volcanic rocks in order to understand the characteristics of volcanic rocks, magmatic evolution processes during their genesis and implications on their emplacement.

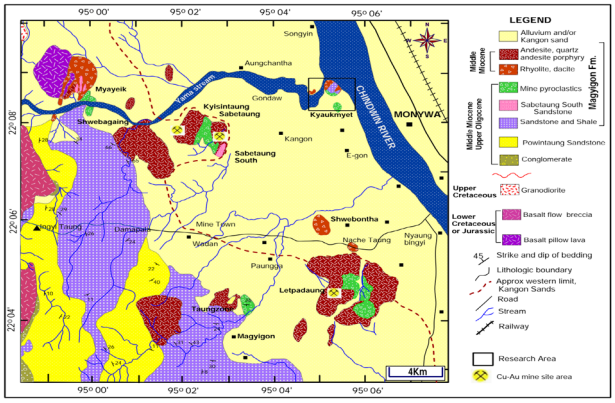

Figure 2. Regional geological map of Monywa copper-gold district and the black rectangle is the Kyaukmyet prospect, modified from [10].

2. Geology of the Kyaukmyet Prospect

The Kyaukmyet prospect is located in the western part of Chindwin River (Monywa city), Monywa district, which is a part of the Wuntho Popa magmatic arc (Figure 1,2). The geology of the Kyaukmyet area is characterized by the occurrence of sedimentary, volcanic, and volcaniclastic rocks of the Late Oligocene to Middle Miocene Magyigon Formation. Physiographically, the Kyaukmyet area is situated at the confluence of two large rivers including the Yama Stream and the Chindwin River. In the Kyaukmyet prospect, exposed rock units are dominated by a sedimentary succession consisting of cherty or siliceous mudstone, siltstone, and quartzofeldspathic sandstone and volcaniclastic and volcanic units of tuffaceous rocks, lapilli tuff, and rhyolite (Figure 3). In the research area, a simplified geological map indicates the presence of rhyolite and lapilli tuff as the predominant rock units

at the northern and southeastern part of the Kyaukmyet prospect. These rocks are further intruded by small distributed silicified sandstone, mudstone and siltstone unit. In outcrop, the fresh surface of the rhyolites are usually yellowish to light grey colour and flow banding nature (Figure 4a,4b). The surfaces of the lapilli tuffs are often coated by white to reddish colour ash in fresh surface due to alteration effects (Figure 4c,4d) Stratigraphically, silicified sandstone, mudstone, and siltstone are the oldest rock units. These units crop out in the western and central parts of the research area. Geological structures in the research area prominently trend in an ENE-WSW direction. This structural trend would be controlled by movement along the Chindwin and Monastery Faults. It has been speculated that these northeast-trending structures might be subjected to dextral movement similar to the movement on the well-studied Sagaing Fault [11,12].

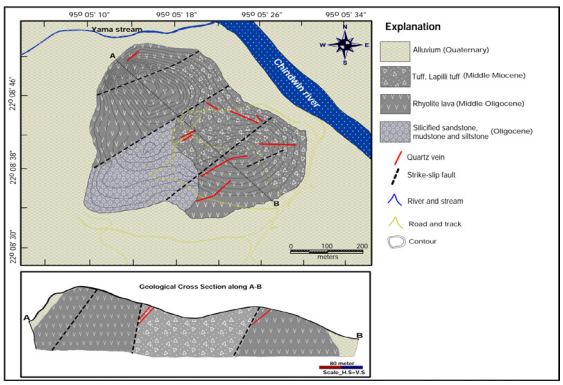

Figure 3. Simplified geological map of the Kyaukmyet prospect, Monywa district, central Myanmar and cross section along A-B is also shown modified from [13].

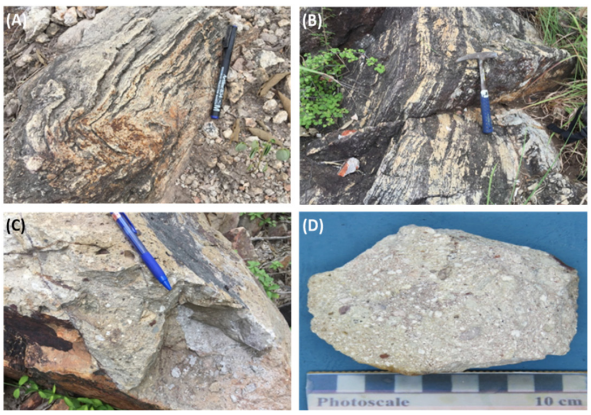

Figure 4. Representative field photographs of (a,b) flow banding outcrop nature of rhyolite unit, (c) lapilli tuff unit showing white to reddish colour ash in fresh surface due to alteration effects, and (d) hand specimen sample of lapilli tuff.

3. Materials and Methods

Based on the field and petromineralogical studies, a total of thirty-four (34) representative samples were collected from the surface outcrop in the Kyaukmyet prospect area. Of these samples, 10 representative samples were prepared for thin-sections with a thickness of approximately 0.03 mm and studied under polarizing microscope NIKON E600POL in order to examine their mineralogical compositions as well as textural characteristics. Subsequently, a total of 24 representative rock samples were selected for whole-rock geochemistry. The concentrations of major and minor elements of 12 volcanic rocks were analyzed by X-ray fluorescence Spectroscopy using a RIGAKU RIX-3100, with relative standard deviations < 5%. For quality control, the reference sample JA-3 was applied as standard sample. The XRF analyses were conducted at the Department of Earth Resource Engineering, Mineral Resource lab, Kyushu University, Fukuoka, Japan and the X-ray machine was carried out at a voltage of 50 kV and a current of 50 mA, scanning speed: automatic and 4°/min for the determination of major and trace elemental compositions. The loss on ignition (LOI) was measured for all of volcanic rock samples by weight difference after ignition at 105°C for 1.5 h first, followed by 500°C for 1 h and 900°C for 2 h. In this study, rare earth elements (REEs) of the 12 samples of volcanic rocks were also analyzed in the same institute by Inductively Coupled Plasma-Mass Spectrometry (ICP-MS) using the open system rock digestion method.

4. Results and Discussion

4.1 Petrographic Characteristics

The rhyolite lava shows as a trachytic texture, which represents preferred orientation of the minerals (Figure 5a,5b). It is dominantly composed of quartz, plagioclase, alkali feldspar and trace amount of biotite and opaque minerals which are embedded in a flow banded rhyolite nature (Figure 5a,5b).

Quartz displays that anhedral to subhedral and plagioclase occurs as phenocrysts, usually euhedral and K-feldspar, also as phenocrysts shows alteration and albitization. The size of the phenocrysts generally ranges from 0.2 mm to 2.5 mm and groundmass minerals <0.1 mm respectively. Phenocrysts of plagioclase and K-feldspar are subhedral to anhedral and developed a wide range of size characterizing trachytic texture (Figure 5a,5b). Flow direction is marked by the presence of parallel oriented plagioclase, biotite and quartz bands defining a preferred orientation.

Rhyolite lava also displays as a porphyritic texture and consists predominantly of quartz, K-feldspar and traces

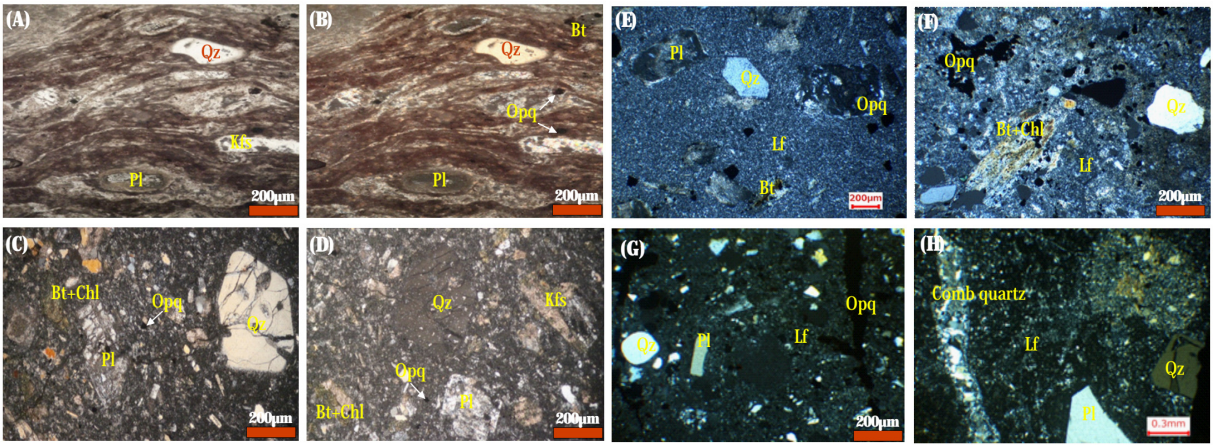

Figure 5. Representative photomicrographs showing common textures in the volcanic rocks (a-b) phenocrysts of euhedral plagioclase, K-feldspar and anhedral to subhedral quartz in trachytic texture of rhyolite, (c-d) euhedral quartz phenocrysts with hexagonal outline in rhyolite, plagioclase, K-feldspar and biotite in an aphanitic matrix, (e) plagioclase, quartz and opaque minerals observed in the lithic fragments, (f) quartz, opaque mineral (pyrite) and biotite altered to chlorite occur in the lithic fragments, (g,h) quartz, plagioclase, comb quartz and opaque minerals occurred in the lithic fragments. Mineral abbreviations: Qz, quartz; Pl, Plagioclase; Bt, biotite; Chl, chlorite; Opq, opaque mineral; Lf, lithic fragment.

amount of biotite and opaque minerals. The phenocrysts of quartz and K-feldspar are distributed throughout a hypocrystalline matrix. In general, phenocrysts of quartz crystals are larger than K-feldspar and it often contains euhedral with corrosion gulfs. The size of the phenocrysts generally ranges from 0.4 mm to 4 mm and groundmass minerals, <0.2 mm. Phenocrysts of amphibole and biotite are much rare, and are partially chloritized. Opaque minerals occur as finely dispersed throughout the rock. The content of quartz is approximately 35% of the total volume of the constituent minerals. Quartz occurs as phenocrysts as well as a groundmass. Some phenocrysts of quartz are characterized by the occurrence of euhedral hexagonal outline (Figure 5c,5d). Between crossed-nicols, it gives first order grey interference color. K-feldspar belonged to subhedral with a grain size that varied from 0.5 to 4.0 mm. Plagioclase crystals have a tabular and elongated shape and commonly occur with corroded and broken edges (Figure 5c,5d). It belonged to subhedral to euhedral, ranges from 0.8 to 3 mm in size, and typically displays sharp contacts. Feldspar is also comprised of phenocrysts as well as a groundmass and some feldspar phenocrysts show perthitic texture and incline extinction with extinction angle 22°. Between cross-nicols, it yields nearly parallel or straight extinction. Biotite contains 6% of total volume of constituent minerals. It is well recognized by its color yellow or yellowish brown and its perfect one set cleavage. Sometimes, it is altered to chlorite (Figure 5c,5d). Other opaque minerals also present in minor amount.

In the research area, lapilli tuff is primarily composed of fine to medium-grained crystalline quartz with lithic fragment cemented by the fine-grained matrix. This unit is mainly comprised of 40-50% of quartz, 20-30% of clay minerals, 20-25% of plagioclase and 5-10% of opaque minerals respectively. Quartz occurs as phenocrysts and spherulite in the lithic fragments which is associated with opaque mineral (pyrite) (Figure 5e-g). Chlorite appears as the replacement of biotite and illite occurring as the replacement of plagioclase (Figure 5f). The lapilli tuff unit is characterized by porphyritic and fragmental textures. They are strongly altered and the size of fragments ranges from 0.1mm to 1mm in diameter. Originally, this unit has the moderately sorted with grains surrounded by cryptocrystalline volcanic material as a matrix. In addition, quartz veinlet and comb quartz occur in the lithic fragments (Figure 5h).

4.2 Whole Rock Geochemistry

4.2.1 Geochemical Classification

Major (wt%), trace and rare earth element (ppm) concentrations of the volcanic rock samples from the Kyaukmyet prospect are shown in Table 1 and Table 2. The volcanic rocks from the Kyaukmyet prospect mainly comprised of rhyolite and lapilli tuff. These volcanic rocks show 71.84-86.29 wt.% SiO_2, 0.099-0.338 wt.% TiO_2, 6.707-19.29 wt.% Al_2O_3, 0.483-2.881 wt.% FeO, 0.312-0.89 wt.% MgO, 0.38-0.432 wt.% Na_2O, 0.083-5.483 wt.% K_2O, 0.071-0.128 wt.% CaO, 75-160 ppm Zr, 51-590 ppm Ba, 21-210 ppm Sr, 5-8 ppm Nb, 12-18 ppm Y, 1-196 ppm Rb, 3-49 ppm Cr Table 1.

Table 1. Whole-rock major- and trace-element concentrations of volcanic rocks from the Kyaukmyet prospect.

Sample ID	KMR17	KMR14a	KMR12	KMR9	KMR2	KMR7	KMLP5	KMLP3	KMLP9	KMLP10	KMLP6	KMLP4
Major elements (in wt%)												
SiO_2	78.33	73.79	81.68	78.47	71.95	71.84	82.59	83.37	85.69	86.29	84.22	85.27
TiO_2	0.194	0.207	0.099	0.187	0.219	0.216	0.321	0.27	0.312	0.338	0.257	0.238
Al_2O_3	13.58	17.94	9.098	13.48	15.47	19.29	9.041	6.723	7.002	7.167	6.707	7.682
FeO	0.529	0.82	0.833	0.483	0.947	0.84	1.658	2.02	2.881	0.76	2.382	2.033
MnO	n.d	n.d	n.d	n.d	n.d	n.d	n.d	0.002	n.d	n.d	0.004	n.d
MgO	0.783	0.312	0.663	0.763	0.889	0.341	0.593	0.692	0.408	0.727	0.678	0.369
CaO	0.128	0.08	0.117	0.116	0.12	0.085	0.08	0.082	0.097	0.077	0.13	0.071
Na_2O	0.413	0.378	0.432	0.378	0.409	0.384	0.388	0.385	0.384	0.401	0.387	0.379
K_2O	1.337	0.083	5.483	1.296	1.616	0.095	1.043	1.413	0.199	1.226	1.186	0.204
P_2O_5	0.028	0.079	0.008	0.037	0.19	0.08	0.055	0.065	0.026	0.003	0.043	0.071
H_2O	4.6	6	1.5	4.71	7.2	6.79	3.89	4.16	2.89	2.83	3.46	3.42
S	0.028	0.016	0.011	0.023	0.809	0.018	0.245	0.712	0.059	0.127	0.464	0.138
Total	**99.95**	**99.71**	**99.92**	**99.94**	**99.82**	**99.98**	**99.90**	**99.89**	**99.95**	**99.95**	**99.92**	**99.88**
Trace elements (in ppm)												
V	13	30	6	13	10	21	19	15	20	22	14	22
Cr	21	10	5	8	11	3	33	25	48	49	25	33
Co	24	23	37	29	32	17	20	38	32	29	22	25
Ni	10	6	10	10	6	7	8	7	10	10	5	7
Cu	12.04	5.03	20.08	0.4	43.07	3.03	11.01	6.07	10.02	13.01	40.01	16.02
Zn	8.4	7.1	11.02	12.7	11.01	22.8	22.1	10.92	16.31	11.8	13.2	21.9
Pb	27.39	12.01	0.8	14.45	11.08	3.09	34.06	4.02	0.09	31.06	3.19	1.19
As	48	23	38	35	106	25	128	162	84	19	127	463
Mo	8	14	5	7	13	14	7	8	4	5	6	7
Rb	64	1	196	62	56	0	47	62	7	67	62	6
Sr	63	113	31	73	210	107	64	78	68	21	40	157
Ba	59	103	299	113	590	96	70	450	107	51	335	387
Y	13	16	18	14	14	16	17	18	15	18	12	16
Zr	135	145	75	130	155	152	160	137	138	157	131	129
Nb	6	6	8	7	7	7	7	5	6	7	5	6

Table 2. Rare earth element (ppm) concentrations of volcanic rocks from the Kyaukmyet prospect.

Sample ID	KR17	KR14a	KR12	KR9	KR2	KLP4	KLP7	KLP3	KLP10	KLP9	KLP5	KLP6
Rare earth elements (in ppm)												
La	25.4	10.7	26.9	22.6	23.1	25.7	20.5	13.6	11.9	38.3	18.34	18.2
Ce	44.7	19.9	47.9	41.5	43.2	48.0	36.4	26.6	22.0	64.2	35.05	32.4
Pr	4.10	1.83	4.56	3.83	4.13	4.71	3.5	2.78	2.23	5.76	3.49	3.27
Nd	15.2	6.43	18.9	14.9	16.1	19.0	13.6	11.0	8.88	22.34	15.2	12.9
Sm	1.76	0.91	2.50	1.86	2.21	2.73	2.11	1.44	1.45	2.72	2.298	1.82
Eu	0.54	0.31	0.64	0.45	0.33	0.67	0.56	0.31	0.29	0.56	0.64	0.37
Gd	2.41	1.21	3.26	2.85	2.81	3.48	2.82	1.95	1.69	3.75	2.75	2.4
Tb	0.21	0.14	0.33	0.23	0.32	0.31	0.27	0.18	0.24	0.32	0.25	0.21
Dy	1.58	1.18	1.71	1.57	2.16	1.78	1.75	1.25	1.49	2.19	1.55	1.19
Ho	0.23	0.21	0.25	0.24	0.35	0.32	0.26	0.19	0.30	0.33	0.24	0.17
Er	0.83	0.71	0.88	0.76	1.21	0.98	0.89	0.65	0.93	0.899	0.74	0.67
Tm	0.14	0.12	0.13	0.14	0.23	0.15	0.16	0.09	0.17	0.15	0.12	0.10
Yb	0.94	1.04	1.12	1.01	1.74	1.04	1.05	0.87	1.17	1.18	1.13	0.85
Lu	0.15	0.15	0.15	0.16	0.25	0.16	0.16	0.12	0.198	0.15	0.16	0.13

On the Nb/Y-Zr/TiO_2 chemical classification diagram [14], all volcanic samples fall within the field of rhyolite/dacite (Figure 6a). The tectonic settings of volcanic rocks are adopted classification scheme of Zr-TiO_2 discrimination diagram [15]. In the Zr-TiO_2 plot diagram, most of rock samples are plotted in the field of the volcanic arc setting (Figure 6b). It is also possible that the overlap is due to the involvement of sub-continental lithosphere in magma genesis as pointed out by Watters and Pearce (1987) [16]. According to binary plot diagram of SiO_2 versus Na_2O+K_2O (Irvine and Baragar, 1971) [17], volcanic rocks of the Kyaukmyet prospect area are shown the nature of subalkaline to alkaline affinity (Figure 7a). AFM diagram is commonly used to distinguish between tholeiitic and calc-alkaline differentiation trends in the sub-alkaline magma series. Volcanic rocks from the Kyaukmyet prospect were plotted on the AFM diagrams [17], Triangular AFM plot suggests that most of volcanic rocks fall within the sub-alkaline field (Figure 7b). Calc-alkaline is typical magma resulted from subduction zone [18].

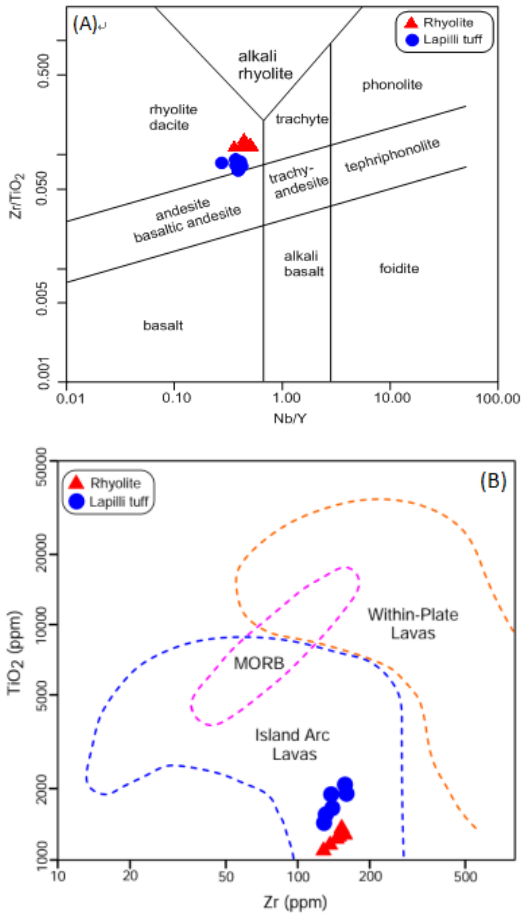

Figure 6. (a) Zr/TiO_2 vs Nb/Y plot diagram showing volcanic rocks classification [14], (b) Zr-TiO_2 tectonic discrimination diagram for volcanic rocks of the Kyaukmyet prospect [15].

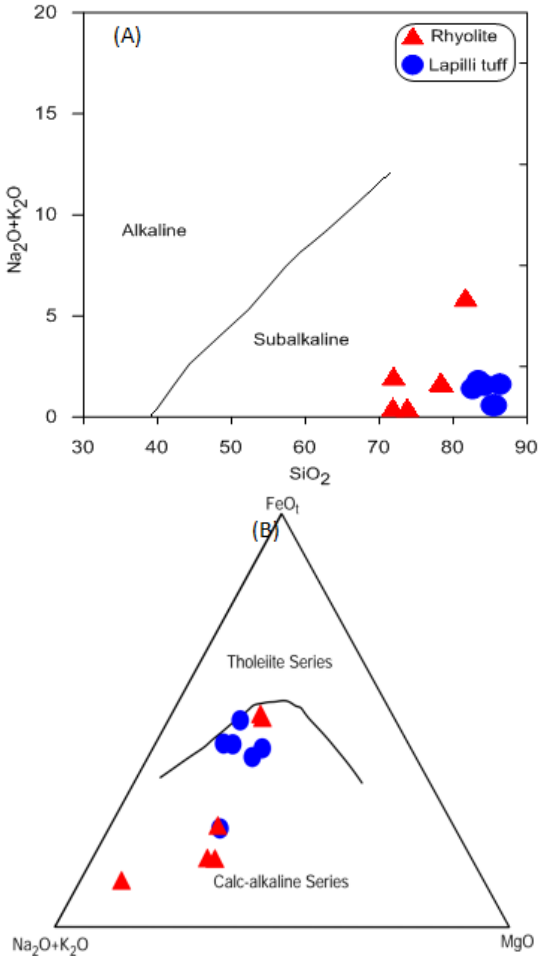

Figure 7. (a) Alkali-silica diagram for determining subalkaline and alkaline field and (b) AFM diagram showing whole-rock composition in terms of Na_2O+K_2O, total iron as FeO and MgO [17].

4.2.2 Geochemistry of Trace Elements

In the research area, most of the volcanic rock samples have been altered. In order to determine the compositional change which, accompany hydrothermal alteration. Generally, Zr is used as an immobile element during hydrothermal alteration because of very high radius. For the magmatic evolution processes, SiO_2 and some of major oxide elements cannot be used as a result of alteration effect. Therefore, immobile element (Zr) is used in order to instead of SiO_2 in this study. Trace element contents of the Kyaukmyet volcanic rock samples are plotted on the variation diagram to show Zr versus Sr, Y, NB, Rb, Ba and Cr (Figure 8).

Trace element variation diagram in this study exhibits that Cr versus Zr display negatively correlation (Figure 8) which are recognized to be mobile with altered volcanic rock during hydrothermal alteration. In addition, compati-

ble element Cr decreases with Zr increasing fractionation. Sr, Ba versus Zr negative correlation that is subjected to be most mobile during alteration (Figure 8). Additionally, they show a fairly positive correlation between Zr and Nb and Y (Figure 8). This positive trend is considered to be immobile in the volcanic rocks. Furthermore, Zr versus Rb and Nb are enriched immobile while impacting hydrothermal alteration.

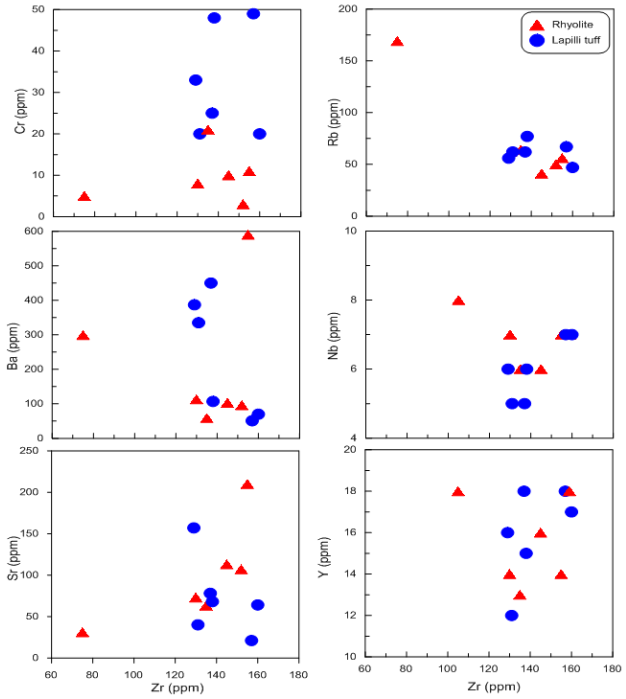

Figure 8. Trace elements variation diagram for volcanic rocks of the Kyaukmyet prospect with Zr.

In the chondrite-normalized diagram (Boynton, 1984) (Figure 9), the volcanic rocks (rhyolite and lapilli tuff) are almost enriched than LREE/HREE ratio. The concentrations of light rare earth elements (LREE) of rhyolite and lapilli tuff rock units are generally elevated (La; 10.7-38.3 ppm, Ce; 19.9-64.2 ppm, Pr; 1.83-5.76 ppm, Nd; 6.43-22.34 ppm and Sm; 0.91-2.72 ppm) in contrast to the depleted heavy rare earth elements (HREE). In this figure, the rhyolite and lapilli tuff rock units are relatively enriched than LREE/HREE ratio. Moreover, the chondrite-normalized REE patterns of rhyolite and lapilli tuff rock units are similar to those of the upper continental crust (Figure 9). They show LREE enrichment but HREE depletion in which all samples display negative Eu anomalies indicating its deplection in the upper continental crust. This would probably be resulted from the removal of feldspar (Plagioclase) from the source rock during the crystal fractionation [18].

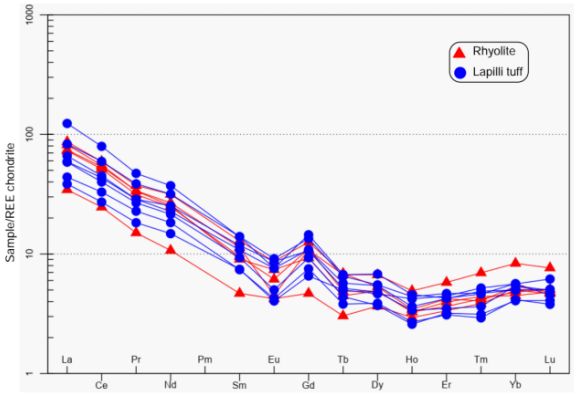

Figure 9. Chondrite-normalized spider diagrams for volcanic rocks from the Kyaukmyet prospect. Using the normalization and ordering scheme of [19].

5. Conclusions

Petrographical studies of volcanic rocks (rhyolite and lapilli tuff) from the Kyaukmyet area point out that they were composed mainly of quartz, plagioclase (phenocryst), K-feldspar and opaque minerals. Accessory minerals in these rocks are opaque mineral, biotite and chlorite. In some cases, plagioclases are strongly altered to clay minerals, sericite, and chlorite. On the other hand, volcanic rocks (rhyolite, lapilli tuff) display that trachytic and porphyritic textures with phenocrysts of quartz, plagioclase, and K-feldspar in which various shades of colour i.e. colourless, pink, grey etc. In this study, geochemical and tectonic discrimination diagrams indicated that volcanic rocks are plotted in the rhyolite/dacite field as well as calc-alkaline area. In trace element variation diagram, Zr displays negatively correlated with Cr and Ba which are considered to be mobile with altered volcanic rocks during hydrothermal alteration. On the other hand, Zr shows a fairly positive correlation between Nb and Y. This positive trend is suggested to be that immobile in the volcanic rocks. On the basis of the chondrite normalized spider diagrams, LREE have strongly enriched to HREE in this area which indicated negative Eu anomaly and subduction tectonic setting.

Author Contributions

T.N.O., K.Z.O and T.Z carried out the fieldworks and developed the concepts, designed on this research. T.N.O. collected the data and samples as well as conducted the laboratory analysis and wrote this manuscript with contribution on discussion from K.Z. All authors were contributed in reading, comments and giving the annotations on this manuscript.

Funding

This study was supported by AUN/SEED-Net and JICA program.

Conflicts of Interest

The authors declare no conflict of interest.

Acknowledgements

This paper is a section of the first author's PhD thesis completed at Department of Geological Engineering, Faculty of Engineering, Gadjah Mada University, Yogyakarta, Indonesia. The authors would like to express sincere thanks to AUN/SEED-Net and JICA program for their financial support. We are extremely grateful to Prof. Dr. Akira Imai and Assoc. Prof. Dr. Kotaro Yonezu as well as laboratory members from the Department of Earth Resource Engineering, Kyushu University, Japan for their supports for laboratory analysis and insightful suggestions on data interpretation. Special thanks are also given to Mr. Kyaw Zin Oo and Mr. Than Zaw for their kind helps and supports during the fieldwork. Finally, we are grateful to Prof. Dr. Khin Zaw who help and valuable suggestions into the geological information of Monywa district.

References

[1] Searle, M.P., Noble, S.R., Cottle, J.M., Waters, D.J., Mitchell, A.H.G., Hlaing, T. and Horstwood, M.S.A. Tectonic Evolution of the Mogok Metamorphic Belt, Burma (Myanmar) Constrained by U-Th-Pb Dating of Metamorphic and Magmatic Rocks. Tectonics, 2017, 26, TC2083.

[2] Mitchell, A.H.G., Htay, M.T., Htun, K.M., Win, M.N., Oo, T. and Hlaing, T. Rock Relationships in the Mogok Metamorphic Belt, Tatkon to Mandalay, Central Myanmar. Journal of Asian Earth Sciences, 2007, 29, 891-910.

[3] Lee, H.-Y., Chung, S.-L. and Yang, H.-M. Late Cenozoic Volcanism in Central Myanmar: Geochemical Characteristics and Geodynamic Significance. Lithos, 2016, 245, 174-190.

[4] Liu, C.Z., Chung, S.-L., Wu, F.-Y., Zhang, C., Xu, Y., Wang, J.-G., Chen, Y. and Guo, S. Tethyan Suturing in Southeast Asia: Zircon U-Pb and Hf-O Isotopic Constraints from Myanmar Ophiolites. Geology, 2016, 44, 311-314.

[5] Gardiner, N.J., Robb, L.J. and Searle, M.P. The Metallogenic Provinces of Myanmar. Applied Earth Science, 2014, 123, 25-38.

[6] Zaw, K., Meffre, S., Lai, C.K., Burrett, C., Santosh, M., Graham, I., Manaka, T., Salam, A., Kamvong, T., Cromie, P. Tectonics and metallogeny of mainland Southeast Asia - A review and contribution. Gondwana Res, 2014, 26 (1), 5-30.

[7] Mitchell, A.H.G., Chung, S.L., Oo, T., Lin, T.H., Hung, C.H. Zircon U-pb ages in Myanmar: Magmatic-metamorphic events and the closure of a neo-Tethys ocean? J. Asian Earth Sci. 2012, 56, 1-23.

[8] United Nations. Geology and Exploration Geochemistry of the Pinlebu-Banmauk area, Sagaing Division, Northern Burma "Draft", Technical Report No. 2. DP/UN/ BUR-72-002, Geological Survey and Exploration Project. United Nations Development Programme. United Nations, New York, 1978, (p. 69).

[9] Knight, J., Zaw, K. The geochemical and geochronological framework of the Monywa high sulfidation Cu and low sulfidation Au-epithermal deposits, Myanmar. Poster No. 104 presented at the SEG, Conference; 27-30 September, 2015, Hobart, Tasmania, Australia.

[10] Mitchell, A.H.G., Myint, W., Lynn, K., Htay, M.T., Oo, M., Zaw, T. Geology of the High Sulfidation Copper Deposits, Monywa Mine, Myanmar. Resource Geology, 2011, 61: 1-29.

[11] Zaw, K. Comments on transcurrent movements in the Myanmar-Andaman Sea region. Geology, 1989, 17: 93−95.

[12] Zaw, K. Geological, petrological and geochemical characteristics of granitoid rocks in Burma: with special reference to the associated W-Sn mineralization and their tectonic setting. Journal of Southeast Asian Earth Sciences, 1990, 4: 293-335.

[13] Htet, W.T. Volcanic-hosted gold-silver mineralization in the Monywa mining district, central Myanmar. PhD. Dissertation, 2008, Mandalay University, Myanmar.

[14] Pearce, J. A. A user's guide to basalt discrimination diagrams. In: Wyman, D. A. (ed.) Trace Element Geochemistry of Volcanic Rocks: Applications for Massive Sulfide Exploration. Geological Association of Canada, Short Course Notes, 1996, 12, 79-113.

[15] Pearce, J. A. Trace element characteristics of lavas from destructive plate boundaries. In: Thorpe R.S. (ed.) Andesites: Orogenic Andesites and Related Rocks. John Wiley & Sons, Chichester, 1982, pp. 525-548.

[16] Watters, B.R. and Pearce, J.A. Metavolcanic rocks of the La Ronge Domain in the Churchill Province, Saskatchewan: geochemical evidence for a volcanic arc origin, *in*: Pharaoh, T.C., Beckinsale, R.D., Richard, D. (Eds.), Geochemistry and Mineralization of Pro-

terozoic Volcanic Suites Geological Society, Special Publications, 1987, vol.33, pp. 167-182.

[17] Irvine, T.N., and Baraga, W.R.A. A guide to the chemical classification of the common volcanic rocks. *Can. J. Earth Sci*, 1971, 8, 523-548.

[18] Wilson M. *Igneous petrogenesis*, 1989, Unwin Hyman, London.

[19] Boynton, W.V. Cosmochemistry of the Rare Earth Elements: Meteorite Studies. In: Henderson, P., Ed., Developments in Geochemistry, Elsevier Sci. Publ. Co., Amsterdam, 1984, 63-114.

BILINGUAL PUBLISHING CO.
Pioneer of Global Academics Since 1984

Journal of Geological Research
https://ojs.bilpublishing.com/index.php/jgr-a

ARTICLE

Analysis of Groundwater Quality in Jabal Sarage and Charikar Districts, Parwan, Afghanistan

Hafizullah Rasouli*

Department of Geology, Geoscience Faculty, Kabul University, Jamal Mina 1006, Kabul, Afghanistan

ARTICLE INFO

Article history
Received: 15 September 2021
Revised: 28 October 2021
Accepted: 30 October 2021
Published Online: 3 November 2021

Keywords:
Groundwater
Water quality
Total Dissolved Soled (TDS)
Solved Salt in Water (SSW)

ABSTRACT

This groundwater research is carried out groundwater quality in Jabal Sarage and Charikar Districts. The main objective of this research is to find out natural causes of drinking water contaminations (toxic elements and components), that are leaching from soluble arrangement of rocks, sediments and soil by surface water at the infiltration time, toward the groundwater. For completion this research I used two categories of water analysis; one is areal analysis, and another is laboratory analysis. In areal analysis ten wells have been recovered by this research in Jabal Sarage and Charikar Distracts, a number of Electro-Conductivity, water temperature, dissolved oxygen in water, Total Dissolved Soled (TDS) and the Resolved Salt in Water (SSW), determination Partible ground at areal complete. For laboratory works I used chemical device of Spectra- photo model. From comparing mean of chemical and physical parameters with standards. pH, K, Na, Mg, Cl, Fe, F, TH, Ca and SO_4 all are normal and we can use them for drinking and irrigation waters. The challenges that I faced during this research are; absence of research in this area and lack of geological equipment's.

1. Introduction

Afghanistan is a country dominated by a dry climate, with most of the area Characterized by effects of global climate changes on hydrological systems, especially on mountain snow and glacier melting, can modify the timing and amount of in mountain watersheds. Therefore, accurate stream flow simulation and forecast is of great importance to water resources management and planning [25]. The key watercourses drain at the snowmelting times (from January to May), raining periods (March to April) and occasionally through quick overflowing terms (May to August), the main elevations of snow cover is Parwan Maintains series, Wardak, Loger, Baba, Spingher, Salang, Kohkurugh, Koha Safi, Hindu Kush mountains ranges in Afghanistan" [1,24,25], as well as here is certain cold provinces for example; Bamyan, Wardak, Loger, Badakhshan, Pangesher, Parwan, some parts of Kabul, snow covers these areas from September to November and its storing is used for water in Afghanistan [5,6,24].

Likewise, in north sides of Afghanistan, here are specific glaciers; Pamir Badakhshan, Mymai Badakhshan, Panjsher mountains range that belong to the Hindu Kush mountains series in Afghanistan. These are main sources

*Corresponding Author:
Hafizullah Rasouli,
Department of Geology, Geoscience Faculty, Kabul University, Jamal Mina 1006, Kabul, Afghanistan;
Email: hafizullah.rasouli133@gmail.com

DOI: DOI: https://doi.org/10.30564/jgr.v3i4.3717

for Panjsher, Helmand and Koner Rivers [2-4]. In particular provinces, we use rivers as a mean for irrigations and water supply (Drinking water), such as; Bamyan, Panjsher, Wardak, Parwan, Helmand and Kandahar, Kapesa, but in some of these provinces for instance; Wardak, Parwan, Panjsher spending from spring, and in several provinces for drinking and irrigation benefit from Kariz water, and some other provinces benefit from wells [3].

In these basins, all regolith and sediments are transported from different points of Parwan, mountains by sudden floods and Panjsher, Sanlang, Gurband and Shetal Rivers its accumulated at the different thickness in different locations of this basin. The Parwan Basins belongs to Quaternary (Pleistocene) and Neogen geological periods, different sediments are deposited after one another and forms of morphology, which we can see at the different reliefs. Types of sediments in this basin directly belong the kinds of rocks located in surrounding mountains. In these sediments, we can see Garnete, Biotite and Muscovite minerals particles. The surrounding mountains of this basin are formed from metamorphic rocks like; Schist, Gneiss and Slate that is called Crystalline [19].

Hydrogeological and geological studies are very important for these sedimentary basins, because in all villages, health centers and industrials organizations groundwater is from wells, Kariz and spring. The Panjsher, Sanlang, Gurband and Shetal Rivers are main rivers flows between these basin and more groundwater recharge from river bank and bed, especial in snowmelting season. The aquifers of this sedimentary basin are located prolonging of these Rivers and its tributaries. The more aquifers are between different sizes of sediments (sands and gravels). The hydrogeology of Jabal Sarage and Charikar sedimentary basins belong to the different aquifer that are located prolonging mountain range in longitudinal valley. The thickness and depth of aquifers are related to the slope and distance from mountain range, generally near to mountain and slope areas there are gravels and angular materials, but far from mountains are rounded and fine materials like bolder, cobble, pebble, granule, sands and silts. For drinking water generally using shallow wells, deep wells, but in some places benefit from spring water at the fracture zones and they install pipe scam for gravity pumping system and distributed water among villages [22].

The Degree of acidic is belonging to the soils pH, and formation of acids belong to the chemical characteristics of soils. Also related to the elements and components that are located at the air and after rains washing the air and infiltrate in the soils. Activities of some animal and different plants also will be acidification of soils. In addition mutual effect of biochemical, solution particles of rocks and minerals that located between soils and its absorption by colloids done some reactions of Cation exchange capacity and basic exchange capacity in some parts of soils mass. The groundwater movements from aquifer layers by different speeds and wash soluble materials from different layers. Some soluble load from parent materials produced different elements and components. Industrial activities for example; burn coal and oil in the predictable materials factory, vehicles and permanent melting of plastics and metals at the result more amount of different gases gone to the atmosphere with different type of precipitations again come down to the earth surface and product different toxic elements between soils. Due to many years of wars we couldn't conduct many researches. So, many researches are accommodated to be carried out and one of these research is soil, air and water pollution [23].

The basins can be described as a valley fill basins, where are filled with Quaternary and Tertiary sediments, gravels, and sedimentary rocks. Quaternary sediments are typically less than 80 m thick in the valleys. The underlying Tertiary sediments have been estimated to be as much as 1000 m thick in the valley Center. The gravel and sand were deposited mainly in the river channels. Describe the Lataband Formation as Quaternary terrace sediments younger Pleistocene age overlying conglomerates. The surrounding mountains are primarily composed of Paleoproterozoic gneiss and Late Permian through Late Triassic sedimentary rocks. The interbasin ridges, composed of metamorphic complex rocks, are Paleoproterozoic gneiss. The Khengal and basement rocks are over thrust by schist mélange, which has been called the Cottagay Series, in the northern Salang range. The sediments of Khengal series is started from Jurassic and belongs to the Thythes Ocean in Afghanistan [20].

Triassic clays and Paleozoic schist form impermeable substratum of this aquifer. These carbonate formations burrow under the Mio-Plio-Quaternary cover in the basins, which forms a deep confined aquifer. The depth of the Miocene Marls forming the impermeable roof of this aquifer is about 1500 m in the contact with Prerif Ridges at drilling point. The fracture rocks constitute the groundwater reservoirs. The main parameters for the migration of fluids in fractured rocks are the main geological characteristics of the fracturing, drainage, topography and rainfall. The hydrogeological context of different regional structures implies the existence of groundwater tables. E1 Hajeb-Ifrane Tabular is a free water table circulating in the Limestone's and Dolomites. It is supplied directly by precipitation [12-15].

Three rivers flow 12 months, such as Helmand, Panjsher, Koner, but particular rivers related to snowmelting sea-

sons and rainy periods for example Kabul, Paghman, and Loger River. The third river is related to the flooding seasons, its involving of some valleys and mountains areas [8,9]. As the result of 20 years climate change and drought in Afghanistan, the irrigation and drinking water using from groundwater storages (wells, Kariz and springs), its percolated from surface waters, during snowmelting periods [5,2]. In Afghanistan, for one year storing 75 million meter cubic fresh water, from this water is 57 million meter cubic consist of surface water, from these only 18 million meter cubic involves groundwater. Meant from 100 % in Afghanistan 76 % waters consist of surface water and 24 % water consist of groundwater [7,10].

1.1 The Main River Basins of Afghanistan

Afghanistan mainly has four river basins that contains:

Amodarya Basin, it consists the Wakhan, Kokcha, Konduz, Andrab and Khenjan Basins; North Rivers Basin, Balkhab and Sarepol Rivers Basins; West River Basin, Harirud, Marghab, Shrine Tagab, Adraskan, Koshan, Kaysar, Gulran and Khasherud; Helmand River Basin, Arghandab, Gazny, Trang, and Musa Qala [11].

In this research I investigated water quality in Jabal Sarage and Charikar Districts have of Parwan Province. The main independent of this study is to nominate dissimilar kinds element, components in Groundwater in Jabal Sarage and Charikar Districts. The Parwan is placed in north sideways of Kabul Province. The climate of this province is simi-arid, wind direction is flows from north toward south, and it is started from Hindu Kush Mountains Ranges [6,18]. The hydro - meteorological situations in the winter seasons snow fall and at the spring seasons having rain fall, the amount of whole annual precipitation is 300-400 mm, and at Salang Mountain total annual precipitation is 800-1000 mm, the higher mean air temperature is between 25 - 30 ºC at the summer season and lower air temperature winter season is -25 at the Salang and at the Jabal Saraj is -5 to -10 ºC. The landscape of Parwan Province has been formed from mountains, the main mountains of Parwan province are Salang and Pangesher mountains to plain areas of Kohdaman, the Hundukush mountains range is like wall at the north part of this province continues. The Jabal Saraj, Dowshakh and Paghman mountains range is located at the west side of this province [27].

1.2 The Main Rivers of Parwan

Here are four main streams contain of: Panjsher, Sanlang, Gurband and Shetal Rivers. The Gurband River sourced from 2911 m a.s.l. Besides its flows from west to northwest of 11km among Hindu Kush and Paghman Mountain, afterward some km at Shekh Ali valley, Gurband and Surkh Parsa joining with Panjsher watercourse. Panjsher River starts from Khawak Kotal, Kotal Anjiman and Bazark from 3000 m a. s. l then 150 km link with Kabul River, the total length of this river is 320 km and 125 km is in the Panjsher Province [5,8]. The south Salang River, begins from south Salang, after transient from Jabal Sarage connected with Panjsher River and in Sarobi District join with Kabul River, the total length of this river is 438mm [28] (Figures 1 and 2).

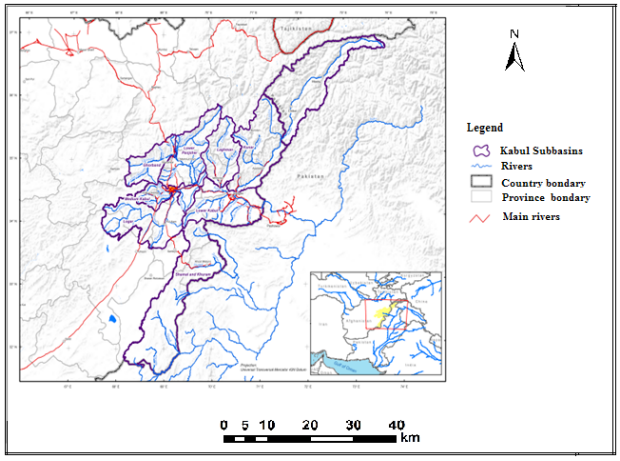

Figure 1. Watercourses map of Parwan and Kabul Basins, Afghanistan.

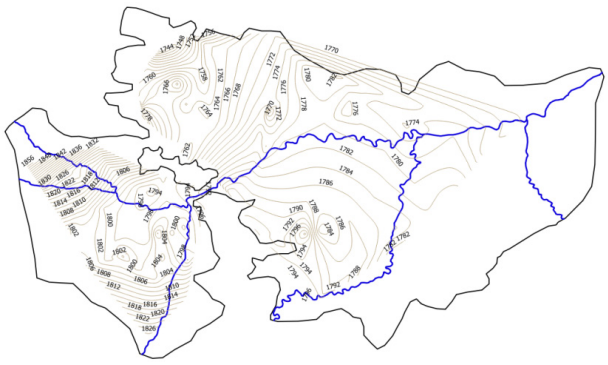

Figure 2. Contour line map of Parwan and Kabul subbasins.

2. Study Area

Parwan Province is located in the north side of Kabul Province (Figure 3). The environment of this province is Simi-arid, additional wind route from Hindu Kush Mountains series. In winter terms consuming snowfall and in spring seasons covering by rainfall, overall yearly precipitation is 300-400 mm, and the whole annually precipitation in Salang highlands from 800-1000 mm, higher mean air temperature at summer season exists among 25-30 ºC

and minor air temperature in winter periods minimum temperature in Salang is -25 and in Jabal Saraj are -5 to -10 ºC. The setting of Parwan Province Mountains form area and the main highlands of Parwan are Salang and Pangesher Mountains towards plain areas of Kohdaman, remain similar barrier at northern sections of this region [9-11].

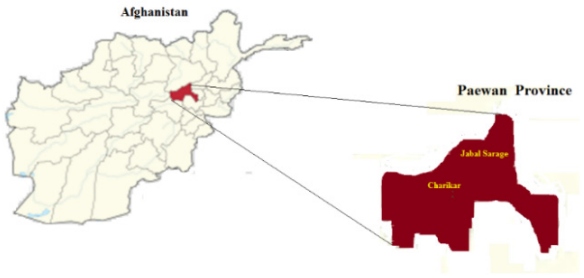

Figure 3. Location map of Jabal Sarage and Charikar districts, Parwan, Afghanistan.

3. Discussions on Groundwater Parameters

Previously wherever distributed the Chemical and Physical factors in Jabal Sarage and Charikar Districts, now I want to give brief information about some physical and chemical happening, that are involved in groundwater of this investigations:

3.1 Electro-Conductivity of Water

The conductivity is measurement principles of current in any solution, and its shows the quantity of salt solved in water. At some time the electro-conductivity related to the water temperature that having at the period of measurement. One of the aids of this study is very easy it can be conducted at the site. In this research we need for three times [12-15]. At the usual situations agreeing to the norms of Afghanistan (ANSA, 2011) the EC [29], the world health organization (WHO) and Asian Countries the electro conductivity is 1500µs/cm [34].

3.2 pH

For pH demonstrations used acidic and basic situations of water, in this research we found the pH of water via pH- meter [29]. The normal conditions pH agreeing to 6.5-8.5, the pH [31,16] and giving the World Health Organization (WHO) and Asian Countries are 6.5-8.5 [32].

3.3 Hardness of Water

The resistance of water belongs to particular anions and cations in the present water, these are particular salts which consist of; Mg^{2+}, K^{+}, Sr^{2+}, Fe^{2+}, Al^{3+}, Mn^{2+}, Ca^{2+} and with some anions CO_3^{2-}, Cl^{-}, $SO4^{2-,}$ NO^{3-}, SiO_3^{2-} and HCO_3^{-}, it's continuously exist in the form of Solutes (mg. L^{-}) conditions, [17]. The main method for measurement of Total Hardness is consisting 2340-CEDTA titrimetric. For this method we must use buffer of (NH_4 OH+NH_4 Cl), in addition the pH = 10-10.1 must be [32]. The common circumstances TH according to ANSA (2011) is 500 mg/l, the TH [31], and the world health organization (WHO) and Asian Countries is 500 mg/l [32].

3.4 Cations and Anions

a. Calcium (Ca)

In this research we found the quantity of Ca in groundwater by Photometer tool (test- Ray). Additional Ca we can discover in natural water, it's placed in mother rocks that are transitory from rock. Usually calcium is found in Carbonates, bicarbonates and sulfides [34]. Similarly, in salty water we can discover at form of Calcium chlorides and Calcium bicarbonates, nevertheless for some time if we find the Calcium bicarbonates its related hardness of waters and Calcium sulfites, Calcium nitrites and Calcium chlorides are main reasons for continuously hardness of waters. For Ca ions 10 mL adding in water, afterward 0.4 ml Sodium hydroxide for basic environment, it must be pH = 8-12, after one spoon of Monoxide indicator (C_6 H_8 N_6 O_6) adding and via solution E.D.T.A to changing the color. In normal conditions Ca according to [30], 200 mg/l, quantity of Ca according to the World Health Organization (WHO) and Asian Countries is 200 mg/l [29].

b. Sodium (Na)

This element is solvable and can be found in groundwater. In salty water this element is more than 1-100 gr. $^{-}$L. When we want to modification water to soft water using $NaCO_3$ via exchange of Na basic element add to this solution. At the usual situations water necessity consuming lesser amount of Na to protect water from toxic waste. In usual conditions Na is according to 200 mg/l [30], and Na according to World Health Organization (WHO) and Asian Countries is 200 mg/l [30].

c. Potassium (K)

As all know the K is one of the elements, that is often found in nature, but not exceeds from 30 mg. $^{-}$L. Agreeing to European Union, the more concentration of salts in the water is among 10-12 mg.-L determined. The normal conditions K is allowing to 10 mg/l [23], and the World Health Organization (WHO) and Asian Countries is 10 mg/l [29].

d. Iron (Fe)

For Iron amount we use two tubes A and B, in this case we acquire some potable water and wash these tubes. At the same time in every tube we add 20 mL potable water. After three minutes determined the quantity of Iron. Here

is diverse colors and compare color with chart for selection the amount of irons in water. This test must be repeated three times. The normal conditions Fe 0.3 mg/l, and the World Health Organization (WHO) and Asian Countries quantity of Fe is 0.3 mg/l [27].

e. Sulfides (SO_4)

This measuring Turbidity meter, via this device presentation the amount of Sulfides in water and this test is necessary to repeat three times. The concentration of sulfides in water is 100 mg. $^{-}$L. From changed origin sulfides solved in water, the main sources of its Gypsum and other sulfides. Sulfides in sea water added as of oxidation of sulfides, sulfites and Neosulfites [13,14]. Extra sulfides at the groundwater added from industrial activities and some factories using H_2SO_4, for example paper and Leeds factories its dispersal from chimney of factories. At the normal conditions according to, 250 mg/l [31], the Sulfides and the World Health Organization (WHO) and Asian Countries is 250 mg/l [34].

f. Chlorides

The method for chlorides determination of groundwater, we can fix on the surface and groundwater, now this technique 10 ml groundwater collected in flask and two drops of Potassium chromite added, after that 0.0141 N Slurnitrites ($AgNO_3$) also added to altered color towards yellow and red. The Chlorides normal conditions rendering to 250 mg/l, the World Health Organization (WHO) and Asian Countries select 250 mg/l. At changing color Chromite precipitated in waters. Chlorides can be calculated by the next formula [12-16].

mg CL-/ L = (A-B). F.N. 354 50/mL of model

A = Titration solution for sampling

F = factor (1.03)

B = Titration solution for potable water (0.1)

N = Normality Slurnitrites

g. Fluorine (F)

In this investigation for fluorine determination, added 10 mL in flask, after 2 CC solution for three minutes staying. The F normal conditions according to 1.5 mg/l, and F via World Health Organization (WHO) and Asian Countries consist of 1.5 mg/l [30-34].

h. Arsenic (Ar)

For determination amount of Ar in groundwater, 50 mL sample of water added, afterwards add Zink for 20 mins, and after comparing filter with Chart for finding amount of Ar in water [31].

i. Magnesium (Mg)

For Mg, I used software. In this software I can find the quantity of Mg. In normal situations Mg giving to mg/l, the World Health Organization (WHO) and Asian Countries quantity of Mg is 30 mg/l [29-33].

4. Method and Materials

This inquiry completes two categories of water analysis: one is a real analysis, and another is research laboratory analysis. In areal analysis I investigated and tested ten wells in Jabal Sarage and Charikar Distracts, a number of electro - conductivity, water temperature, dissolved oxygen in water, Total Dissolved Soled (TDS) and the Resolved Salt in Water (SSW) at areal complete, and at laboratory works selected chemical and physical analysis used for determination 18 parameters.

In this research measure dissimilar physical and chemical consideration at the groundwater of Jabal Sarage District, as it's explain in Tables 1 and 2:

Table 1. The physical parameters devices as used for this research.

No	Parameter	Unite	Name of measurement devices	The location of measurement
1	EC	s/Cmμ	Partible ground, Water temperature Conductivity, Electro - Conductivity meter and pH-meter, 2340-CEDTA titrimetric ,	Areal (site)
2	pH			
3	Hardness	Mg/L		
4	Color	Mg/L		
5	T	C°		

Table 2. Chemical parameters that found in this investigation in groundwater of Jabal Sarage district.

No	Elements	Unite	Device of measurements	Type of test
1	Ca	Mg/L	Spectra- photo model DR3900	Laboratory analysis
2	K			
3	Na			
4	SO_3			
5	NO_4			
6	Cl			
7	F			
8	Fe			
9	NO_3			
10	SO_4			
11	Mg			
12	Ca/H			
13	HCO_3			
14	CO_3			
15	AlK			
17	Cl_2			
18	TDS			

5. Results and Discussion

In this research I used physical and chemical limitations at the groundwater of SamadKhankhel, Chingay, Hashamkhel, Nasratkhel, and Qasamkhel villages have in Jabal Sarage District and Malakhel, Salehkhel, Azizbigkhel and Babakhel villages related to Charikar District of Parwan Province, Afghanistan. These parameters involves; Hardness, Turbidity, Color, Temperature, Electro-conductivity (EC), pH, Ca, K, Na, SO_3, NO_4, Cl, Fe, NO_3, SO_4, Mg, F,

Ca/H, Fe, HCO_3, CO_3, AlK, Cl_2 and TDS.

As described follows:

5.1 Hardness

In this research for measurement of Total Hardness consisting 2340-CEDTA titrimetric, in this method I use buffer of (NH_4 OH+NH_4 Cl), in addition the pH = 10 -10.1 must be. The Maximum amount of hardness is in Salehkhel village well its 857 (mg.L$^-$), and minimum amount of is in Qasamkhel which is 535 (mg.L$^-$). The main reason of high amount of Hardness in Salehkhel is Cl in groundwater, which is acidic, but the minimum amount of in Qasamkhel village that belongs to basic is 8. For better understand we can see (Figure 4).

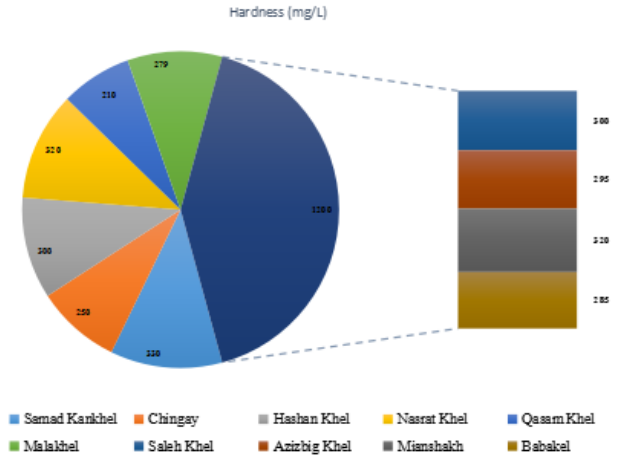

Figure 4. Hardness of groundwater in Jabal Sarage and Charikar districts.

5.2 Turbidity

Turbidity belongs to the amount of solution and smaller particles in water, which change its color. In this research we used for measuring the turbidity of water by turbidity mater (mg.L$^-$). For this we can use TDS (Total Dissolved Solid). Generally the turbidity of water in this research was no problem and all groundwater was clear and we can use for drinking. The turbidity in all well and groundwater water was zero which is equal to the international standards for groundwater's. For better understand we can use (Figure 5).

5.3 Color

Generally, the color of water is almost green, but the other colors belong to the existence of organic and inorganic materials, which is solvable in waters (mg.L$^-$). In inorganic materials, existence of some elements and components that are existing in rock, sediments and soils in ground and surface waters. In this research the color of groundwater is almost green and having no any problems we can use for drinking and irrigation. For better understanding see (Figure 6).

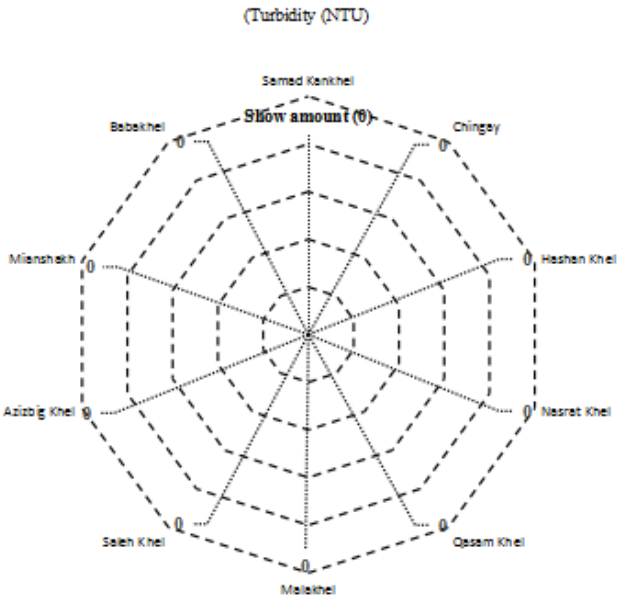

Figure 5. Turbidity of groundwater in Jabal Sarage and Charikar districts.

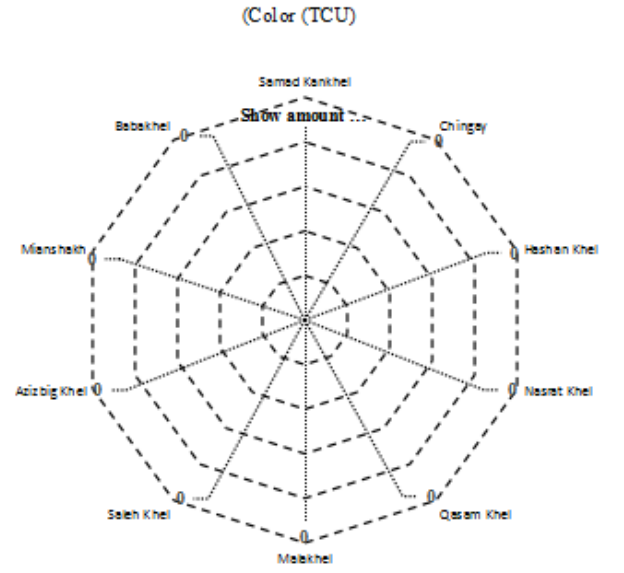

Figure 6. Color of groundwater in Jabal Sarage and Charikar districts.

5.4 Temperature

The Temperature of groundwater belongs to the depth of groundwater, volcanic eruptions and geographical locations. From view point of temperature the ground divided in six categories', it consists of: very cold (5 ˚C), lately

cold (10 ˚C), warm water (18 ˚C), almost warm (25 ˚C), Warm (37 ˚C) and very warm (more than 40 ˚C). In this research in all groundwater temperature is around 22 ˚C, and this is better and suitable for drinking and all uses. For better understand we can use (Figure 7).

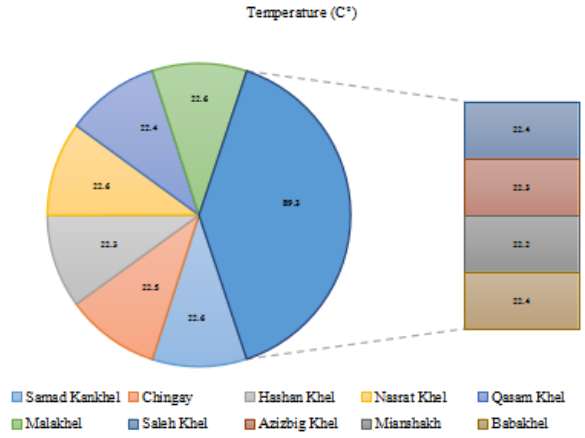

Figure 7. Temperature of groundwater in Jabal Sarage and Charikar districts.

5.5 Electro–Conductivity (EC)

The Electroconductivity shows the amount of salts (µs/cm). In this research we used Electrocoductivity mater for measurement of groundwater, in same time the electro-conductivity related to the water temperature that having at the period of measurement. It is worth to mention that, this research has been done three times for every sampling. The EC of this research is normal and can be used for drinking water. For better understanding we can use (Figure 8).

5.6 pH

As all know pH show demonstration of acidic and basic situations in waters, in this research we found the pH of water by pH- meter. The pH of this research neutral (7), but in two villages (SamadKhankhel, Chingay) are basic its 8.1 and 8, but no higher basic we can use for drinking and irrigations water . For better understand we can use (Figure 9).

5.7 Chemical Parameters

The chemical parameters consisting elements and components that exist at the composition of rocks, sediments and soils, that are leaching by surface waters during percolation washing from one horizon to another horizon and eventually adding to the groundwater and saturation zone. As well as during movements of groundwater among different layers and washing mining carried to at the solved groundwater's. In this research I found different elements and components such as Ca, K, Na, SO_3, NO_4, Cl, Fe, NO_3, SO_4, Mg, F, Ca/H, Fe, HCO_3, CO_3, AlK, Cl_2 and TDS. In all villages wells of this research are normal and equal to international standards and we can use for drinking and irrigations. For better understand we can use (Figure 10).

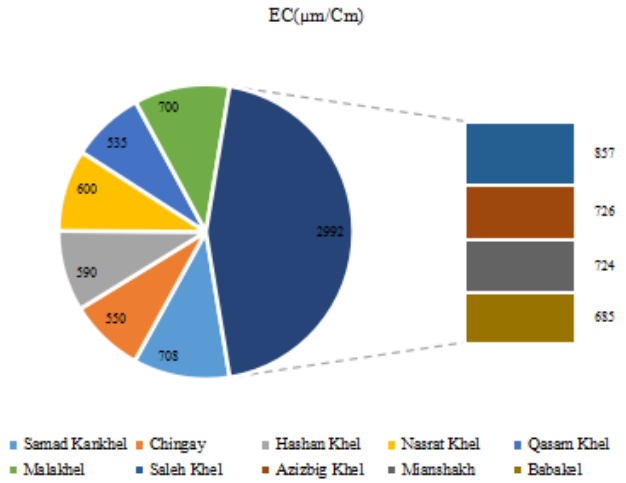

Figure 8. Electrocoductivity of groundwater in Jabal Sarage and Charikar districts.

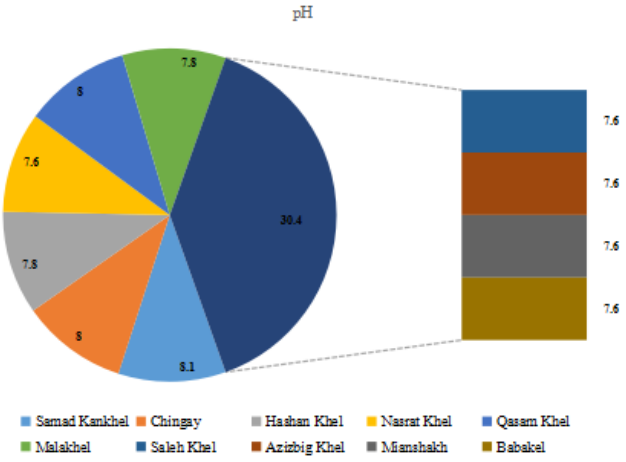

Figure 9. pH of groundwater in Jabal Sarage and Charikar districts.

5.8 Comparing Means and International Standards

In this research for better understanding and accurate research works, I compared mean of some parameters such as EC, pH, K, Na, Mg, Cl, Fe and F are equal permitting to the global values, but TH, Ca and SO_4 are minor from universal and international values besides its not toxic aimed at health and we can using for drinking and irrigation water. For better understanding, we can use (Figure 11). The Physical and Chemical of groundwater

Table 3. Physical parameters for groundwater of this research.

District	Villages	Parameters					
		Hardness ([1]mg/L)	Turbidity ([2]NTU)	Color ([3]TCU)	Temperature ([4]C°)	EC ([5]µs/Cm)	pH
Jabal Sarage	Samad Khankhel	330	0	0	22.6	708	8.1
Jabal Sarage	Chingay	250	0	0	22.5	550	8
Jabal Sarage	Hasan Khel	300	0	0	22.3	590	7.8
Jabal Sarage	Nasrat Khel	320	0	0	22.6	600	7.6
Jabal Sarage	Qasam Khel	210	0	0	22.4	535	8
Charikar	Qasam Khel	279	0	0	22.6	700	7.8
Charikar	Saleh Khel	300	0	0	22.4	857	7.6
Charikar	Azizbig Khel	295	0	0	22.3	726	7.6
Charikar	Mianshakh	320	0	0	22.2	724	7.6
Charikar	Babakhel	285	0	0	22.4	685	7.6

Table 4. Chemical parameters for groundwater of this research.

District	Villages	Parameters																	
		Ca (mg/L)	Na ≈	K ≈	SO4 ≈	Cl ≈	F ≈	Mg ≈	Ca/H ≈	HCO_3 ≈	CO_3 ≈	SO_4 ≈	AlK ≈	Cl_2 ≈	T/H ≈	NO_3 ≈	Fe ≈	As ≈	TDS ≈
Jabal Sarage	Samad Khankhel	110	19	9.2	78	84	0.3	14	143	180	0	55	2.3	0	287	0	0.2	0	414
Jabal Sarage	Chingay	105	12	4.6	32.3	72	0.3	12	145	180	0	56	3.3	0	310	0	0.3	0	412
Jabal Sarage	Hasan Khel	95	13	5.2	34.7	74	0.2	11	150	212	0	70	3.4	0	300	0	0.3	0	415
Jabal Sarage	Nasrat Khel	100	14	5.3	33.1	75	0.1	14	153	181	0	56	2.7	0	256	0	0.2	0	433
Jabal Sarage	Qasam Khel	120	16	5.4	16.3	66	0.2	12	145	150	0	65	3.1	0	285	0	0.2	0	445
Charikar	Qasam Khel	105	26	5,4	58	37	0,3	11	145	190	0	58	3.8	0	285	0	0.3	0	413
Charikar	Saleh Khel	120	32	9,1	70	88	0,2	13	150	210	0	70	4.2	0	320	0	0.3	0	476
Charikar	Azizbig Khel	95	25	5,1	67	52	0,2	15	225	167	0	67	3.3	0	295	0	0.2	0	433
Charikar	Mianshakh	90	27	5,5	65	52	0,3	15	150	170	0	65	3.4	0	300	0	0.2	0	439
Charikar	Babakhel	90	25	3,5	59	37	0,2	15	145	166	0	59	3.1	0	279	0	0.3	0	410

1 Mille gram/ Liter
2 Nepeleo Turbite Unite
3 Total Color Unite
4 Centigrade
5 Micro Semins/Centi meter

quality in the Tables 3 and 4 are detail explained.

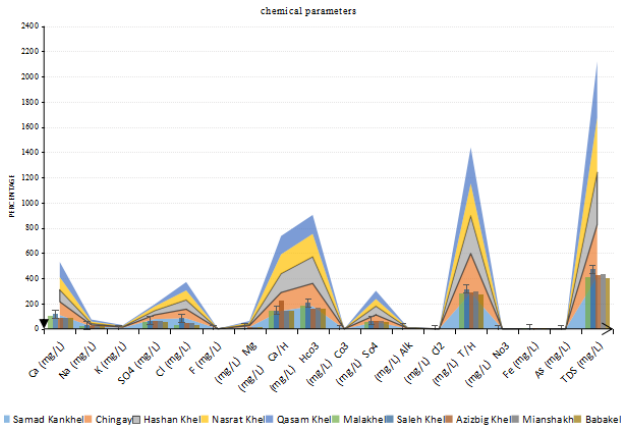

Figure 10. Chemical parameters in Jabal Sarage and Charikar Districts, Parwan, Afghanistan.

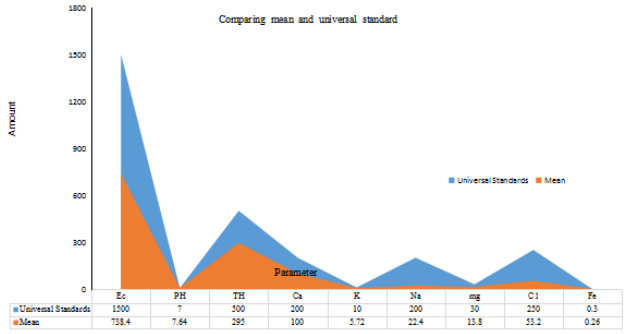

Figure 11. Comparing mean chemical, physical limitations and universal standards of its in Jabal Sarage and Charikare district.

6. Conclusions

The groundwater quality analysis is used to determine physical and chemical parameters from Jabal Sarage and Charikar Districs (drinking water 10 rings of wells), Parwan Province, in Afghanistan. The calculated mean of physical and chemical parameters EC, hardness, temperature, pH, color and turbidity for Samad Khankhel, Chingay, Hasankhel, Nastrat Khel and Qasam Khel, are 597 µm/Cm, 282 mg/L, 22.48 ˚C, 7.8, 0 TCU and 0 NTU respectively, and for Malakhel, Saleh Khel, Azizbig Khel, Mianshakh and Babakhel are 738.4 µm/Cm, 295.5 mg/L, 22.38 ˚C, 7.6, 0 TCU and 0 NTU respectively. The mean of these parameters show good results with equal to international standards. The chemical parameters of Ca, Na, K, SO4, Cl, F, Mg, Ca/H, HCO_3, CO_3, SO_4, AlK, Cl_2, T/H, NO_3, Fe As and TDS are almost appropriate and equal to the international standards, we can used for drinking and irrigations water. The results obtained suggest that the water quality can be used efficiently in the other province of groundwater in Afghanistan.

Acknowledgements

I extend my thanks to my faculty members who helped us put this paper together.

References

[1] Banks et al. (2014). Hydrogeological Atlas of Faryab Province, Northern Afghanistan. Ministry of Rural Rehabilitation &Development, Kabul.

[2] Banks, David, and Soldal, Oddmund, (2002). Towards a policy for sustainable use of Groundwater by non-governmental organizations in Afghanistan: Hydrogeology Journal, v. 10, no. 3, p. 377.

[3] Broshears, R.E., Akbari, M.A., Chornack, M.P., Mueller, D.K., and Ruddy, B.C. (2005). Inventory of ground-water resources in the Kabul Basin, Afghanistan: U.S. Geological Survey Scientific Investigations Report 2005-5090, 34 p.

[4] Bohannon, R.G., (2005). Geologic map of quadrangle 3468, Chak-e-Wardak (509) and Kabul (510) quadrangles: Afghan Open-File Report (509/510) 2005-1001.

[5] Bohannon, R.G., and Turner, K.J., (2007). Geologic map of quadrangle 3468, Chak Wardak-Syahgerd (509) and Kabul (510) quadrangles, Afghanistan: U.S. Geological Survey. Open- File Report 2005–1107–A. 1 sheet.

[6] Böckh, E.G., (1971). Report on the groundwater resources of the city of Kabul, report for Bundesanstalt für Geowissenschaften und Rohstoffe BGR file number 0021016, 43 p.

[7] Dojlido, J. R., and G. A. Best. (1993). Hydrochemistry of Water and Water Pollution". Ellis Harwood, New York, 363 pp.

[8] Hessami, E. B. (2017). Afghanistan's Water Plans Complicated by Worried Neighbors, New Secur. Beat [online] Available from: https://www.newsecuritybeat.org/2017/03/afghanistans-waterplans- Complicated-worried-neighbors/ (Accessed 26 January 2019).

[9] Houben. George. Tunnermeier. Torg. (2003). Hydrogeology of Kabul Basin Part 1 (BGR). Kabul. Afghanistan5pp, 14pp.

[10] Japan International Cooperation Agency (JICA), (2007a). The study on groundwater resources Potential in Kabul Basin in the Islamic Republic of Afghanistan: 3rd Joint Technical Committee, Sanyu Consultants, Inc., Kabul, Afghanistan.

[11] Jain, R. (2018). In Parched Afghanistan, Drought

Sharpens Water Dispute With Iran, US News World Rep.[online] Available from: https://www.usnews.com/news/world/articles/2018-07-16/inparched- Afghanistan-drought-sharpens-water-dispute-with-iran (Accessed 26 January 2019.

[12] Belhassan, K. (2020). Hydrogeology of the Ribaa-Bittit springs in the Mikkes Basin (Morocco). International Journal of Water Resources and Environmental Science 9 (1): 07-15, 2020 ISSN 2311-2492, © IDOSI Publications, 2020.
DOI: 10.5829/idosi.ijwres. 2020.9.1.14537.

[13] Belhassan, K. (2020). Relationship between River and Groundwater: Water table Piezometery of the Mikkes Basin (Morocco. International Journal of Water Resources and Environmental Science 9 (1): 01-06, 2020 ISSN 2311-2492, © IDOSI Publications, 2020.
DOI: 10.5829/idosi.ijwres. 2020.9.1.14536.

[14] Belhassan, K. (2011). Hydro-geological Context of Groundwater Mikkes and different variations of Its springs flow (Morocco). Research Journal of Earth Science 3 (1): 15-26, 2011, ISSN 1995-9044, © IDOSI Publications, 2011.

[15] Belhassan, K. (2011). Relationship flow-Rainfall in the stream Mikkes (Morocco). Research Journal of Earth Science 3 (1): 39-44, 2011, ISSN 1995-9044, © IDOSI Publications, 2011.

[16] Matthew King and Benjamin Sturtewagen. (2010). Making the Most of Afghanistan's River Basins, Opportunities for Regional Cooperation, The East West Institute,11 East 26th Street, 20th Floor, New York, NY 10010, U.S.A. 1-212-824-4100. PP, 1-13.

[17] Myslil, Vlastimil, Eqrar, M. Naim, and Hafisi, M., (1982). Hydrogeology of Kabul Basin (Translated from Russian): sponsored by the United Nations Children's Fund and the Ministry of Water and Power, Democratic Republic of Afghanistan.

[18] Proctor & Redfern International Limited (1972). Water supply, sewerage, drainage and solid waste Systems for Greater Kabul - Joint Interim Master Plan.- Report on behalf of the Royal Government of Afghanistan, WHO, UNDP.- Toronto. BGR-Archiv-Nr. 0030084.

[19] Rasouli, H. and Safi, A. G. (2021). Geological, Soil and Sediment Studies in Chelsaton Sedimentary Basin, Kabul, Afghanistan. International Journal of Geosciences, 12, 170-193. https://doi.org/10.4236/ijg.2021.122011.

[20] Rasouli H. Sarwari, M. H., Khairuddin R.' Said A. H. **(**2020**).** Geological Study of Tangi Mahipar Mountain Range along Kabul Jalalabad road, Afghanistan https://dx.doi.org/10.4236/ojg.2020.1010044.

[21] Rasouli H. (2020). Application of soil physical and chemical parameters and its Comparing in Kabul sedimentary basins, Kabul, Afghanistan http://dx.doi.org/10.24327/ijrsr.2020.1102.5095.

[22] Rasouli H., (2020). WELL DESIGN AND STRATIGRAPHY OF SHEERKHANA DEEP WELL IN CHAK DISTRICT, WARDAK, AFGHANISTAN. International Journal of Geology, Earth & Environmental Sciences ISSN: 2277-2081, and Open Access, Online International Journal Available at http://www.cibtech.org/jgee.htm2020Vol.10 (2) May-August, pp.54-68/Rasouli.

[23] Rasouli H., (2017). THE WAYS OF ACID ACCUMULATION IN KABUL BASIN SOILS AND ITSEFFECTS ON ANIMALS AND PLANTS, KABUL, AFGHANISTAN. International Journal of Geology, Earth & Environmental Sciences ISSN: 2277-2081, and Open Access, Online International Journal Available at http://www.cibtech.org/jgee.htm 2020Vol.10 (2) May-August, pp.44-53/Rasouli.

[24] Rasouli H., (2019). A STUDY ON SOME RIVER SEDIMENTS, HYDROLOGY AND GEOLOGICAL CHARACTERISTICS IN CHAK SEDIMENTARY BASIN, WARDAK, AFGHANISTAN. International Journal of Geology, Earth & Environmental Sciences, ISSN: 2277-2081, and Open Access, Online International Journal Available at http://www.cibtech.org/jgee.htm2019 Vol.9 (2) May-August, pp.49-61/Rasouli.

[25] Rasouli, H. Kayastha, R. B., Bikas, C. B., Ahuti S., Arian, H. and Armstrong, R. (2015). Estimation of Discharge From Upper Kabul River Basin, Afghanistan Using the Snowmelt Runoff Model. Journal of Hydrology and Meteorology, 9, 85-94. https://doi.org/10.3126/jhm.v9il.15584.

[26] Robert E. Broshears, M. Amin Akbari, Michael P. Chornack, David K. Mueller, and Barbara C. Ruddy. (2005). Inventory of GroundWater Resources in the Kabul Basin, Afghanistan Scientific, For More information about the USGS and its products: 1-888-ASK-USGS World Wide Web: http://www.usgs.gov.

[27] Shahid Ahmad, (2010). TOWARDS KABUL WATER TREATY: MANAGING SHARED WATER RESOURCES-POLICY ISSUES AND OPTIONS, International Union for Conservation of Nature and Natural Resources. PP 1-11.

[28] Thamas Himmelsbach, (2003). Hydrogeology of the Kabul basin part III: Modeling approach, Conceptual and numerical ground water models, Foreign office

of the Federal Republic of Germany (AA-Gz: GF07 385.28/3 16/03. P 15-50.

[29] Torge, T., Georg, H., and Thomas, H. (2003). Hydrogeology of the Kabul Basin Part I: Geology, aquifer characteristics, climate and hydrography. Foreign office of the Federal Republic of Germany. BGR record no.: 200310277/05.

[30] WHO, (2011). Arsenic in drinking-water. Background document for development of WHO guidelines. For drinking-water quality. WHO, Geneva.

[31] WHO, (2010). Preventing disease through healthy environments. Exposure to arsenic: a major public Health concern. WHO, Geneva.

[32] WHO, (2009). WHO Handbook on Indoor Radon: A Public. Health Perspective (Geneva, Switzerland: World Health Organization).

[33] WHO, (2011). Uranium in drinking-water. Background document, for development of WHO guidelines for drinking-water quality. WHO, Geneva.

[34] WHO, (2003). Zinc in drinking-water. Background document for, development of WHO. WHO, Geneva.

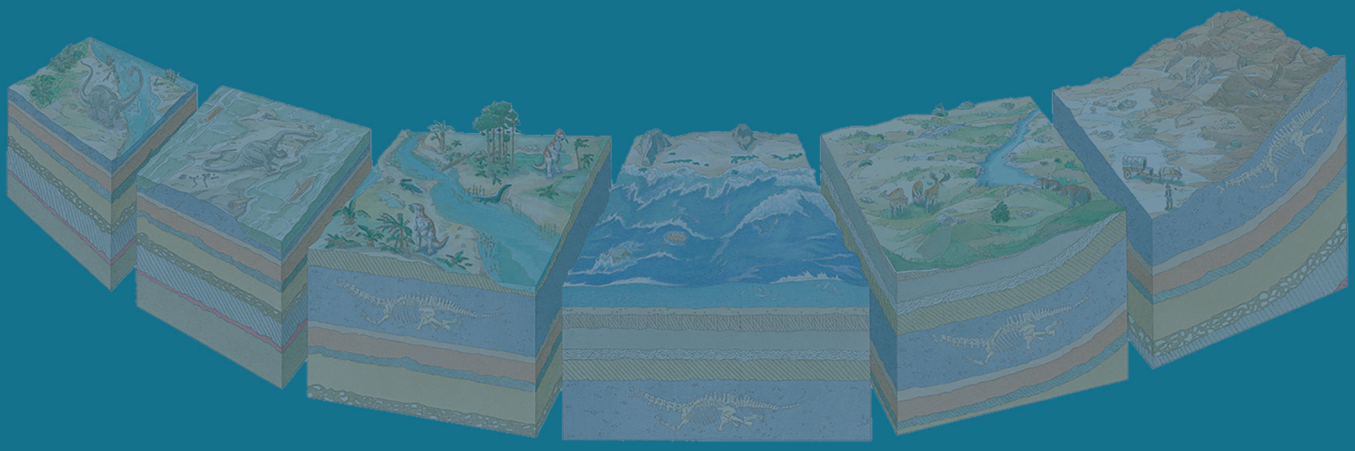

BILINGUAL
PUBLISHING CO.
Pioneer of Global Academics Since 1984

Tel:+65 65881289
E-mail: contact@bilpublishing.com
Website:ojs.bilpublishing.com

ISSN 2630-4961
04
9 772630 496218